

**EGE UNIVERSITY GRADUATE SCHOOL OF NATURAL  
AND APPLIED SCIENCES**

**DOCTORAL THESIS**

**DEVELOPMENT OF FUNCTIONAL SURFACES FOR  
ELECTROCHEMICAL DETECTION OF THIOLS**

**Meliha ÇUBUKCU**

**Supervisor: Prof. Dr. Fatma Nil ERTAŞ**

**Co-Supervisor: Assoc. Prof. Dr. Ülkü ANIK**

**Department of Chemistry**

**Code: 405.03.01**

**Presentation Date: 07.12.2012**

**Bornova-İZMİR**

**2012**



**Yüksek Kimyager Meliha Çubukcu** tarafından **Doktora** tezi olarak sunulan “**Development of Functional Surfaces For Electrochemical Detection of Thiols**” başlıklı bu çalışma E.Ü. Lisansüstü Eğitim ve Öğretim Yönetmeliği ile E.Ü. Fen Bilimleri Enstitüsü Eğitim ve Öğretim Yönergesi'nin ilgili hükümleri uyarınca tarafımızdan değerlendirilerek savunmaya değer bulunmuş ve **07.12.2012** tarihinde yapılan tez savunma sınavında aday oybirliği/oyçokluğu ile başarılı bulunmuştur.

**Jüri Üyeleri:**

**İmza**

<b>Jüri Başkanı</b>	<b>: Prof.Dr.F.Nil ERTAŞ</b>	.....
<b>Raportör Üye</b>	<b>: Doç Dr.Ülkü ANIK</b>	.....
<b>Üye</b>	<b>: Prof.Dr.Ümran YÜKSEL</b>	.....
<b>Üye</b>	<b>: Prof.Dr.Suna TİMUR</b>	.....
<b>Üye</b>	<b>: Prof.Dr.Zekerya DURSUN</b>	.....



**ÖZET****TİYOLLERİN ELEKTROKİMYASAL TAYİNİ İÇİN FONKSİYONEL  
YÜZEYLERİN GELİŞTİRİLMESİ**

ÇUBUKCU, Meliha

Doktora Tezi, Kimya Anabilim Dalı

Tez Danışmanı: Prof. Dr. Fatma Nil ERTAŞ

İkinci Tez Danışmanı: Doç. Dr. Ülkü ANIK

Aralık 2012, 120 sayfa

Biyolojik öneme sahip moleküllerin, pratik, ekonomik ve etkin tayininde elektrokimyasal biyosensörleri de içeren elektrokimyasal yöntemler sıklıkla kullanılmaktadır. Bu çalışmada farklı malzemelerle modifiye edilmiş farklı türde elektrotlar ve voltammetri ile santrifüj yönteminin bileşiminden oluşan sentri-voltammetri yöntemleri kullanılarak duyarlı ve etkin elektrokimyasal yöntemlerin geliştirilmesi amaçlanmıştır ve model olarak glutatyon (GSH) bileşiği kullanılmıştır. Bu bağlamda nanoyapı temelli elektrotlar ve uygun şekilde tasarlanan biyosensör sistemleri geliştirilmiştir. Bunların dışında santrifüj ve voltammetri yöntemlerinin bileşiminden oluşan sentri-voltammetri yöntemi de bu bileşiklerin tayininde ilk kez uygulanmıştır. Sentri-voltammetri yöntemi uygulanırken silika jel ve altın nanopartikül (AuNp) gibi taşıyıcı çökeleklerden faydalanılmıştır. Ayrıca AuNp, çok duvarlı karbon nanotüp (MWCNT) gibi nanomalzemeler de sentri-voltammetrik tekniklerin uygulamasında kullanılmışlardır. Tüm yöntemler için deneysel parametreler optimize edildikten sonra, yöntemlere ilişkin analitik özellikler belirlenmiştir. Daha sonra optimize sistemler ile seçilen örneklere standart katma yöntemi uygulanmış ve oldukça iyi geri kazanım değerleri elde edilmiştir.

**Anahtar Sözcükler:** glutatyon, sensör, biyosensör, sentri-voltammetri, nanomateryaller, taşıyıcı çökelek



**ABSTRACT****DEVELOPMENT OF FUNCTIONAL SURFACES FOR  
ELECTROCHEMICAL DETECTION OF THIOLS**

ÇUBUKCU, Meliha

PhD in Chemistry

Supervisor: Prof. Dr. Fatma Nil ERTAŞ

Co-Supervisor: Assoc. Prof. Dr. Ülkü ANIK

December 2012, 120 pages

Electrochemical methods including electrochemical biosensors are widely used for practical, economical and effective detection of some biologically important molecules. In this work, various types of electrodes modified with different materials and also centri-voltammetry-a combination of centrifuge with voltammetry- was planned to use for developing sensitive and effective method for detection of these materials and glutathione (GSH) was chosen as model materials. For this purpose, nanomaterial based electrodes and biosensing systems were prepared. Besides these systems, centri-voltammetry which includes the centrifugation and voltammetry was applied for detection of this substance for the first time. In centri-voltammetric application carrier precipitates like silica gel and gold nanoparticles (AuNps) were used. Also nanomaterials like AuNp and multi-walled carbon nanotubes (MWCNT) were introduced with this technique. After the experimental parameters were optimized for all techniques, analytical characteristics were examined. Then these methods were applied for GSH detection by means of standard addition technique in selected samples and promising recovery values were obtained.

**Keywords:** glutathione, sensor, biosensor, centri-voltammetry, nanomaterials, carrier precipitate





## ACKNOWLEDGEMENTS

I would like to express my deep gratitude to my supervisors Prof. Dr. F. Nil ERTAŞ and Assoc. Prof. Dr. Ülkü ANIK for their encouragement, patience and valuable guidance during the whole period of my research. I also would like to express my sincere gratitudes to Prof. Dr. Suna Timur and Prof. Dr. Zekerya DURSUN for their valuable suggestions throughout the study.

I also thank to all of the members of the chemistry department from Ege University and Muğla Sıtkı Koçman University.

I would like to thank The Scientific and Technological Research Council of Turkey and Ege University Research Found for financial support during this study. I would like to thank NE-KA Kalıp Makina San.Tic.Ltd.Şti. for helping making Centri-Cell.

I would like to thank to PhD student Serdar ÇEVİK for his support and valuable assistance, advice. I also would like to thank warmly to my friends Msc. Yeliz YAVUZ and Rsc. Assist Sema ASLAN and all my laboratory colleagues for their friendly helping, collaboration and fellowships, who assisted me during my study.

Finally, I would like to thank my family for immortal confidence, their support and encouragement for my education in any difficulties.

At last but not least I would like to thank with whole my heart Özgür CESUR for his patience, encouragement and understanding throughout the study.



## CONTENTS

	<u>Page</u>
ÖZET .....	v
ABSTRACT .....	vii
ACKNOWLEDGEMENTS.....	ix
CONTENTS .....	xi
LIST OF FIGURES .....	xv
LIST OF TABLES.....	xxi
SYMBOLS AND ABBREVIATION.....	xxiii
1. INTRODUCTION .....	1
1.1. Thiols .....	1
1.1.1. Cysteine .....	3
1.1.2. <i>N</i> -acetylcysteine.....	4
1.1.3. Homocysteine .....	4
1.1.4. Glutathione .....	5
1.2. Methods Developed for Thiolic Compound Analysis .....	13
1.2.1. Spectrophotometric assay .....	13
1.2.2. Fluorometric assay.....	13
1.2.3. Bioluminescence assay .....	14
1.2.4. Capillary electrophoresis .....	14
1.2.5. Chromatographic methods.....	15
1.2.6. Electrochemical techniques .....	18
1.3. Biosensors.....	24
1.4. Nanotechnology .....	26
1.4.1. Nanocomposites.....	27
1.4.2. Nanoparticles .....	28
1.5. Centri-voltammetry.....	36
1.6. The Aim of the Thesis .....	38
2. EXPERIMENTAL.....	39
2.1. Instrumentation .....	39

## CONTENTS (Continue)

	<u>Page</u>
2.2. Reagents .....	41
2.3. Electrode Preparation .....	43
2.3.1. Preparation of bismuth film electrode (BiFE) .....	43
2.3.2. Preparation of bare GCPE .....	43
2.3.3. Preparation of AuNp/Al <sub>2</sub> O <sub>3</sub> .TiO <sub>2</sub> /GCPE .....	43
2.3.4. Preparation of QCM sensors .....	44
2.3.5. Preparation of AuNp/nano-micro TiO <sub>2</sub> based GCPE .....	44
2.3.6. Preparation of 4% MWCNT-CPE .....	44
2.3.7. Preparation of Chit/GSH-P <sub>x</sub> /PtNp onto the GCPE .....	45
2.3.8. Preparation of GSH-P <sub>x</sub> (immob)/PtNp/GCPE .....	45
2.3.9. Preparation of 4% Fe <sub>3</sub> O <sub>4</sub> Np/GSH-P <sub>x</sub> (immob) modified GCPE .....	46
2.4. Procedures .....	46
2.4.1. Procedure for BiFE .....	46
2.4.2. Procedure for AuNp/Al <sub>2</sub> O <sub>3</sub> .TiO <sub>2</sub> /GCPE .....	46
2.4.3. Procedure for AuNp/nano-micro TiO <sub>2</sub> based GCPE .....	47
2.4.4. Procedure for 4% MWCNT-CPE .....	48
2.4.5. Procedure for Chit/GSH-P <sub>x</sub> /PtNp onto the GCPE .....	48
2.4.6. Procedure for GSH-P <sub>x</sub> (immob)/PtNp/GCPE .....	48
2.4.7. Procedure for 4% Fe <sub>3</sub> O <sub>4</sub> Np/GSH-P <sub>x</sub> (immob) modified GCPE .....	49
2.5. Sample Application .....	50
2.5.1. Sample application for AuNp/Al <sub>2</sub> O <sub>3</sub> .TiO <sub>2</sub> nanopowder/GCPE .....	50
2.5.2. Sample application for 4% MWCNT-CPE .....	50
2.5.3. Sample application for GSH biosensor .....	51
3. RESULT and DISCUSSION .....	52
3.1. Development of Composite Electrodes for Voltammetric Studies .....	52
3.1.1. Studies with BiFE .....	52
3.1.2. Studies with AuNp/Al <sub>2</sub> O <sub>3</sub> .TiO <sub>2</sub> modified GCPE .....	52
3.1.3. Studies with AuNp/nano-micro TiO <sub>2</sub> based GCPE .....	64

## CONTENTS (Continue)

	<u>Page</u>
3.2. Centri-voltammetric Studies.....	66
3.2.1. Optimization of the experimental parameters.....	68
3.2.2. Analytical characteristics.....	76
3.2.3. Sample application.....	79
3.3. Biosensor Studies with Pt Modified GCPE.....	80
3.3.1. Electrodeposition of PtNps by cyclic voltammetry .....	80
3.3.2. The Effect of presence of PtNps into electrode structure .....	82
3.3.3. The EIS characterization of GSH biosensor .....	83
3.3.4. Optimization of experimental parameters .....	85
3.3.5. Analytical characteristics.....	91
3.3.6. Interference study .....	93
3.3.7. Sample application.....	93
3.3.8. Biosensor studies with 4% Fe <sub>3</sub> O <sub>4</sub> Np modified GCPE.....	94
3.4. Biocentri-voltammetric Analysis of GSH .....	95
3.4.1. Biocentri-voltammetry with GSH-Px <sub>(immob)</sub> /GCPE .....	95
3.4.2. Biocentri-voltammetry with GSH-Px <sub>(immob)</sub> /PtNp/GCPE biosensor.....	97
4. CONCLUSION .....	99
REFERENCES .....	103
CURRICULUM VITAE.....	119



## LIST OF FIGURES

Figure	Page
1.1 Structures of biological aminothiols .....	2
1.2 Glutathione synthesis and metabolism. (a) Glutamylcysteine synthetase; (b) glutathione synthetase; (c) $\gamma$ -glutamyl cyclotransferase; (d) oxoprolinase; (e) $\gamma$ -glutamyl transpeptidase; (f) peptidase.....	8
1.3 The pathways of GSH-Px enzyme .....	10
1.4 Excitation signal for DP voltammetry .....	19
1.5 Schematic diagram of a voltammetric cell .....	22
1.6 The principle of a biosensor.....	25
1.7 Schematic representations of nanocomposite materials with characteristics length scale: (a) nanolayered composites with nanoscale bilayer repeat length; (b) nanowire composites composed of a matrix with embedded filaments of nanoscale diameter; (c) Nano particle composites composed of a matrix with embedded particles of nanoscale diameter.....	28
1.8 Schematics of an individual (A) SWCNT, (B) MWCNT and (C) DWCNT.....	31
2.1 FRA 2 modulated $\mu$ -AUTOLAB Type III.....	39
2.2 An conventional electrochemical working set-up (A) and a centri- voltammetric set-up (B) relating with the triple electrode system.....	40
2.3 Centri-voltammetric cell; (A) whole cell, (B) parts of the cell.....	41
2.4 Schematic representation for the fabrication of a GSH biosensor.....	47
2.5 (A) Adsorption process, (B) the stages of centri-voltammetry.....	49
3.1 Cyclic voltammograms of 1 mM GSH at (a) for bare GCPE, (b) AuNp modified GCPE, and (c) AuNp and $\text{Al}_2\text{O}_3\cdot\text{TiO}_2$ nanopowder modified GCPE in 0.05 M PBS (pH 7.0) at a scan rate of $100 \text{ mVs}^{-1}$ .....	53
3.2 The different scan rates for 1.0 mM GSH at the AuNp/ $\text{Al}_2\text{O}_3\cdot\text{TiO}_2$ nanopowder/GCPE (A) in 0.05 M PBS (pH 7.0); a) 5, (b) 10, (c) 25, (d) 50, (e) 100, (f) 250, (g) 500, (h) 750, and (i) $1000 \text{ mVs}^{-1}$ . Inset: the curve of peak current ( $I_p$ ) vs $v^{1/2}$ .....	54

## LIST OF FIGURES (Continue)

<u>Figure</u>	<u>Page</u>
3.3	The SEM images of bare GCPE (a) with an accelerating potential of 10.00 kV, and AuNp/Al <sub>2</sub> O <sub>3</sub> .TiO <sub>2</sub> nanopowder/GCPE with different magnification of (b) 1.00 kx, (c) 2.00 kx, (d) 3.52 kx and acc. potential of 6.00 kV ..... 55
3.4	The QCM responses of differently modified sensors; (A) GSH aqueous solution, (B) Al <sub>2</sub> O <sub>3</sub> .TiO <sub>2</sub> /AuNp/GSH suspension..... 56
3.5	DP voltammograms of 250 μM GSH on the sensor response at different portions of Al <sub>2</sub> O <sub>3</sub> .TiO <sub>2</sub> nanopowder: a to f: 2, 4, 8, 10, 20 and 30%, respectively; conditions: PBS (0.050 M, pH 7.0), 20 μL AuNp ..... 57
3.6	The effect of optimum Al <sub>2</sub> O <sub>3</sub> .TiO <sub>2</sub> nanopowder curve of AuNp/Al <sub>2</sub> O <sub>3</sub> .TiO <sub>2</sub> nanopowder/GCPE..... 58
3.7	DP voltammograms of 250 μM GSH on the sensor response at different volumes of AuNp: (a) 1 μL, (b) 2 μL, (c) 5 μL, (d) 10 μL, (e) 20 μL, (f) 30 μL; conditions: 0.05M PBS (pH 7.0) ..... 59
3.8	The effect of AuNp amount for 250 μM GSH at AuNp/Al <sub>2</sub> O <sub>3</sub> .TiO <sub>2</sub> nanopowder/GCPE..... 60
3.9	DP voltammograms of 250 μM GSH on the sensor response at different pH ranges: (a) 6.0, (b) 6.5, (c) 7.0, (d) 7.5, (e) 8.0, (f) 8.5; conditions: 0.05M PBS, 20 μL AuNp ..... 61
3.10	The effect of pH (from 6.0 to 8.5) on current values for 250 μM GSH at AuNp/ Al <sub>2</sub> O <sub>3</sub> .TiO <sub>2</sub> nanopowder /GCPE ..... 62
3.11	Calibration graph for GSH at AuNp/Al <sub>2</sub> O <sub>3</sub> .TiO <sub>2</sub> nanopowder/ GCPE at lower concentration (A) and higher concentration (B), conditions: in 0.05 M PBS (pH 7.0), 25°C ..... 63
3.12	The effect of nano-micro TiO <sub>2</sub> amount on the sensor response ..... 65
3.13	The linear range of nano-micro TiO <sub>2</sub> /AuNp/GCPE..... 65



## LIST OF FIGURES (Continue)

<u>Figure</u>	<u>Page</u>
3.14 DP voltammetric responses of the 4% MWCNT/CPE with centri-voltammetry (a) background, (b) 400 $\mu$ M GSH, (c) a+ 1 mg silica gel, (d) c+ AuNp, in 0.05 M PBS (pH 7.0). Inset: A comparison of (a) bare CPE and (b) 4% MWCNT modified CPE for 400 $\mu$ M GSH including silica gel and AuNp.....	67
3.15 The centri-voltammetric responses of 4% MWCNT/ CPE for various amounts of silica gel added into 10 mL of solution; (a) 0.5 mg, (b) 1 mg, (c) 1.5 mg, (d) 2.0 mg, (e) 2.5 mg, 2 $\mu$ L AuNp, 0.05 M PBS (pH 7.0).....	69
3.16. The effects of silica gel amount added into 10 mL of cell solution containing 250 $\mu$ M GSH on the sensor response.....	70
3.17 The centri-voltammetric responses of 4% MWCNT/ CPE for various amounts of AuNp; (a) 10 $\mu$ L, (b) 20 $\mu$ L, (c) 30 $\mu$ L, (d) 40 $\mu$ L, (e) 50 $\mu$ L, 1 mg silica gel, 0.05 M PBS (pH 7.0) .....	71
3.18 The effect of AuNp amount for 250 $\mu$ M GSH on the sensor response ....	72
3.19 The effect of pH for 250 $\mu$ M GSH on the sensor response .....	72
3.20 The centri-voltammetric responses of 4% MWCNT/ CPE for different adsorption time; (a) 1 min, (b) 2 min, (c) 5 min, (d) 7 min, (e) 10 min, (f) 20 min, 1 mg silica gel, 30 $\mu$ L AuNp, 0.05 M PBS (pH 7.0).....	74
3.21 The effect of adsorption time for 250 $\mu$ M GSH on the sensor response ..	75
3.22 The effects of a) centrifugation time, b) centrifugation speed on the centri-voltammetric results obtained for 250 $\mu$ M GSH.....	76
3.23 DP voltammetric response curves of 4% MWCNT-modified CPE obtained for different concentration GSH. Inset: the linear range of GSH sensor .....	77
3.24 Electrodeposition of PtNps onto bare GCPE with cyclic voltammetry in 0.1 M KCl at 50 mV.s <sup>-1</sup> for 50 cycles.....	80

## LIST OF FIGURES (Continue)

<u>Figure</u>	<u>Page</u>
3.25 DP voltammetric responses of different concentration of GSH for (A) GSH-P <sub>x</sub> (immob)/PtNp/GCPE and (B) Chit/GSH-P <sub>x</sub> /PtNp/GCPE; for (A) (a) background, (b) 100 μM GSH:50 μM H <sub>2</sub> O <sub>2</sub> , (c) 250 μM GSH:125 μM H <sub>2</sub> O <sub>2</sub> (d) 500 μM GSH:250 μM H <sub>2</sub> O <sub>2</sub> , for (B) (a) background, (b) 100 μM GSH:50 μM H <sub>2</sub> O <sub>2</sub> , (c) 500 μM GSH:250 μM H <sub>2</sub> O <sub>2</sub> 0.05 M PBS (pH 7.0) .....	81
3.26 DP voltammetric responses of (a) GSH-P <sub>x</sub> immobilized Pt electrode, (b) GSH-P <sub>x</sub> (immob)/PtNp/GCPE for 100 μM GSH. Conditions: 0.05 M PBS (pH 7.5), GSH:H <sub>2</sub> O <sub>2</sub> =2:1 μM.....	82
3.27 DP voltammograms of (a) background for GSH-P <sub>x</sub> (immob)/GCPE, and in the presence of 100 μM GSH:50 μM H <sub>2</sub> O <sub>2</sub> at a (b) GSH-P <sub>x</sub> (immob)/GCPE, (c) PtNp modified GSH-P <sub>x</sub> (immob)/GCPE. Conditions: 0.05 M PBS (pH 7.0).....	83
3.28 Nyquist plots of the biosensing electrode response at different stages in the electrode assembly process: bare GCPE (X); GSH-P <sub>x</sub> /GCPE (■) and PtNp/GSH-P <sub>x</sub> /GCPE (▲). All spectra were recorded in the presence of 1 mM [Fe(CN) <sub>6</sub> ] <sup>3-/4-</sup> in 0.05 M PBS (pH 7.5), as a redox-active indicator. Frequency range: 10 <sup>4</sup> to 0.01 Hz, 0.05V amplitude .....	84
3.29 DP voltammetric responses of 100 μM GSH: 50 μM H <sub>2</sub> O <sub>2</sub> on the biosensor response at various enzyme amount: (a) 1.0 U, (b) 2.0 U, (c) 5.0 U, (d) 10.0 U, (e) 15.0 U; conditions: PBS (0.05M, pH 7.0), potential range of 0 V and +0.7 V.....	86
3.30 The effect of optimum enzyme amount curve of GSH-P <sub>x</sub> (immob)/PtNp/GCPE.....	87
3.31 DP voltammetric responses of different GSH/H <sub>2</sub> O <sub>2</sub> ratio on the biosensor response; (a) 0.1:1 GSH:H <sub>2</sub> O <sub>2</sub> , (b) 0.5:1 GSH:H <sub>2</sub> O <sub>2</sub> , (c) 1:1 GSH:H <sub>2</sub> O <sub>2</sub> , (d) 2:1 GSH:H <sub>2</sub> O <sub>2</sub> , (e) 5:1 GSH:H <sub>2</sub> O <sub>2</sub> , (f) 10:1 GSH:H <sub>2</sub> O <sub>2</sub> . Conditions: PBS system (0.05M, pH 7.0), [GSH]=50.0 μM, T=25°C ....	88
3.32 Effect of the GSH/H <sub>2</sub> O <sub>2</sub> ratio in the GSH biosensor performance .....	89

## LIST OF FIGURES (Continue)

<u>Figure</u>	<u>Page</u>
3.33 DP voltammetric responses of different pH values on the biosensor response; (a) pH 5.0, (b) pH 5.5, (c) pH 6.0, (d) pH 6.5, (e) pH 7.0, (f) pH 7.5, (g) pH 8.0. Conditions: phosphate buffer solution system (50 mM), GSH:H <sub>2</sub> O <sub>2</sub> =2:1 μM .....	90
3.34 The effect of the pH in the GSH biosensor performance.....	91
3.35 The linear range for the GSH biosensor .....	92
3.36 DP voltammetric response of the synthetic plasma sample for 25 μM GSH in 0.05 M PBS, GSH:H <sub>2</sub> O <sub>2</sub> =2:1 μM.....	94
3.37 DP voltammograms recorded with (A) GCPE+GSH-Px <sub>(immob)</sub> , (B) GCPE+4% Fe <sub>3</sub> O <sub>4</sub> Np+GSH-Px <sub>(immob)</sub> for different concentrations of GSH: (a) 100 μM GSH:50 μM H <sub>2</sub> O <sub>2</sub> , (b) 200 μM GSH:100 μM H <sub>2</sub> O <sub>2</sub> , (c) 400 μM GSH:200 μM H <sub>2</sub> O <sub>2</sub> , (d) 600 μM GSH:300 μM H <sub>2</sub> O <sub>2</sub> , (e) 800 μM GSH:400 μM H <sub>2</sub> O <sub>2</sub> , (f) 1mM GSH:500 μM H <sub>2</sub> O <sub>2</sub> in 0.05 M PBS (pH 7.0) .....	95
3.38 The biocentri-voltammograms of GCPE+GSH-Px <sub>(immob)</sub> for 50 μM GSH+25 μM H <sub>2</sub> O <sub>2</sub> ; (a) without centri, (b) with centri. Conditions: 0.05 M PBS (pH 7.0), V <sub>centr</sub> : 3000 rpm, t <sub>centr</sub> : 3 min.....	96
3.39 The centri-voltammograms recorded with GCPE+GSH-Px <sub>(immob)</sub> ; (a) centri-voltammetric background, (b) 100 μM GSH+50 μM H <sub>2</sub> O <sub>2</sub> , (c) 100 μM GSH+50 μM H <sub>2</sub> O <sub>2</sub> +1mg silica gel. Conditions: 0.05 M PBS (pH 7.0), V <sub>centr</sub> :3000 rpm, t <sub>centr</sub> :3min .....	97
3.40 DP voltammetric responses of the developed biosensor for 100 μM GSH:50 μM H <sub>2</sub> O <sub>2</sub> ; (a) no carrier material, (b) 0.5 mg Tenax, (c) 1 mg Silica gel, (d) 0.15 mg Activated Carbon in 0.05 M PBS (pH 7.5), t <sub>ads</sub> :5 min, t <sub>cent</sub> :3 min, V <sub>cent</sub> :3000 rpm .....	98
3.41 DP voltammetric responses of the developed biosensor (a) 100 μM GSH: 50 μM H <sub>2</sub> O <sub>2</sub> , (b) 1 mg Activated Carbon. 0.05 M PBS, t <sub>ads</sub> : 5 min, t <sub>cent</sub> :4 min, V <sub>cent</sub> :4000 rpm .....	98



**LIST of TABLES**

<u>Table</u>	<u>Page</u>
1.1 Chromatographic methods for bioanalysis of thiol compounds.....	17
1.2 Electrochemical bioanalysis of thiol compounds .....	24
1.3 Selected nanomaterials .....	27
1.4 Different functions of nanoparticles in electrochemical sensor systems.....	32
1.5 Gold nanoparticle-based electrochemical enzyme biosensors.....	34
3.1 A comparison of the analytical characteristics of differently modified electrochemical sensors for detection of GSH.....	63
3.2 A summary of the recent investigations for GSH detection strategies based on various types of methods .....	78
3.3 The comparison of analytical characteristics with reported on centri- voltammetry and biocentri-voltammetry .....	79
3.4 A comparison of the analytical characteristics of differently modified electrochemical biosensors for detection of GSH.....	92



## ABBREVIATIONS

<u>Abbreviation</u>	
AA	Ascorbic acid
AcCySH	<i>N</i> -acetylcysteine
ADH	Alcohol dehydrogenase
Al <sub>2</sub> O <sub>3</sub> .TiO <sub>2</sub>	Aluminum titanate
ASV	Anodic stripping voltammetry
AuNp	Gold Nanoparticle
BiFE	Bismuth Film Electrode
CE	Capillary electrophoresis
CNT	Carbon nanotube
cGPx	Cytosolic glutathione peroxidase
CPE	Carbon paste electrodes
CySH	Cysteine
DP	Differential-pulse voltammetry
DTNB	5,5'-dithiobis-(2-nitrobenzoic)-acid
DWCNT	Double-walled carbon nanotube
EC-CZE	Electrochemical detection-Capillary zone electrophoresis
EIS	Electrochemical impedance spectra
EMLC	Electrochemically modulated liquid chromatography
ESI-MS	Electrospray mass spectrometry
FCCa	Ferrocene carboxylic acid
Fe <sub>3</sub> O <sub>4</sub> Np	Fe <sub>3</sub> O <sub>4</sub> nanoparticles
FMN	Flavin mononucleotide
FPLC	Fast protein liquid chromatography
GCE	Glassy carbon electrode
GCPE	Glassy carbon paste electrode
GCS	γ-glutamylcysteine synthetase
GI-GPx	Glutathione peroxidase of the gastrointestinal system
GOx	Glucose oxidase
GS	Glutathione synthetase
GSH	Glutathione
GSSG	Glutathione disulfide
GSH-Px	Glutathione peroxidase
GR	Glutathione reductase
HCySH	Homocysteine

**ABBREVIATIONS (Continue)**Abbreviation

HMDE	Hanging mercury drop electrode
HPCE	High-performance capillary electrophoretic
HPLC	High-performance liquid chromatography
H <sub>2</sub> O <sub>2</sub>	Hydrogen peroxide
LC	Liquid chromatography
Met	Methionine
MO <sub>x</sub> Nps	Metal Oxide Nanoparticles
MRI	Magnetic resonance imaging
MS	Mass spectrometry
MTs	Metallothioneins
MWCNT	Multi-walled carbon nanotubes
NADPH	Reduced nicotinamide-adenine dinucleotide phosphate
Nps	Nanoparticles
OPA	o-phthaldialdehyde
PCs	Phytochelatins
Pen	d-penicillamine
pGP <sub>x</sub>	Plasma glutathione peroxidase
PG	Pyrolytic graphite
PHGP <sub>x</sub>	Phospholipid hydroperoxide glutathione peroxidase
PBS	Phosphate Buffer Solution
PtNp	Platinum Nanoparticles
PQQ	Pyrroloquinoline quinone
QCM	Quartz crystal microbalance
ROS	Reactive Oxygen Species
RSD	Relative standard deviation
SIM	Selected-ion-monitoring
SO <sub>x</sub>	Sulphydryl oxidase
SWCNT	Single-walled carbon nanotube
TP	Tiopronin
TRIS-HCl	Tris (hydroxymethyl)-aminomethane
Trp	Tryptophan
UV	Ultraviolet
XOD	Xanthine oxidase



## 1. INTRODUCTION

As a natural by-product the normal metabolism of oxygen produces the reactive oxygen species (ROS). ROS has unpaired electrons in the outer valence shell since they are highly reactive. Some environmental stress such as exposure to ultraviolet (UV) radiation or heat, contact with oxidative chemicals can cause an increment considerably to the concentrations of ROS. Levels of ROS are also connected with many diseases such as cancer, inflammation, cardiovascular disease, neurodegenerative disease, diabetes, age-related macular degeneration, and HIV infection (Huang et al., 2011).

Enhanced generation of ROS and impaired antioxidant detoxification cumulate into a situation known as oxidative stress. This will cause significant damage to cell structures and contributes to an imbalance between oxidative and reductive reactions. It is reflected in intracellular thiol redox status and extracellular thiol/oxidized thiol balance (Schafer and Buettner, 2001; Moriarty-Craige and Jones, 2004; Lee and Britz-McKibbin, 2009; Jones and Liang, 2009; Lee et al., 2010).

For that reason, it is important to establish the concentrations of individual thiols and oxidized thiols in diagnosis, monitoring the progression, and evaluating the treatment of the diseases mentioned above (Huang et al., 2011).

### 1.1. Thiols

The most reactive nucleophilic reagents are the thiols within all the biological components investigated. Several different forms of cysteine residue presents in vivo: reduced free thiol ( $-\text{SH}$  or  $-\text{S}^-$ ), thiyl radical ( $-\text{S}^\bullet$ ), disulfide ( $-\text{S}-\text{S}-$ ), sulfenic acid ( $-\text{SOH}$ ), sulfinic acid ( $-\text{SOOH}$ ), sulfonic acid ( $-\text{SOOOH}$ ), and S-glutathionylated and S-nitrosylated ( $-\text{SNO}$ ) forms. Thiols have unique chemical properties to take part in a variety of chemical redox reactions and the coordination of metals (Holmgren and Sengupta, 2010).

These properties make it a key residue in enzymatic catalysis, protein folding and trafficking, and reactive oxygen and nitrogen species signaling (Holmgren and Sengupta, 2010; Le Moan et al., 2008). Sulfur containing molecules are known to possess a variety of roles within physiological systems.

The biological aminothiols, such as cysteine (CySH), *N*-acetylcysteine (AcCySH), homocysteine (HCySH), and glutathione (GSH), are critical physiological components and widely occur in animal tissues and fluids (Figure 1.1). Especially, many biological and chemical systems introduce a crucial process related with the reversible oxidation-reduction reactions between thiols and the corresponding disulphides (Eq 1).

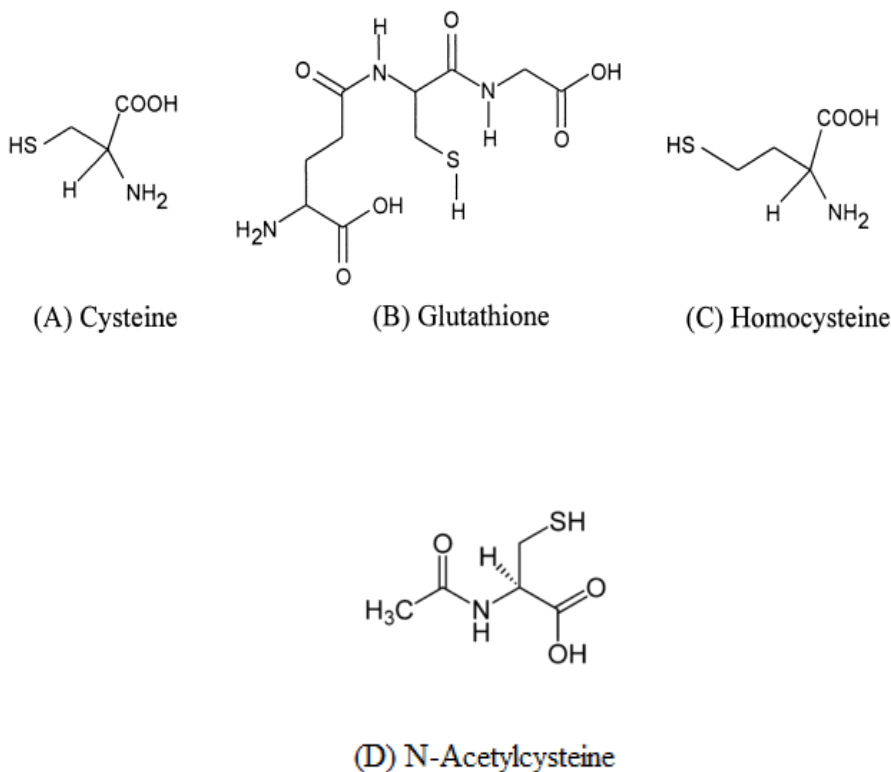
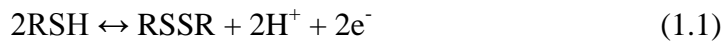


Figure 1.1 Structures of biological aminothiols

Thiols are the most essential indicator molecules in biological systems. For instance, when the increased homocysteine levels have been involved in coronary artery disease (McCully, 1996 and 1997), high levels of the disulfide cystine in the urine are characteristic of kidney dysfunction (Jocelyn, 1972). One of the key indicators is the ratio of glutathione (GSH) to glutathione disulfide (GSSG) for the redox status of cells and, thus, a marker for cellular oxidative stress (Meister and Anderson, 1983).

Thus, correct determination of the alterations in thiol levels supplies a vital comprehension into proper physiological functions or in the diagnosis of disease states (Inoue and Kirchhoff, 2000). For example, especially, premature arteriosclerosis, occlusive vascular and neurodegenerative disorders, leukemia, diabetes, and acquired immunodeficiency syndrome (AIDS) (Toyo'oka, 2009, White et al, 2002).

Moreover, cysteine-rich peptides, such as metallothioneins (MTs) and phytochelatins (PCs) are essential components to help for understanding their physiological roles. For instance, d-penicillamine (Pen) and tiopronin (TP) are also well studied as therapeutic pharmaceuticals which has sulfhydryl compounds in its structure (Toyo'oka, 2009).

### **1.1.1. Cysteine**

CySH is an amino acid which synthesized by the liver. It is implied in a diversity of significant cellular functions, including protein synthesis, detoxification, and a metabolic process. Although its biological importance is well-known, the level of CySH in physiological fluids, such as plasma and urine, has recently been documented as an important indicator for numerous clinical disorders (Toyo'oka, 2009).

### **1.1.2. N-acetylcysteine**

AcCySH also completely appears due to the acetylation in the kidney in human (Tsikas et al., 1998). The active site of AcCySH, which is sulfhydryl group, cooperates with the disulfide bonds of mucous glycoproteins by breaking the protein network into less viscous strand (Majima et al., 2002). It is known that AcCySH generally used mucolytic agent for management into respiratory tracts to loosen secretions. Moreover, AcCySH is usually implicated for the treatment acetoaminophen overdose. Administration of AcCySH has also been encountered in systemic sclerosis, HIV infection and septic shock (Atmaca, 2004; Failli et al., 2002; Galley et al., 1997; Toyo'oka, 2009).

### **1.1.3. Homocysteine**

Demethylation of methionine (Met) produces endogenous sulfhydryl-containing amino acids called HCySH. Under standard situations, the intracellular concentration of HCySH is retained low because of the re-methylation reactions to Met and catabolism via the trans-sulfuration pathway. Enzyme reactions control these alterations hereby 15-20 mmol HCySH are synthesized in humans each day. However most of them are exchanged to CySH or Met under the enzymatic control of cystathionine  $\beta$ -synthase or methionine synthase and methylenetetrafolate reductase.

Normal human plasma has concentration the total homocysteine in the range between 5 and 15  $\mu$ M. Therefore, the concentration greater than 15  $\mu$ M for elevated plasma may be the consequence of inherited disorders corresponding metabolism. During the last decade, the improvement in the detection of HCySH has rapidly developed in physiological fluids. Recent studies demonstrate that altered levels of HCySH in plasma (hyperhomocysteinemia) may be significant risk factor and an indicator for certain diseases including cardiovascular disease (Toyo'oka, 2009).

#### 1.1.4. Glutathione

Reduced glutathione ( $\gamma$ -L-glutamyl-L-cysteinylglycine, GSH), a tripeptide, is the most abundant non-protein thiol in biological systems and occurs in various cells of animals, plants and bacteria. It is reported that GSH can be taken from diet or can be synthesized *de novo* in the liver.

Recently, GSH has been encountered in biological processes such as catabolism, metabolism, transport and altered levels of GSH in plasma have been implicated in a number of pathological conditions including macular degeneration, diabetes, Alzheimer's, Parkinson's and HIV diseases (Toyo'oka, 2009; Meister and Anderson, 1983). It is an important antioxidant that detoxifies reactive oxygen and drug metabolites (Chen et al., 2006; Raouf et al., 2009). In such cases, two GSH molecules form a molecular of oxidized glutathione (GSSG) via the formation of double-sulfur bond (Chen et al., 2006). Intracellularly, it is found in millimolar concentrations, plasma and urine containing lower tGSH levels. The intracellular level of glutathione is much greater than that of cysteine and cystine. Therefore, GSH serves as a storage form of cysteine moieties (Pastore et al., 2003; Meister and Larsson, 1989). The total glutathione can be present as free or bound to proteins in cells.

Free GSH is present mainly in its reduced form, which can be converted to the oxidized form during oxidative stress. It can be reverted to the reduced form by the action of the enzyme glutathione reductase. The relative amounts of the reduced and oxidized forms of glutathione (GSH/GSSG) show the redox status which is a critical determinant in cell and some disease.

The glutathione redox couple is present in concentrations range between 1 and 10 mM for mammalian cells under standard conditions by means of the reduced GSH predominating over the oxidized form (Pastore et al., 2003; Chai et al., 1994). Glutathione is composed of two characteristic structural features: a  $\gamma$ -glutamyl linkage and a sulphydryl group. These moieties of the tripeptide make possible its participation in a fascinating number and diversity of functions.

It can be said that glutathione contributes in transhydrogeneration reactions which involved in the formation. It participates in conservation of the sulphydryl groups of other molecules, such as coenzyme A, various enzymes and proteins.

Minimizing capacity of the formation of deoxyribonucleotides by ribonucleotide reductase and the reduction of dehydroascorbate to ascorbate is reduced by glutathione. Glutathione has a role in the detoxification of hydrogen peroxide, other peroxides and free radicals. Several xenobiotics collaborate with glutathione so that GSH contributes in the detoxification of these xenobiotics. They are eventually excreted in the urine or feces in the form of mercapturic acids (Pastore et al., 2003; Meister and Larsson, 1989).

#### **1.1.4.1. Biochemistry of GSH**

The intracellular level of GSH is changed in the range of the millimolar level (0.5-10 mM) in mammalian cells while micromolar concentration is characteristically present in plasma. Mitochondria contains a small proportion of the total cellular GSH pool, which is about 10-15%, and it reaches a concentration similar to that found in the cytosol (Pastore et al., 2003; Griffith and Meister, 1985).

GSH is synthesized in the cell by the sequential actions of  $\gamma$ -glutamylcysteine synthetase (GCS) and glutathione synthetase (GS) in a series of six-enzyme-catalysed reactions (Pastore et al., 2003; Meister 1973; Meister and Anderson, 1983). This process given in Figure 1.2 was termed as the  $\gamma$ -glutamyl cycle.

GSH can be readily oxidized to its disulfides (GSSG). Consequently, the ratio of both forms is critical for the characterization of the oxidative stress in living systems. GSH contributes in the defense against free radicals and ROS induced during metabolism.

GSH prevents formation of free radicals and detoxifying cells which conserves the living cells against hypoxia, toxicity, mutagenicity or transformation by radiation and carcinogens. GSH also has a role for the inactivation of some exogenous compounds such as drugs and pollutants.

The altered levels of GSH in physiological liquids have been linked to specific pathological conditions and closely associated with several human diseases, especially premature arteriosclerosis, occlusive vascular leukemia, diabetes, AIDS and cataracts (Toyo'oka, 2009; Roederer et al., 1992; Meister, 1994).

The diagnosis of several human diseases exhibits that it is important for the determination of aminothiols in physiological fluids. These facts speed up the research of the measurement of the aminothiols in biological models and the development of highly sensitive and selective methods for analysis. Since the biological thiols is required for high detection sensitivity (Toyo'oka, 2009) they have no specific physicochemical properties (e.g., strong absorption in UV-VIS regions or native fluorescence).

Moreover, the measurement of thiols has to be careful owing to their instability in aqueous medium and their affinity to oxidize to disulfides. In addition, since the extraction of these thiols from biological matrices difficult, they are generally highly polar and water soluble. As a result, the fields of biological and clinical sciences require a robust method (Toyo'oka, 2009).

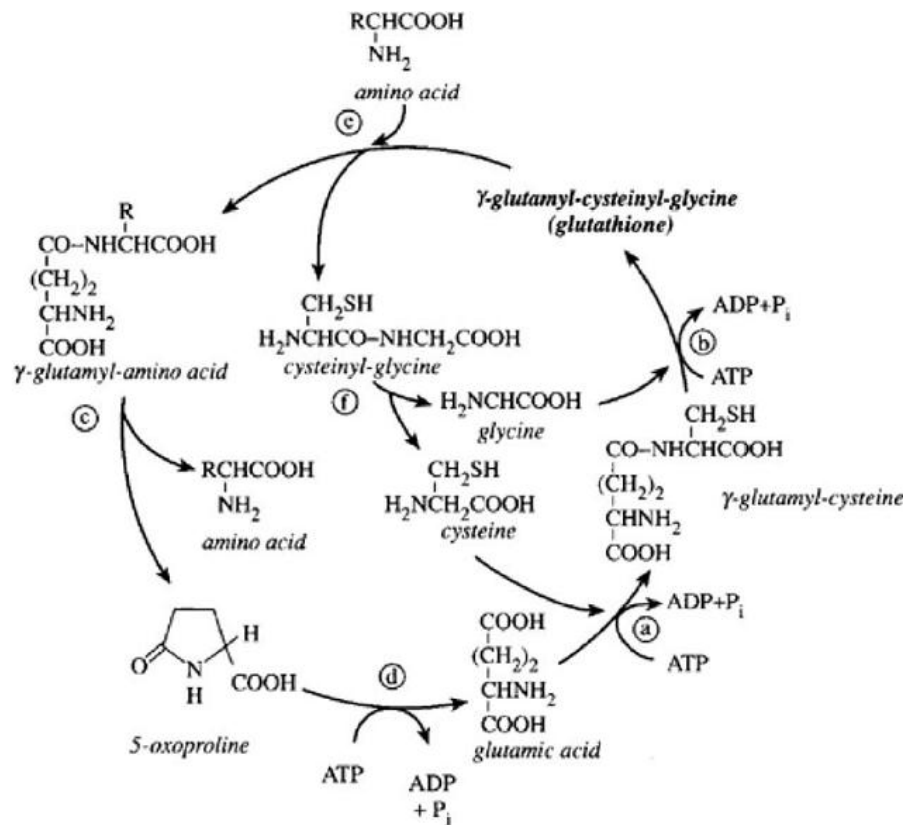


Figure 1.2. Glutathione synthesis and metabolism. (a) Glutamylcysteine synthetase; (b) glutathione synthetase; (c) g-glutamyl cyclotransferase; (d) oxoprolinase; (e) g-glutamyl transpeptidase; (f) peptidase (Pastore et al., 2003).

#### **1.1.4.2. Enzymatic mechanism of GSH**

Glutathione peroxidase (GSH-Px) and glutathione reductase (GR) are the main enzymes that participate in the GSH metabolism. They have substantial function such as, GSH-Px plays an essential role in the removal of hydrogen peroxide (H<sub>2</sub>O<sub>2</sub>) and lipid peroxides from the cells, while the GR regulates the ratio of reduced and oxidized glutathione in erythrocytes (Meister and Anderson, 1983; Matés et al., 2000; Rover Jr. et al., 2001). These enzymes raised up a scavenging of oxyradical products in tissues, minimizing damages caused by these species working together with catalase and superoxide dismutase (Matés et al., 1999).

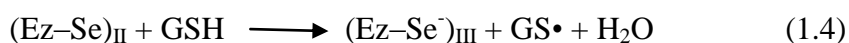
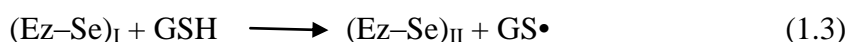
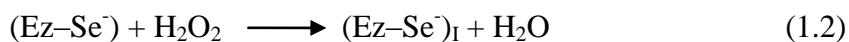


GSH-Px belongs to the family of selenoproteins gradually (Lehmann et al., 2001; Scheller et al., 2002) containing selenocysteine in the catalytic centre (Ip et al., 1991) and are the most extensively studied selenoproteins (Flohé, 1989). The function of many of the selenoproteins discovered is still unknown.

Glutathione peroxidases have four different types of classes which are the cytosolic or classical glutathione peroxidase (cGPx), phospholipid hydroperoxide glutathione peroxidase (PHGPx), extracellular or plasma glutathione peroxidase (pGPx), and a glutathione peroxidase of the gastrointestinal system (GI-GPx). All GSH-Px takes place in the hydroperoxide metabolism and oxidative defense system which reduces hydroperoxides like H<sub>2</sub>O<sub>2</sub>, organic hydroperoxides and fatty acid hydroperoxides with the consumption of GSH (Lehmann et al., 2001; Scheller et al., 2002). PHGPx is a monomeric enzyme of 18 kDa. PHGPx, one of the types of glutathione peroxidases, is able to decrease hydroperoxides of complex lipids like phospholipids and cholesterol even when they are positioned in biological membranes (Thomas et al., 1990). Thus, it can defend bio-membranes from oxidative damage. The cGPx has a function of antioxidant device as can be deduced from studies of cGPx knock-out mice (Cheng et al., 1998). The other glutathione peroxidases have further functions.

One of the roles of PHGPx is the regulation of lipoxygenase activities and it also has an essential role in sperm maturation (Ursini et al., 1999). Brigelius-Flohé (1999) reported that tissue-specific functions of the individual glutathione peroxidases have been reviewed recently. The catalytic activity of glutathione peroxidases effects from the redox reaction of selenium which is integrated into the polypeptide chain as selenocysteine. Along with tryptophan and glutamine selenocysteine generates the catalytic triade as has been shown by site directed mutagenesis (Maiorino et al., 1995; Lehmann et al., 2001). According to Lehmann et al. (1998) the catalytic reaction involves the reduced enzyme, which reacts chemically as a selenolate (Ez-Se<sup>-</sup>) with the H<sub>2</sub>O<sub>2</sub> leading, to an activated enzyme (Eq. (2)).

Since the oxidized enzyme needs to be reduced to maintain its activity, it may be performed by an electron donor species like GSH or electrochemically as shown in scheme where  $(Ez-Se)_I$  and  $(Ez-Se)_{II}$  are the enzyme oxidized intermediates, GSH a reducing substrate and  $GS\cdot$  a free radical (Rover et al., 2001).



In the first step, the enzyme reduces the hydrogen peroxide with formation of an enzyme intermediate compound. Then, the oxidized enzyme can be reduced to the native form in two steps. On the other hand, this mechanism is not totally figure out and the different oxidation states of the GSH-Px enzyme have not been decisively recognized (Lehmann et al., 1998). After the enzyme initial activation by hydrogen peroxide, the mechanism can be better realized when GSH renews the enzyme in two steps (Figure 1.3).

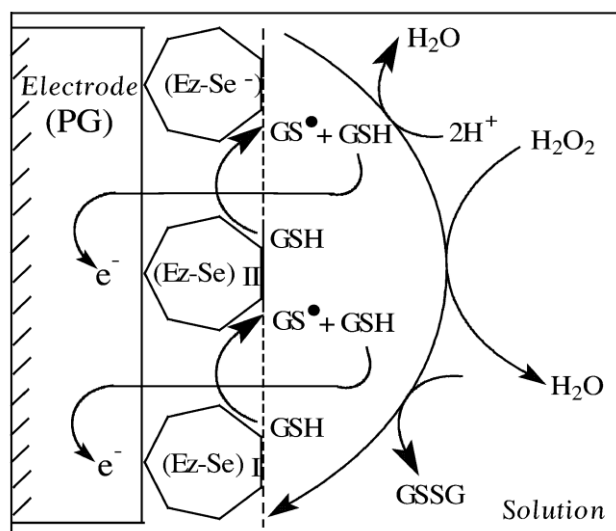


Figure 1.3. The pathways of GSH-Px enzyme (Rover et al., 2001)

A number of methods including Ellman's method (Ellman, 1959), have been reported in the literature for GSH analysis. Ellman's method is the most commonly used assay in biological samples (Ellman, 1959). This method depends on the reaction between GSH and 5,5'-dithiobis(2-nitrobenzoic acid) producing 2-nitro-5-mercapto-benzoic acid, which is monitored spectrophotometrically at 410 nm. This test is not sensitive concerning the other techniques since it is inexpensive and easy to use.

Other methods include high-performance liquid chromatography (Buchberger et al., 1987; Fukunaga et al., 1998; Parmentier et al., 1998; Shi et al., 1999), spectrofluorimetry (Chen et al., 1999), spectrophotometry (Besada et al., 1989; Raggi et al., 1991) and potentiometry (Compagnone et al., 1991). These techniques are not suitable in many cases since a rapid and accurate method for GSH determination is needed and they often require extraction and pre-concentration steps. The interference problems can be encountered because they are less susceptible.

Because of its high sensitivity, voltammetric methods have been applied extensively for GSH detection in the last two decades (Wring et al., 1989; Kulys and Drungiliene, 1991; Nalini and Narayanan, 1998; Kinoshita et al., 1999). Enzymatic methods based on GSH-Px (Mannervik, 1985; Lehmann et al., 1998; Rover Jr. et al., 2001) immobilized onto an electrode surface (Hua et al., 1991; Wring et al., 1992; Carsol et al., 1996) or in-column reactors (Satoh et al., 1988; Satoh et al., 1991; Compagnone et al., 1994) have also been utilized for determination of GSH.

The enzyme catalyzes the oxidation of GSH to the disulfide form (GSSG) in the presence of hydroperoxides ( $\text{H}_2\text{O}_2$  or  $\text{ROOH}$ ), as shown below: (Rover Jr. et al., 2001).



Spectrophotometric assays can be monitored by the consumption of GSH via the absorbance decrease, using the Ellman's reagent (Smith et al., 1988; Austin et al., 1988), or the formation of GSSG by its combination with the reaction catalyzed by glutathione reductase while the NADPH (reduced nicotinamide-adenine dinucleotide phosphate) oxidation is recorded spectrophotometrically or fluorimetrically (Smith et al., 1988; Rover et al., 2001). It is also known that spontaneous GSH oxidation can take place under conditions, especially in the presence of hydrogen peroxide (Wring et al., 1992; Rover et al., 2001).

GSH was oxidized (0.1 mmol/L solution) directly onto the bare pyrolytic graphite (PG) electrode with consecutive additions of peroxide in phosphate buffer at pH >8.0 in the absence of GSH-Px enzyme (Rover et al., 2001). There are some disadvantages that are needed to be overcome for the direct electrochemical oxidation of GSH at unmodified traditional electrodes. These can be described as slow electron transfer reaction of GSH which requires high working potential and strong adsorption of GSH at the surface of metallic electrode that makes GSH detection harder (Chen et al., 2006; Liu et al., 2010).

Rover et al. (2001) reported that there is no GSH electrooxidation even when more peroxide was added into the solution at pH values <8.0, thus it is suggested that the GSH oxidation process was pH dependent. These results are very similar to those obtained by Hua et al. who investigated the GSH oxidation (Hua et al., 1991). They established a peak concerning to hydrogen peroxide oxidation which appears at a potential of 0.88 V vs. SCE (pH 7.0) in phosphate buffer. It is observed that the reaction between GSH and hydrogen peroxide permitted GSH measurement by the electrooxidation through the enzymatic reaction catalyzed by the immobilized GSH-Px (Rover et al., 2001).

## **1.2. Methods Developed for Thiolic Compound Analysis**

### **1.2.1. Spectrophotometric assay**

For a long time, since 1959, there have been various papers which are reported on sulphhydryl compounds and glutathione determination in biological samples. Aside from the spectrophotometric determinations, Owens and Belcher (1965) discovered the most popular assay which is the enzymatic recycling reaction, to determine glutathione concentrations and Tietze (1969) developed this method (Pastore et al., 2003). The determination of total glutathione is allowed by this method and it is more sensitive than those available with the spectrophotometric method using Ellman's reagent. In fact, it uses the yeast GR to reduce GSSG to GSH, and the Ellman's reagent, 5,5'-dithiobis-(2-nitrobenzoic)-acid (DTNB) to measure the absorbancy change at 412 nm (Pastore et al., 2003).

### **1.2.2. Fluorometric assay**

Cohn and Lyle (1966) described a fluorometric assay for reduced glutathione based on the reaction between o-phthaldialdehyde (OPA) and amino acids, and it could be utilized for the assay of submicrogram amount of amino acids in biological tissues. Hissin and Hilf (1976) modified this method allowing the determination of both reduced and oxidized glutathione. OPA is used as the fluorescent reagent by this method, so a highly fluorescent derivative is produced by binding the free thiol group of glutathione. Hissin and Hilf (1976) described the similarities between the GSH and GSSG procedures which allow for minimal alteration of sample preparation, assay conditions and instrumentation. The poor specificity is the major disadvantage of this method owing to significant interference by amino acids and other thiols (Pastore et al., 2003).

### **1.2.3. Bioluminescence assay**

Romero and Mueller-Klieser (1998) developed the bioluminescence assay of reduced glutathione and they reported that the biochemical principle is the chemiluminescence of bacterial luciferase. GSH is coupled to the NADP/NADPH+H<sup>+</sup> redox system throughout specific enzymes. The redox system can then be united in a quantitative method to bacterial luciferase via flavin mononucleotide (FMN). Each substance that can be quantitatively coupled to NADP/NADPH+H<sup>+</sup> may be analyzed, thus this enzymatic cascade presents flexibility.

This assay involves small liquid sample and can be utilized in a wider range of GSH concentrations. Its semi quantitative feature is the major drawback of the assay and the disulphide form cannot be detected (Pastore et al., 2003).

### **1.2.4. Capillary electrophoresis**

Capillary electrophoresis (CE) has a highly efficient, ultra small-volume analytical separation technique for the analysis of charged species even in single cells. Piccoli et al. (1994) first explained a high-performance capillary electrophoretic method (HPCE) which provides the simultaneous determination of red blood cells reduced and oxidized glutathione at femtomole levels with a simple Microcon-10 membranes extraction procedure. Lately, a capillary zone electrophoretic method with electrochemical detection (EC-CZE) for glutathione determinations was performed by Jin et al. (2000) in a single red blood cell.

In this assay, the whole cell is injected into a separation capillary and no derivatization or handling of the intracellular fluid is required. Therefore, the quantification of GSH is independent from sample preparation or derivatization. However, the disadvantage of this method compared to the other CE methods is that oxidized glutathione cannot be determined (Pastore et al., 2003).

### **1.2.5. Chromatographic methods**

The selective and sensitive determinations of thiols can be applied by using some popular separation methods which are liquid chromatography (LC) and capillary electrophoresis (CE). A variety of separation and detection techniques, such as GC–MS, LC–MS, LC–ECD, LC–UV, LC–FL, CE–UV and CE–LIF, can probably be employed for the detection of thiols in biological samples.

Various techniques have been utilized to analyze the thiols but there are still some problems which are about the operation of sophisticated instrumentation and/or the complexity of the procedure. It can be said that the approach based on derivatization and separation followed by FL detection is the most frequently used method for the thiol determination due to the high selectivity and sensitivity (Toyo'oka, 2009). Table 1.1 summarizes the chromatographic methods for bioanalysis of thiol compounds.

#### **1.2.5.1. High-performance liquid chromatographic methods**

Recently, the high-performance liquid chromatography (HPLC) is extensively popular in detection of glutathione and related thiols in biological samples. A rapid, highly specific, sensitive (of the order of 0.5 pmol) and reproducible are the properties of HPLC techniques. The selection of appropriate column, derivatization and elution protocols and detection system achieves the simultaneous determination of GSH and other thiols in a single assay (Pastore et al., 2003). HPLC with electrochemical detection stands for an essential device for the analysis of electroactive compounds, including thiols and disulphides, glutathione.

Firstly, Hg pool electrodes were utilized for the determination of glutathione and other thiols (Rabenstein and Saetre, 1977). When a dual Au/Hg amalgam thin layer electrode was developed for the simultaneous determination of glutathione and cysteine, and their respective disulphides (Allison et al., 1984), this method was later simplified and enlarged as well.

Richie and Lang (1987) modified the method of Allison, allowing the determination of a wide range of biologically important thiols and disulphides, and its application in biological samples. Saitoh et al. (2006) introduced the electrochemically modulated liquid chromatography (EMLC) to enhance the separation selectivity of HPLC (Monostori et al., 2009). EMLC works by altering retention through changes in the potential applied to the conductive stationary phase (Saitoh et al., 2008).

Although EMLC potentially suitable for the determination of GSH and GSSG, it has not yet been accepted. Only three recent HPLC methods have employed UV absorbance via detection.

Hansen et al. (2007) measured protein thiols and dithiols in picomolar amounts by using 4-DPS as a derivatizing agent. Vignaud et al. (2004) analyzed disulphides generated from the oxidation of GSH and Cys by using RP-HPLC connected with either direct UV absorbance or ECD (coulometric) detection. Size exclusion was previously executed on a fast protein liquid chromatography (FPLC) system so as to avoid derivatization. ECD was established to supply sensitivity 100 times higher for the disulphides than UV absorbance at 220 nm for underivatized samples. This method allowed the determination not only of GSH, Cys and their symmetric disulphides, but also of their mixed disulfide, GSSG (Vignaud et al., 2004; Monostori et al., 2009).

### **1.2.5.2. Gas chromatography-mass spectrometry**

Capitan et al. (1999) explained that blood or plasma is reduced with dithiothreitol, deproteinized with sulfosalicylic acid, derivatized with ethyl chloroformate, and extracted with diethyl ether in the GC-MS method for analysis of glutathione in biological samples (Pastore et al. 2003; Capitan et al., 1999).

Capillary GC-MS in the selected-ion-monitoring (SIM) mode separated and quantified the *N,S*-ethoxycarbonyl methyl ester derivatives of glutathione and other thiols.



Table 1.1. Chromatographic methods for bioanalysis of thiol compounds (Toyo'oka, 2009)

Analyte	Method	LOD	Reference
Homocysteine (total)	CZE-UV derivatization with CMQT	1.0 $\mu$ M (total)	Kubalczyk et al, 2006
Cysteine, homocysteine, glutathione, cysteineglycine	RP LC-UV derivatization with CMQT	0.1-0.3 nmol/mL (red.) 0.1-2 nmol/mL (total)	Bald et al, 2004
Cysteine (total)	CE-MEKC/UV derivatization with DPDS	2.5 $\mu$ M (total)	Sevcikova et al, 2003
Homocysteine (total)	CE-MEKC/UV derivatization with DPDS	6 $\mu$ M (total)	Sevcikova et al, 2003.
Cysteine, homocysteine, glutathione (reduced and total)	RP LC/ESI-MS (SIM) derivatization with CMQT	3-15 pmol	Guan et al, 2003
Glutathione (total)	CE-MEKC/UV derivatization with DPDS	5 $\mu$ M (total)	Glatz et al, 2000
Cysteine, homocysteine, glutathione, N-acetylcysteine	RPLC/FL derivatization with IAB	1-2 nM	Wang et al, 2004
Cysteine, homocysteine, glutathione (total)	RP LC/FL derivatization with MIAC	1-2 pmol	Benkova et al, 2008
Homocysteine (total)	CE/LIF derivatization with 6-IAF	50 pM	Cause et al, 2000
Cysteine, homocysteine, cysteinylglycine, glutathione (reduced and total)	CE/LIF derivatization with 5-IAF	100-200 pM	Carru et al, 2004
Glutathione	RP LC/FL derivatization with SBD-F, ABD-F, DBD-F	1-3 pmol	Toyo'oka et al, 2001
Cysteine, homocysteine, cysteinylglycine, glutathione (total)	RP LC/FL derivatization with SBD-F		Nolin et al, 2007
Homocysteine (total)	RP LC/FL derivatization with mBBr	2,4 pmol	Chou et al, 2001
Glutathione (reduced and oxidized)	RP LC/FL derivatization with OPA (pre-label)	5.6 14 fmol	Kand'ar et al, 2007

LOD: Limit of Detection, CE: Capillary Electrophoresis, MS: mass spectrometry, FL: fluorescence, UV: ultraviolet, LC: liquid chromatography, RP: Reversed phase, dBBr: dibromobimane, mBBr: monobromobimane, CMQT: 2-chloro-1-methylquinolinium tetrafluoroborate, CZE: capillary zone electrophoresis, DPDS: 2,2-Dipyridylsulfide, DTNB: 5,5'-dithiobis(2-nitrobenzoic acid) (Ellman's reagent), IAB: 3-iodoacetylaminobenzanthrone, 5- or 6-IAF: (5 or 6-iodoacetamidofluorescein), LIF: laser induced fluorescence, MEKC: micellar electrokinetic chromatography, MIAC: *N*-(2-acridonyl) maleimide, OPA: ortho-phthalaldehyde, SBD-F: ammonium 7-fluoro-2,1,3-benzoxadiazole-4-sulfonate, DBD-F: 4-(*N,N*-dimethylaminosulfonyl)-7-fluoro-2,1,3-benzoxadiazole, ABD-F: 4-(aminosulfonyl)-7-fluoro-2,1,3-benzoxadiazole.

Although, high sensitivity and specificity are attractive features, lack of total automation and the relatively high cost of the equipment are the major disadvantages of this method (Pastore et al., 2003).

### **1.2.5.3. Liquid chromatography-mass spectrometry**

Tsikis et al. (2000) reported that mass spectrometry (MS) is a useful technique for the analysis of low-molecular-mass thiols, together with GSH and S-nitrosothiols. In recent times, two liquid chromatographic methods linked with electrospray mass spectrometry (ESI-MS) for the concurrently determination of GSH and GSSG in blood mononuclear cells (Camera et al., 2001) and in liver (Norris et al., 2001) have been explained. In the HPLC–ESI-MS method described by Camera et al. (2001), the samples are injected into a diol column, isocratic eluted and detected by the ESI-MS system.

Prior to the injection, the derivatization with NEM, which prevents GSH auto-oxidation, and the addition of thiosalicylic acid as internal standard and the extraction by acetonitrile steps are applied. The major disadvantages of these methods are the lack of total automation and the relatively high cost of the equipment when compared to the other described methods (Pastore et al. 2003).

### **1.2.6. Electrochemical techniques**

Electroanalytical techniques deal with the interaction between electricity and chemistry, that is, the measurements of electrical quantities, such as current, potential, or charge and their relationship to chemical parameters. Such use of electrical measurements for analytical purposes has found a huge range of applications, including environmental monitoring, industrial quality control, or biomedical analysis (Wang, 2006).

Some advances since the mid-1980s, consisting of the development of ultra microelectrodes, the design of tailored interfaces and molecular monolayer, the coupling of biological components and electrochemical transducers, the synthesis of ionophores and receptors containing cavities of molecular size, the development of ultra trace voltammetric techniques or of high-resolution scanning probe microscopies, and the micro fabrication of molecular devices or efficient flow detectors, have prevented to a considerable increase in the popularity of electroanalysis and to its development into new phases and environments (Wang, 2006).

**Differential-pulse (DP) voltammetry** is a notably helpful technique for measuring trace levels of organic and inorganic species. In DP voltammetry, fixed magnitude of pulses superimposed on a linear potential ramp is applied to the working electrode just before the end of the drop (Figure 1.4).

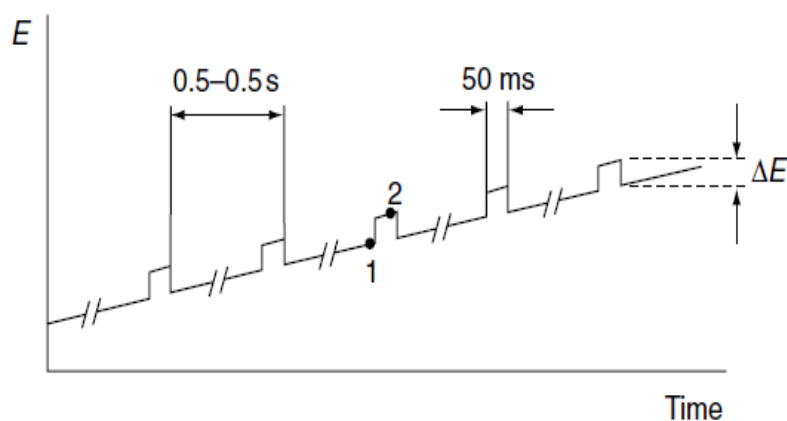


Figure 1.4. Excitation signal for DP voltammetry (Wang, 2006)

As shown in the figure, the current is sampled just before the pulse application (at 1) and again late in the pulse life (after ~40ms, at 2, when the charging current has decayed). The current difference [ $\Delta i = i(t_2) - i(t_1)$ ] is plotted against the applied potential. The resulting DP voltammogram consists of current peaks in which the height is directly proportional to the concentration of the corresponding analyte and the peak potential ( $E_p$ ) can be used to identify the species (Wang, 2006).

The differential-pulse operation produces in a very efficient modification of the charging background current. Therefore, DP voltammetry has sensitivity for metal ions and electroactive substances as low as  $10^{-8}$  M (about 1  $\mu\text{g/L}$ ).

*Cyclic voltammetry* is the most extensively utilized technique for gaining qualitative information about electrochemical reactions. The power of cyclic voltammetry arises from its ability to give information on the thermodynamics of redox processes and the kinetics of heterogeneous electron transfer reactions and on coupled chemical reactions or adsorption processes.

Cyclic voltammetry is often the first experiment executed in an electroanalytical study as it suggests a rapid location of redox potentials of the electroactive species, and suitable evaluation of the effect of media on the redox process (Wang, 2006).

Cyclic voltammetry includes scanning linearly the potential of a stationary working electrode (in an unstirred solution), using a triangular potential waveform. During the potential sweep, the potentiostat measures the current resulting from the applied potential and the resulting plot is termed a cyclic voltammogram.

The cyclic voltammogram comprises single or multiple scans depending on the research and time-dependent function of a large number of physical and chemical parameters (Wang, 2006). It is supposed that only the oxidized form O is present at the beginning. Thus, a negative-going potential scan is chosen for the first half-cycle, starting from a value where no reduction occurs. Since the applied potential comes up the characteristic  $E^\circ$  for the redox process, a cathodic current begins to increase, until a peak is reached.

After traversing the potential region in which the reduction process occurs (at least  $90/n$  mV beyond the peak), the direction of the potential sweep is reversed.

During the reverse scan, R molecules (generated in the forward half-cycle, and accumulated near the surface) are reoxidized back to O, resulting in an anodic peak (Wang, 2006).

Certainly, electrochemical probes offer a major share of the interest in the development of chemical sensors. On the contrary to many chemical measurements, which involve homogeneous bulk solutions, electrochemical processes occur at the electrode-solution interface. The difference between various electroanalytical techniques reveals the type of electrical signal used for the quantitation.

Potentiometric and potentiostatic are the two principal types of electroanalytical measurements. Both types need at least two electrodes (conductors) and a contacting sample (electrolyte) solution, which comprise the electrochemical cell. The electrode surface is thus a connection between an ionic conductor and an electronic conductor.

One of the two electrodes responds to the target analyte and is thus termed the *indicator* (or *working*) electrode (Wang, 2006). The second one, termed the *reference* electrode, is of constant potential which also means independent of the properties of the solution (Figure 1.5).

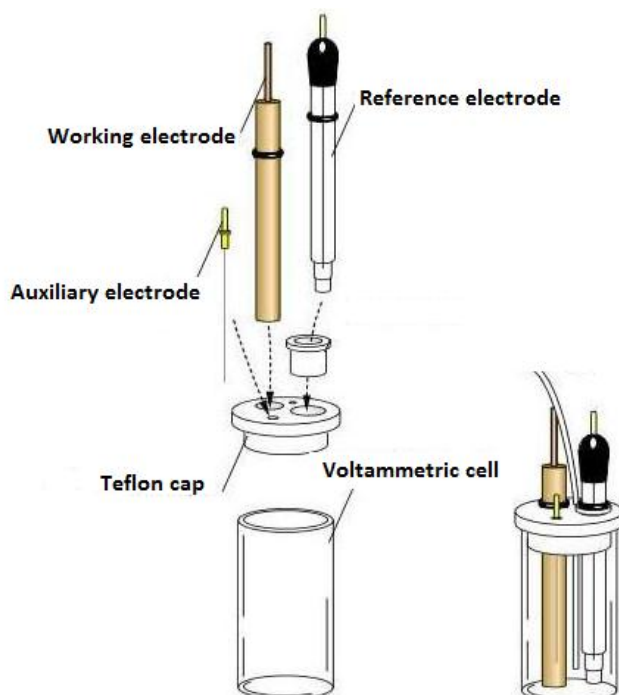


Figure 1.5. Schematic diagram of a voltammetric cell

([http://www.bio-logic.info/potentiostat/glassware\\_cells.html](http://www.bio-logic.info/potentiostat/glassware_cells.html))

Electrochemical techniques are particularly suited to the analysis of organo-sulfur compounds (Simonet, 1993; Chambers, 1978). Simple procedures, fast response and the development in the surface modifications conspire to favor the use of electroanalytical devices (Stulik, 1999). Table 1.2 summarizes the electrochemical bioanalysis of thiol compounds.

Kizek et al. (2004) developed a linear sweep cyclic voltammetry method at hanging mercury drop electrode (HMDE) as a working electrode, which is polarized between potential range between -0.2 and -0.8 V for the measurement of GSH and GSSG. The surface area of the working electrode was  $0.4 \text{ mm}^2$ ; Ag/AgCl/3M KCl served as a reference electrode, and Pt wire as an auxiliary electrode (Monostori et al., 2009; Kizek et al., 2004). It is known that a glassy carbon electrode (GCE) is a good material for modification, and the attachment of carbon nanotube (CNT) layers ends up in an electrode with well-known detection possibilities (Rivas et al., 2007).

It should be noted that CNT-modified GCEs do not primarily serve as stand-alone detectors, but rather as ECDs after chromatographic separations and transducers of the biorecognition event in biosensors for the analysis of biological samples (Rivas et al., 2007; Salimi and Hallaj, 2005).

The preparation of a preheated GCE modified with multi-wall CNTs (MWCNT) and its use in the detection of GSH, Cys and thiocytosine was reported by Salimi and Hallaj (2005). The electrocatalytic oxidation of 14 thiols, containing GSH, HCys, Cys and NAC, was tested by Han and Tachikawa (2005) at a GCE coated with a single-wall CNT (SWCNT) film. When increased catalytic features of this electrode compared with bare GC and diamond electrodes, it was further developed by its modification with pyrroloquinoline quinone (PQQ) (Han and Tachikawa, 2005).

Salimi and Pourbeyram (2003) constructed a renewable three-dimensional sol-gel CCE chemically modified with  $\text{Ru}[(\text{tpy})(\text{bpy})\text{Cl}]\text{PF}_6$  and used for the amperometric detection of GSH and Cys. This modified electrode provided the advantages of high sensitivity, a short response time and long-term stability (Monostori et al., 2009).

Table 1.2. Electrochemical bioanalysis of thiol compounds (White et al., 2002)

Analyte	Method	LOD ( $\mu\text{M}$ )	Reference
GSH	D-DPV	160	Hua et al, 1991
GSH	D	0.867	Wring et al, 1991
GSH	D-CSV	0.0004	Le Gall et al, 1993
CSH, GSH	D	N/S	Zhao et al, 1993
CSH	D-CSV	nM	Von Wandruska et al, 1993
CSH GSH	D-CCSV	0.001 0.010	Banica et al, 1994
CSH	D-CCSV	0.001	Banica et al, 1994
HCSH CSH GSH	CE	0.5 1 5	Huang et al, 1995
GSSG	D-CCSV	0.008	Banica et al, 1995
CSH, GSH	CE-PED	0.5	Owens et al, 1997
CSH	D-PED	0.1	Johll et al, 1997
CSH	Ind-CV	N/S	Lawrence et al, 2000
CSH	Ind-SWV	4	Hignett et al, 2001
CSH, GSH, HCSH	Ind-CV	6 1 7	Lawrence et al, 2001

D=Direct Measurement, Ind=Indirect Measurement, PED=Pulsed Electrochemical Detection, CSV=Cathodic Stripping Voltammetry, CCSV=Catalytic Cathodic Stripping Voltammetry, CV=Cyclic Voltammetry, SWV=Square Wave Voltammetry, DPV=Differential Pulse Voltammetry, CSH=Cysteine, GSH=Glutathione, HCSH=Homocysteine, GSSG=Oxidized GSH, N/S=Not Specified

### 1.3. Biosensors

A biosensor is a device constituted by a biorecognition layer for the purpose of which is the biomolecular recognition of the analyte, and a transducer for the conversion of the biorecognition event into a useful electrical signal (Figure 1.6).

Biorecognition elements constitute of enzymes, antigens, antibodies, nucleic acids, receptors and tissues. Biosensors can be divided into two categories depending on the nature of this element: enzymatic (involving a biocatalytic event) and affinity (involving an affinity event) biosensors (Rivas et al., 2007).



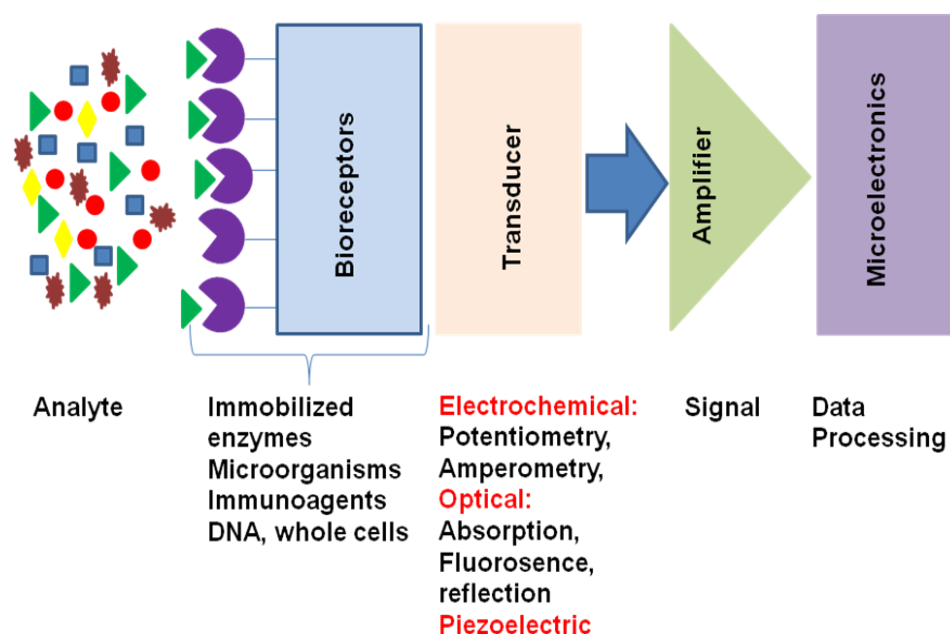


Figure 1.6. The principle of a biosensor

Biosensors are dedicated to evaluating various analytical techniques for monitoring low-molecular-weight analytes, proteins, nucleic acids and whole cells under normal and disease states. With recent advances in nanotechnology, development of nanomaterial bioconjugates is growing enormously towards translation into biomolecular recognition layers on surfaces (Kerman et al., 2008).

Nanomaterials have been used to modify metal, glass or carbon surfaces in connection with electrochemical and optical sensing. Electrochemical biosensors combining with nanomaterials can be presented as simple, efficient tools to determine the concentration of analytes and the response-time functions of target biomolecules to the drugs or the toxic reagents (Kerman et al., 2008; Hernandez-Santos et al., 2004; Wang, 2003; Katz et al., 2004; Luo et al., 2006).

A membrane modified with GR and sulphydryl oxidase (SO<sub>x</sub>) onto the surface of spectrographic graphite rods was integrated by Timur et al. (2008). The biosensor reaction could be monitored by O<sub>2</sub> consumption, which is associated with the concentration of GSSG or GSH during the enzymatic reaction.

When GR and SO<sub>x</sub> combine in the same matrices, they allow the detection of GSSG and GSH easily. This biosensor has also been applied as an ECD after HPLC separation (Timur et al., 2008).

The indirect detection of current has also been represented on biosensing approach. The immobilized horseradish peroxidase on a rotating disk facilitates the oxidation of catechols in the presence of H<sub>2</sub>O<sub>2</sub>, back electrochemical reduction of which is discovered on a GCE surface. When GSH and Cys are included into the solution, they take part in Michael addition reactions with catechols to form the corresponding thioquinone derivatives. So, it reduces the peak current obtained proportionally to the increase in their concentration (Monostori et al., 2009; Ruiz-Diaz et al., 2006).

#### **1.4. Nanotechnology**

Nanoscale science and technology is a youthful and rapidly increasing field that includes nearly every discipline of science and engineering. With rapid advances in molecular electronics, DNA-based self-assembly, and manipulation of individual atoms via a scanning tunneling microscope, nanotechnology has become the principal focus of the scientists (Cammarata, 2004).

Nanotechnology can be expressed as the formation and development of materials with structural characteristics in between those of atoms and bulk materials, with at least one dimension in the nanometer range (1 nm = 10<sup>-9</sup> m). Table 1.3 summarizes typical nanomaterials of different dimensions.

Properties of materials in nanometric dimensions are significantly different from those of bulk materials. Suitable control of the properties of nanometer-scale structures can lead to new devices and technologies for miniaturization (Rao et al., 2004).

Table 1.3. Selected nanomaterials (Rao et al., 2004)

Nanostructure	Size (approx.)	Materials
Nanocrystals and clusters (quantum dots)	diam. 1–10 nm	Metals, semiconductors, magnetic Materials
Other nanoparticles	diam. 1–100 nm	Ceramic oxides
Nanowires	diam. 1–100 nm	Metals, semiconductors, oxides, sulfides, nitrides
Nanotubes	diam. 1–100 nm	Carbon, layered metal chalcogenides
Nanoporous solids	pore diam. 0.5–10 nm	Zeolites, phosphates etc.
2-Dimensional arrays (of nano particles)	several nm <sup>2</sup> –mm <sup>2</sup>	Metals, semiconductors, magnetic Materials
Surfaces and thin films	thickness 1–1000 nm	A variety of materials
3-Dimensional structures (superlattices)	Several nm in the three Dimensions	Metals, semiconductors, magnetic materials

### 1.4.1. Nanocomposites

Nanocomposites can be defined as multiphase materials in which one or more of the phases have at least one dimension of order 100 nm or less. Most nanocomposites that have been expanded and exhibited technological significance have been constituted of two phases, and can be microstructurally categorized into three principal types; (a) Nanolayered composites consist of alternating layers of nanoscale dimension; (b) nanofilamentary composites consist of a matrix with embedded nanoscale diameter filaments; (c) nanoparticulate composites consist of a matrix with embedded nanoscale particles (Figure 1.7).

The properties of nanocomposites can exhibit synergistic enhancements over those of the component phases individually. Nevertheless, abnormal and regularly improved properties can be realized by minimizing the physical dimension(s) of the phase(s) down to the nanometer length scale (Cammarata, 2004).

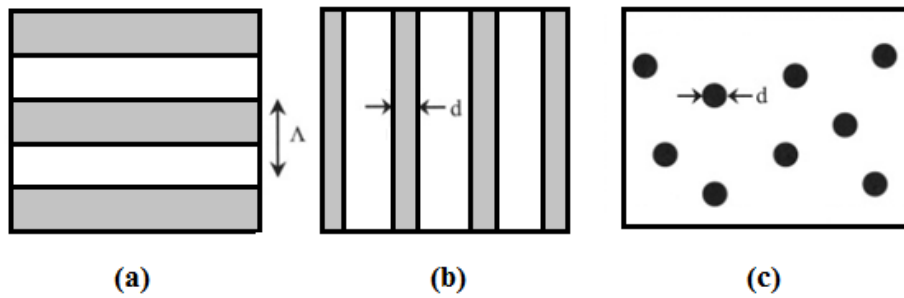


Figure 1.7. Schematic representations of nanocomposite materials with characteristics length scale: (a) nanolayered composites with nanoscale bilayer repeat length; (b) nanowire composites composed of a matrix with embedded filaments of nanoscale diameter; (c) Nano particle composites composed of a matrix with embedded particles of nanoscale diameter (Cammarata, 2004).

### 1.4.2. Nanoparticles

Recently, a large amount of electrode development has intensified on various things miniature: nanotubes, nanoballs, nanodots and especially nanoparticles (Banks et al., 2005; Dai et al., 2004; Zhong et al., 2000; Narayan and Tiwari, 2006). This strong attention is because of their unique optical, magnetic, electronic and chemical properties.

Consequently, it changes enormously from those of the bulk material. Another notable example of this is FeAl powder: while the typical powder is nonmagnetic and fragile, it is converted into ferromagnetic and ductile upon being made ultrafine (Welch and Compton, 2006; Phung et al., 2003).

Nanoparticles (Nps) are charming a significant attention as applicable biomedical materials and research into them is increasing because of their unique physical and chemical properties.

These Nps can be consist of a variety of materials including noble metals (e.g. Au, Ag, Pt, Pd), semiconductors (e.g. CdSe, CdS, ZnS, TiO<sub>2</sub>, PbS, InP, Si), magnetic compounds (e.g. Fe<sub>3</sub>O<sub>4</sub>, Co, CoFe<sub>2</sub>O<sub>4</sub>, FePt, CoPt) and their combinations (core-shell Nps and other composite nanostructures).

Drug carriers, labelling and tracking agents, vectors for gene therapy, hyperthermia treatments and magnetic resonance imaging (MRI) contrast agents can be exemplified as biomedical applications of Nps (Thanh et al., 2010).

There are four main advantages for the usage of nanoparticle-modified electrode when compared to a macro-electrode corresponding to electroanalysis: high effective surface area, mass transport, catalysis and control over local microenvironment. On the other hand, modification of an inexpensive base material with nanoparticle can direct to a larger surface area-to-volume ratio for the expensive metal, lowering the cost of the electrode (Welch and Compton, 2006). The large effective surface area may result larger number of active sites and often a higher signal-to-noise ratio.

The effect of nanoparticle size within an array on the peak current was illustrated by Simm et al. and they have compared it to that of a macro-electrode. The peak current at a macro-electrode for a simple, one electron reduction is given by the Randles-Ševcík equation:

$$I_{\text{peak}} = 2.69 \times 10^5 n^{3/2} D^{1/2} C_{\text{bulk}} \nu^{1/2} A \quad (1.6)$$

where  $I_{\text{peak}}$  is the peak current in amperes,  $n$  is the number of electrons transferred in the rate determining step,  $D$  is the diffusion coefficient in  $\text{cm}^2 \text{s}^{-1}$ ,  $C_{\text{bulk}}$  is the bulk concentration of active species in solution in  $\text{mol cm}^{-3}$ ,  $\nu$  is the scan rate in  $\text{V s}^{-1}$  and  $A$  is the surface area in  $\text{cm}^2$ . On the contrary, the overpotential, needed for a reaction to become kinetically viable, can be decreased by using the catalytic properties of some nanoparticles. For example, gold nanoparticles display catalytic effect of upon dopamine oxidation so its potentials could be distinguished from those of ascorbic acid (Raj et al., 2003).

It can be said that the gold nanoparticle modification enlarged the reversibility of the dopamine oxidation reaction. Thus, it is irreversible at a bulk gold electrode, by facilitating faster electron transfer kinetics (Welch and Compton, 2006).

The obvious peak potential is subjected to the relative “strengths” of these catalytic and mass transport effects when using a nanoparticle electrode. This is a particularly advantageous quality of nanoparticles because a change in the position of the voltammetric peak potential arising from the species of interest can separate it from peaks due to common interferences resulting in a more highly selective electrochemical analysis, as in the abovementioned example where interference from ascorbic acid could be eliminated in the case of dopamine (Katz et al., 2004; Raj et al., 2003; Welch and Compton, 2006).

It can be mentioned that there are some disadvantages to the high reactivity found with nanoparticles; for instance the electrode passivization can emerge due to aerial oxidation (Phung et al., 2003; Rellinghaus et al., 2001; Welch and Compton, 2006).

#### **1.4.2.1. The functions of nanoparticles**

Such nanoparticles; e.g. metal nanoparticles, oxide nanoparticles, semiconductor nanoparticles, and even composite nanoparticles have been commonly utilized in electrochemical sensors and biosensors.

Even though these nanoparticles participate into different roles in different electrochemical sensing systems based on their unique properties, the fundamental functions of nanoparticles can be primarily assorted as: 1) immobilization of biomolecules; 2) catalysis of electrochemical reactions; 3) enhancement of electron transfer; 4) labeling biomolecules and 5) acting as reactant. The roles that different nanoparticles have played in electrochemical sensor systems are summarized in Table 1.4 (Luo et al., 2006).

#### **1.4.2.2. Types of nanoparticles**

*CNTs* have created great interest in future applications based on their field emission and electronic transport properties, their high mechanical strength and their chemical properties since their discovery in 1991.

CNTs can be virtually used in many areas such as, field emission devices, nanoscale transistors, tips for scanning microscopy or components for composite materials and, they are one of the most commonly used building blocks of nanotechnology. They are 100 times the tensile strength of steel, thermal conductivity better than all but the purest diamond, and electrical conductivity similar to copper, but especially with the ability to carry much higher currents is the fascinating feature for CNTs. CNTs consist of single-walled, multi-walled and double-walled structures (Fig. 1.8). SWCNTs (Fig. 1.8-A) compose of a cylindrical graphite sheet of nanoscale diameter restricted by hemispherical ends. SWCNTs have diameters typically  $\sim 1$  nm with the smallest diameter reported to date of 0.4 nm.

The MWCNTs (Fig. 1.8-B) comprise of several layers of graphene cylinders that are concentrically nested like rings of a tree trunk with a layer spacing of 0.3-0.4 nm. MWCNTs tend to have diameters in the range 2-100 nm. The MWCNT can be considered as a mesoscale graphite system, whereas the SWCNT is truly a single large molecule (Merkoçi, et al., 2005; Anık and Çubukçu, 2008).

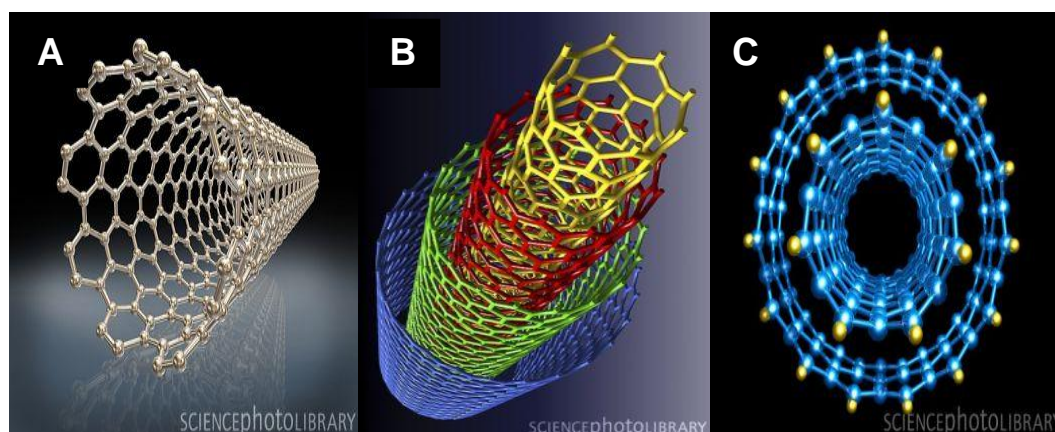


Figure 1.8. Schematics of an individual (A) SWCNT, (B) MWCNT and (C) DWCNT.

([www.sciencephotolibrary.com](http://www.sciencephotolibrary.com))

Table 1.4. Different functions of nanoparticles in electrochemical sensor systems (Xiliang et al., 2006)

<b>Functions</b>	<b>Properties used</b>	<b>Typical nanoparticles</b>	<b>Sensor advantages</b>	<b>Typical examples</b>
Biomolecule immobilization Antibody	Biocompatibility; large surface area	Metal nanoparticles (Au, Ag); Oxide nanoparticles (SiO <sub>2</sub> , TiO <sub>2</sub> )	Improved stability	immobilized onto Au nanoparticles remains stable for 100 days
Catalysis of reactions Enhancement of electron transfer	High surface energy Conductivity; tiny dimensions	Metal nanoparticles (Au, Pt) Metal nanoparticles (Au, Ag,); oxide nanoparticles (TiO <sub>2</sub> , ZrO <sub>2</sub> )	Improved sensitivity and selectivity Improved sensitivity; direct electrochemistry of proteins	H <sub>2</sub> O <sub>2</sub> sensor based on Prussian Blue nanoparticles with a sensitivity of 103.5 mA mM <sup>-1</sup> cm <sup>-2</sup> Electron transfer rate of 5000 s <sup>-1</sup> for glucose oxidase enhanced by gold nanoparticles
Labeling biomolecules	Small size; modifiability	Semiconductor nanoparticles (CdS, PbS); metal nanoparticles (Au, Ag)	Improved sensitivity; indirect detection	DNA sensor labeled with Ag nanoparticles achieves detection limit of 0.5 pM
Acting as reactant	Chemical activity	Oxide nanoparticles (MnO <sub>2</sub> )	New response mechanism	Lactate biosensor with MnO <sub>2</sub> nanoparticles response 50 times more sensitive than without



DWCNT are a novel class of carbon nanotubes with inner and outer shells (Fig. 1.8-C). They can be approved as the thinnest member of MWCNTs in terms of their structural feature. Although they show properties like those of SWCNTs but offer much higher structural stability than those of SWCNTs (Kuwahara et al., 2006).

**Gold Nanoparticles (AuNps)**, is the most utilized metallic nanoparticles in electroanalytical applications. AuNp is a kind of nanomaterial where it can help proteins to retain their biological activity upon adsorption. AuNp provides a suitable microenvironment similar to that of redox protein with more freedom in orientation. Moreover, it is claimed that this nanoparticle reduces the insulating effect of the protein shell by providing direct electron transfer through the conducting tunnels of gold nanocrystals which causes the penetration of nanomeric edges of gold particles.

By this way, the distance between the electrode and biomolecular redox sites for electron transfer is decreased. Its large surface area and good electronic properties and its utilization for the study of direct electron transfer of redox proteins increase their usage in biosensor construction (Çubukçu et al., 2007 and 2012).

AuNps have also show to comprise of helpful interfaces for the electrocatalysis of redox processes of molecules such as  $\text{H}_2\text{O}_2$ ,  $\text{O}_2$  or NADH included in many significant biochemical reactions (Rashid et al., 2006; Pingarrón et al., 2008). Table 1.5 summarizes AuNp based electrochemical enzyme biosensors.

**Platinum Nanoparticles (PtNps)**, the modification of electrode surfaces with redox-active metal nanoparticles has led to the development of electrochemical sensors with catalytic activity. Especially, PtNps have been extensively used for the design of electrodes.

Table 1.5. Gold nanoparticle-based electrochemical enzyme biosensors (Pingarrón et al., 2008)

Enzyme/electrode	Immobilization mode	Detection	Analyte/sample	Linear Range and LOD	Ref
GOx/gold	Covalent attachment of GOx to a AuNp monolayer-modified AuE	Amperometric ( $E=0.3V$ vs SCE)	Glucose	$2.0 \times 10^{-5}$ - $5.7 \times 10^{-3}$ M LOD: 8.2 $\mu$ M	Zhang et al., 2005
GOx/GCE	GOx and the redox mediator TTF coimmobilized by cross-linking with GA on AuNp modified electrodes with either Cyst or MPA monolayers	Amperometric ( $E=0.20V$ )	Glucose	0.01-10 mM; LOD: $0.7 \times 10^{-5}$ M;	Mena et al., 2005
GOx/CPE	GOx adsorbed on a colloidal AuNp modified CPE	CV	Glucose/serum sample	0.04-0.28 mM; LOD: 0.01 mM <sup>1</sup>	Liu and Ju, 2003
GOx/CNT-Teflon composite electrode	GOx and colloidal gold incorporated into composite electrode	Amperometric ( $E=+0.50V$ )	Glucose/sport beverages	0.05-1 mM; LOD: 17 $\mu$ M	Manso et al., 2007
XOD/gold	Mediator, Prussian Blue deposited on the electrode; XOD entrapped onto pPy film by electrooxidation of XOD and pyrrole; colloidal gold adsorbed onto enzyme electrode	Amperom. ( $E=-0.15V$ )	Xanthine	1-20 $\mu$ M	Liu et al., 2004
ADH/gold	Colloidal gold self-assembled through the thiol groups of an 1,6-hexanedithiol ML and immob. of ADH on colloidal gold	EIS	Ethanol	$1.0 \times 10^{-5}$ - $1.3 \times 10^{-2}$ M; LOD: $8.0 \times 10^{-6}$ M	Liu, Yin, Long et al., 2003
GOx/platinum	Layer-by-layer assembled chitosan/nAu/GOx multilayer films	Amperometric ( $E=0.60V$ )	Glucose/human serum	0.5-32 mM	Wu et al., 2007

PtNps may possibly enhance the surface area and beneficial to electron transfer with strong catalytic properties (Wang et al., 2010). The surface of microelectrodes could be modified with nanostructured Pt films to enhance the surface areas with increased mass transport characteristics and shown to be excellent amperometric sensors for  $\text{H}_2\text{O}_2$  over a wide range of concentrations (Hrapovic et al., 2004). An electrochemical biosensor was generated which consisting of PtNps with a diameter of 2-3 nm by Hrapovic et al (2004). They used this biosensor in combination with SWCNTs for fabricating electrochemical sensors with remarkably improved sensitivity toward hydrogen peroxide.

*Metal Oxide Nanoparticles (MOxNps)*, the immobilization and direct electrochemistry of enzymes and proteins can successfully be generated with many MOxNps such as copper oxide, zinc oxide, titanium oxide, and zirconium oxide (Zheng et al., 2009).

Metal nanoparticles have been used as catalysts in numerous biosensor applications, owing to their superior stability and entire recovery in biochemical redox processes. The affinity of certain thiol-containing substrates to Au nanoparticles has particularly originated dramatic changes in the electrochemistry of substrate enzyme interactions (Kerman et al., 2008).

$\text{Fe}_3\text{O}_4$  nanoparticles ( $\text{Fe}_3\text{O}_4$  Nps) have been utilized to immobilize enzymes, owing to their good biocompatibility, strong super paramagnetic property, low toxicity and easy preparation. In particular, magnetite is found to exist in the human brain and they have generally smaller than 200 nm. Thus, it is important to investigate the bioactivity and biocatalysis of enzymes and proteins as they are captured in the  $\text{Fe}_3\text{O}_4$  Nps (Zheng et al., 2009).

$\text{TiO}_2$  is found to be used a research area in cosmetics, solar cells, batteries, additives in toothpaste and white paint, and others. Recently, there is a significant awareness in using  $\text{TiO}_2$  nanoparticles as a film-forming material as they have high surface area, optical transparency, good biocompatibility, and relatively good conductivity.

In spite of wide application in photochemistry, the use of nano-TiO<sub>2</sub> in electrochemistry is rare due to the low solubility of TiO<sub>2</sub> nanoparticles and the poor stability of the TiO<sub>2</sub> film modified on electrodes (Wu, 2009).

Aluminum titanate (Al<sub>2</sub>O<sub>3</sub>.TiO<sub>2</sub>) is a ceramic oxide and known for its excellent thermal shock resistance resulting from the low thermal expansion coefficient, low thermal conductivity, and low Young's modulus and for its good chemical resistance.

During the past decade, new Al<sub>2</sub>O<sub>3</sub>-based nanocomposite coatings have been widely studied, particularly those containing TiO<sub>2</sub>. The Al<sub>2</sub>O<sub>3</sub>.TiO<sub>2</sub> coatings are of interest since they were found to possess enhanced toughness and wear resistance compared to monolithic Al<sub>2</sub>O<sub>3</sub> coatings (Çubukçu et al., 2012).

### **1.5. Centri-voltammetry**

Centri-voltammetry is a method which combines the advantages of centrifugation and voltammetry. The method offers a practical way for the application of co-precipitation in the same cell allowing direct voltammetric scan afterwards (Anık-Kırgöz et al., 2004). A specially designed voltammetric cell compatible with the centrifuge is used for this purpose.

At the bottom of the cell, an electrode with a flat surface, i.e. platinum electrode, serves as a working electrode and the measuring cell is completed by immersing the other two electrodes.

Various carrier materials can be used for this purpose. Pioneering study with centri-voltammetry includes the enrichment process with a commonly used co-precipitant; Al(OH)<sub>3</sub> (Anık-Kırgöz et al., 2004). The main goal was expressed as to trap the analyte between the alumina layer and the mercury thin film electrode surface by driving force of the centrifuge. A thin layer of Al(OH)<sub>3</sub> at the electrode surface, where the trace metals are preconcentrated, also provides a conductive coating for subsequent voltammetric measurement.

Therefore, centri-voltammetry provides a practical and sensitive method for application of co-precipitation in trace analysis eliminating time consuming and laborious decantation, filtration, and dissolution steps.

In later studies, Amberlite XAD-7 resin was used for pre-concentration and better sensitivity was attained with good reproducibility (Anık-Kırgöz et al., 2005). The main difference of this technique from the conventional stripping voltammetric techniques lies on the deposition process.

In centri-voltammetry most of the analyte can be preconcentrated on the electrode surface by means of an appropriate carrier reagent rather than a small portion of the analyte as in the case of anodic stripping voltammetry (ASV). This constitutes the advantage of the method for attaining lower detection limits by using higher bulk volumes.

Ürkmez and coworkers have applied the method for anodic stripping analysis of mercuric ions at a gold film electrode after reducing with  $\text{NaBH}_4$  (Ürkmez et al., 2009). The procedure does not require a carrier precipitate or resin and sub ppb levels of mercury can be detected by this means

Alternatively, the analyte can be preconcentrated on the electrode surface as its complexes and the centrifugation employed forces the complex to precipitate as a thin film on the electrode surface from bulk solution. By this mean, the method was exploited for determination of molybdenum ions with a various carrier reagents namely; oxine, pyrogallol red and cupferron (Koçak, 2009).

More recently, the scope of the method was expanded by applying centri-voltammetry for detection of biological compounds and therefore, it was named as biocentri-voltammetry (Anık and Çevik, 2011; Çevik et al., 2012). In the former work, a xanthine biosensor was developed by immobilizing xanthine oxidase onto the working electrode of centri-voltammetric cell (Anık and Çevik, 2011). In the latter work, biocentri-voltammetric application, the acetyl choline esterase enzyme activity was monitored biocentri-voltammetrically (Çevik et al., 2012).

## **1.6. The Aim of the Thesis**

Growing demand for more selective and sensitive determinations of biologically important molecules encourages searching for more selective carriers as well as new electrode materials adoptable to the centri-voltammetric cell. In this thesis, novel electrode materials are utilized for biologically important thiol containing molecules, GSH in particular.

Development of composite electrodes including nanoparticles is planned and the results of this study are constituted alternative methods for the investigation of electrochemical detection methods for thiol containing biochemical compounds. Besides, centri-voltammetry developed in this laboratory is utilized for further development of more sensitive results.

## 2. EXPERIMENTAL

### 2.1. Instrumentation

Electrochemical measurements were carried out with a FRA 2  $\mu$ -AUTOLAB Type III (Figure 2.1) electrochemical measurement system from ECO CHEMIE Instruments B.V., (Netherlands) driven by GPES software. AC impedance spectroscopy was performed with also FRA 2  $\mu$ -AUTOLAB Type III. The frequency range measured was from  $10^4$  Hz down to 0.01 Hz with amplitude of 0.01 V and at 0.2 V potential.



Figure 2.1. FRA 2 modulated  $\mu$ -AUTOLAB Type III

QCM measurements were performed on a Quartz Crystal Microbalance Digital Controller, QCM D Model QCM200 instrument. An AT-cut 5 MHz Au/quartz crystal electrode was employed as a working electrode.

The experiments were conducted in a 10 mL voltammetric cell (Metrohm) (Fig. 2.2 (A)) and centri-voltammetric cell made of Delrin, also known as polyacetal or polyformaldehyde (Fig. 2.2 (B)), at room temperature ( $25^{\circ}\text{C}$ ), using a three-electrode configuration. A platinum electrode served as an auxiliary electrode while an Ag/AgCl electrode as a reference electrode, the working electrodes were carbon based nanocomposite paste electrodes.

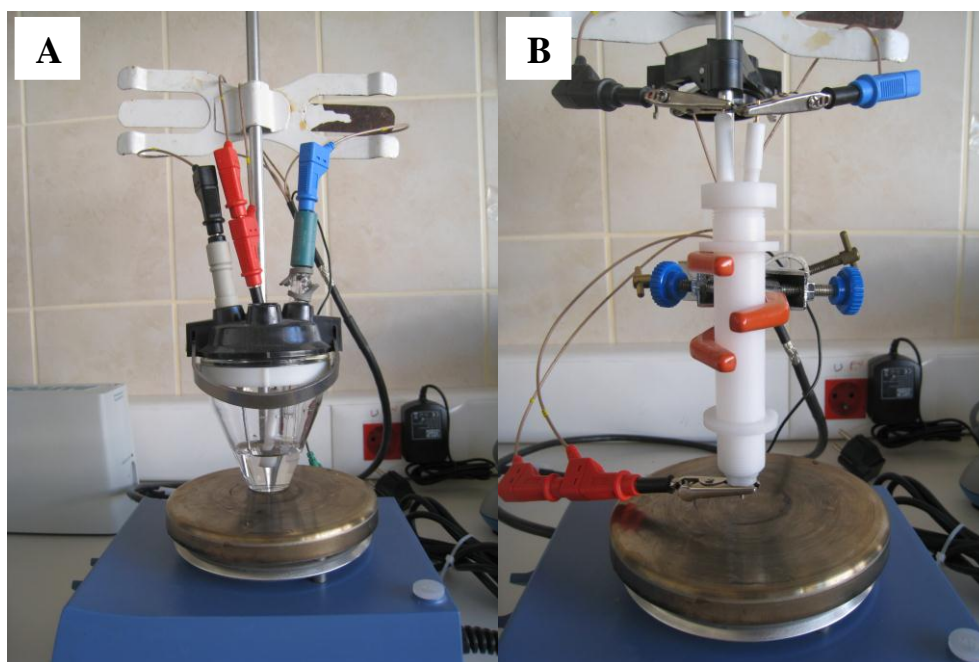


Figure 2.2. A conventional electrochemical working set-up (A) and a centri-voltammetric set-up (B) relating with the triple electrode system

A home-made centri-voltammetric cell was employed for centri-voltammetric measurements (Fig. 2.3(A)). The cell was made of Delrin material and drilled to be suitable for centrifugation with a height of 11 cm, external diameter 1.8 cm and bottom diameter suitable for electrode of 0.7 cm. The centri-voltammetric electrode has also 4 mm diameter (Fig. 2.3(B)). By this means total weight of the centri-cell was reduced to 40.145 g.

The cell consists of a carbon based paste electrodes at the bottom providing a flat surface for collecting the precipitate. The paste electrodes were smoothed with a weighing paper then rinsing with distilled water. After rinsing with distilled water, the electrode was inserted to the bottom of the cell. Upon addition of 10 mL supporting electrolyte, the cell was closed with its cap. Reference and auxiliary electrodes were inserted through the holes of the cap drilled for this purpose.



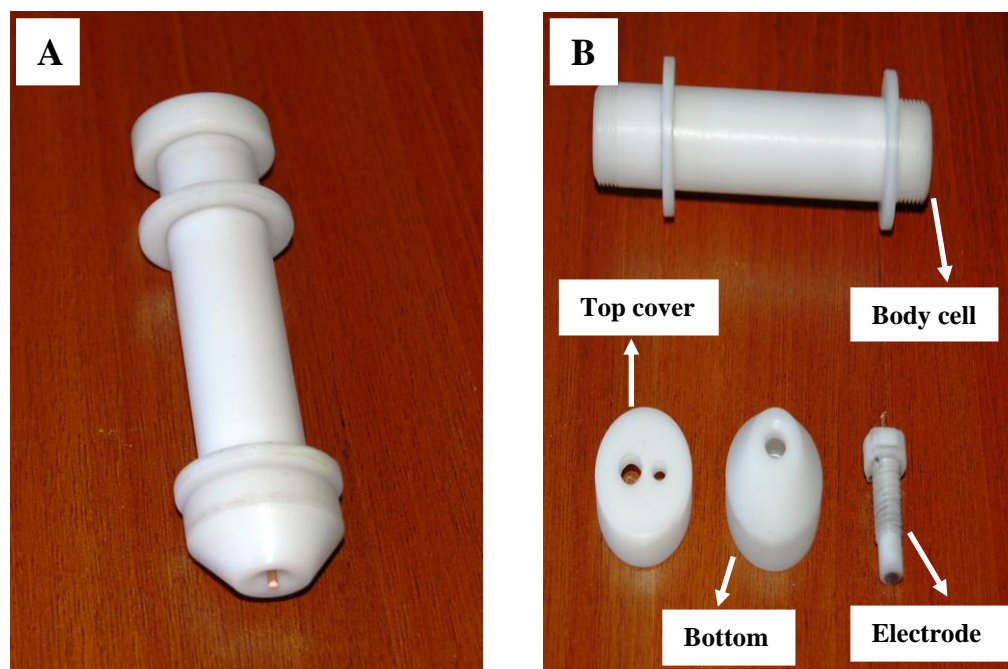


Figure 2.3. Centri-voltammetric cell; (A) whole cell, (B) parts of the cell.

Sigma 3-16PK centrifuge was used for centrifugation for the centri-voltammetric measurements. The home-made centri-voltammetric cell, made from a Delrin tube was constructed to be compatible to the centrifugation system.

All pH measurements were performed using an ORION STAR SERIES model of pH-meter with calibrated its standard calibration solutions. PRECISA XR 205SM-DR model sensitive balance was utilized for weighing the solid chemicals in preparation of chemical solutions. The experimental were all conducted at the room temperature 25 °C.

## 2.2. Reagents

All reagents were of analytical-reagent grade and all solutions were prepared using double distilled water. 0.01 M GSH stock solution was prepared freshly by dissolving the appropriate amount of GSH (L-Glutathione reduced,  $\gamma$ -L-Glutamyl-glycine GSH, cell culture tested, Sigma). PtNp solution was prepared from chloroplatinic acid hexahydrate which obtained from Sigma-Aldrich. KCl (max. 0.0001% Al, puriss, from Riedel-de Haën) solution was used as a background solution for electrochemical deposition of PtNps.

H<sub>2</sub>O<sub>2</sub> stock solutions were prepared freshly by dissolving the appropriate amount of H<sub>2</sub>O<sub>2</sub> (35%, from Merck). K<sub>3</sub>Fe(CN)<sub>6</sub> (99,99+%, d=1,89 g/mL, Sigma-Aldrich) was used for impedance measurements.

Standard stock solution of bismuth (1000 mgL<sup>-1</sup>, AAS standard solution) was obtained from Aldrich and diluted as required. 0.1 M acetic acid/acetate buffer solution (pH 4.5, glacial acetic acid 100%, Merck) was served as supporting electrolyte during bismuth film (Bi-Film) formation. CuSO<sub>4</sub> stock solution was prepared freshly by dissolving the appropriate amount of CuSO<sub>4</sub> (Copper (II) sulfate, anhydrous, powder, 99.99+% metal basis, obtained from Aldrich).

Synthetic plasma samples were prepared by incorporating the reagents into the TRIS-HCl including 140 mM NaCl (99.0-100.1% supplied from Pancreac), 4.5 mM KCl, 2.5 mM CaCl<sub>2</sub> (Calcium chloride dehydrate, ACS reagent, ≥99% from Sigma), 0.8 mM MgCl<sub>2</sub> (magnesium chloride hexahydrate, GR for analysis 99.0-101.0% obtained from Merck), 2.5 mM urea (99.5% pure, used from Horasan Chemistry), and 4.7 mM glucose (D-(+) glucose monohydrate for microbiology from Merck).

10 mM TRIS-HCl (Tris (hydroxymethyl)-aminomethane, TRIS, 99.0-100.1%, supplied from Merck) buffer was used as the background of the synthetic plasma solution. Phosphate buffer solution (PBS) KH<sub>2</sub>PO<sub>4</sub>, Merck/purity 99,995%, 0.05 M, pH 7.0) was served as supporting electrolyte. The pH of buffers was adjusted by adding required amount of sodium hydroxide and hydrochloric acid. For interference study, ascorbic acid (L-ascorbic acid, reagent grade) and L-cysteine (≥98.5% (RT)) were used for this purpose and supplied from Sigma.

Al<sub>2</sub>O<sub>3</sub>.TiO<sub>2</sub> (nanopowder <25nm (BET), 98.5%) was obtained from Aldrich. Glassy carbon spherical powder (20-50 micron, type I) was purchased from Alfa Aesar, while mineral oil was obtained from Sigma-Aldrich and gold colloid from Sigma (0.75A<sub>520</sub> units/mL; 10nm ~0.001% as HAuCl<sub>4</sub>). Graphite powder (particle size <50 μm) was purchased from Merck.

MWCNT (diam.=110-170 nm, length= 5-9 micron, 90+%) and glassy carbon spherical powder, 2-12 micron, 99.95% metal basis were obtained from Aldrich. The silica gel (Silica Gel 60, particle size  $\leq 0.04$  mm ( $\geq 400$  mesh ASTM, for preparative column chromatography, supplied from Fluka), Tenax (TA 60/80 Supelco Analytical) and Charcoal Activated (Merck) was used as a carrier material for centri-voltammetric application. GSH-Px (Glutathione-Peroxidase f.bovine erythrocytes lyoph., powder, white,  $\sim 100$  units/mg) was used from Sigma for biosensor application.

## **2.3. Electrode Preparation**

### **2.3.1. Preparation of bismuth film electrode (BiFE)**

The GCE was polished by hand using alumina slurry on a felt pad prior to Bi-Film formation. BiFE was prepared *ex-situ* by following the usual procedure, which includes introducing Bi solution ( $1.0 \text{ mg L}^{-1}$ ) into a working cell containing 10 mL acetate buffer (0.1 M, pH 4.5) while the solution was stirring with three electrodes configuration. For this process, a deposition potential of  $-1.0 \text{ V}$  was applied for 5 min without applying any deaeration.

### **2.3.2. Preparation of bare GCPE**

Glassy carbon paste electrode (GCPE) was prepared by hand mixing of 80:20 (% w/w) glassy carbon spherical powder and mineral oil. A portion of the resulting paste was then packed firmly into the electrode cavity (3.0 mm diameter and 5.0 mm depth) of a PTFE sieve where electrical contact was established via a copper wire. Prior to its use, the surface of the composite electrode was smoothed with a weighing paper.

### **2.3.3. Preparation of AuNp/Al<sub>2</sub>O<sub>3</sub>.TiO<sub>2</sub>/GCPE**

AuNp/Al<sub>2</sub>O<sub>3</sub>.TiO<sub>2</sub> nanopowder based GCPE was prepared by hand mixing of 60:20:20 (w/w, %) glassy carbon spherical powders/ mineral oil/ Al<sub>2</sub>O<sub>3</sub>.TiO<sub>2</sub> nanopowder and 20  $\mu\text{L}$  AuNp.

A portion of the resulting paste was then packed firmly into the electrode cavity (3.0 mm diameter and 5.0 mm depth) of a PTFE sieve where electrical contact was established via a copper wire. The electrode then, was exposed to air for 25 min to attain a dry surface.

#### **2.3.4. Preparation of QCM sensors**

QCM sensors were prepared as followed procedure. The freshly prepared gold-crystal electrode was injected with a  $\text{Al}_2\text{O}_3\cdot\text{TiO}_2$  nanopowder suspension 100  $\mu\text{l}$  (4mg/250 $\mu\text{L}$ ), a 50  $\mu\text{L}$  AuNp solution, a GSH aqueous solution ( $0.01\text{molL}^{-1}$ ) and the mixture of  $\text{Al}_2\text{O}_3\cdot\text{TiO}_2$  nanopowder, GSH aqueous solution and AuNp solution (150  $\mu\text{L}$ ) for until dryness of the electrode. Then the electrode was rinsed carefully with water to remove the physisorbed materials. After that, the freshly modified electrode was obtained and the QCM sensors were applied for the measurements.

#### **2.3.5. Preparation of AuNp/nano-micro $\text{TiO}_2$ based GCPE**

AuNp/nano-micro  $\text{TiO}_2$  based GCPE was prepared by hand mixing of 60:20:20 (% w/w) glassy carbon spherical powders/ mineral oil/ nano-micro  $\text{TiO}_2$  and 20  $\mu\text{L}$  AuNp. A portion of the resulting paste was then packed firmly into the electrode cavity (3.0 mm diameter and 5.0 mm depth) of a PTFE sieve where electrical contact was established via a copper wire. The electrode then, was exposed to air for 25 min to attain a dry surface.

#### **2.3.6. Preparation of 4% MWCNT-CPE**

MWCNT modified carbon paste electrodes (CPE) were prepared in different portions (66:30:4 % (w/w) graphite powder/mineral oil/MWCNT) by hand-mixing of graphite powder with mineral oil and MWCNT using a spatula. A portion of the resulting paste was then packed firmly into the electrode cavity (3.0 mm diameter and 5.0 mm depth) of a Delrin tube where electrical contact was established via a copper wire. The surface of the resulting paste electrode was smoothed and rinsed carefully with double distilled water.

### 2.3.7. Preparation of Chit/GSH-Px/PtNp onto the GCPE

Electrodeposition of PtNps were incorporated onto the bare GCPE through electrochemical deposition from the stock solution of 0.01 M  $\text{H}_2\text{PtCl}_6$  in 0.1M KCl solution by cyclic voltammetry between -0.70 V and +0.80 V at  $50 \text{ mV}\cdot\text{s}^{-1}$  for 50 cycles (Liu et al., 2010).

After modification of electrode with PtNp, 20  $\mu\text{L}$  GSH-Px enzyme solutions (from 26 U/mL GSH-Px enzyme stock solutions) was casted onto the PtNp modified GCPE and allowed to dry in the air for a while. Then, 20  $\mu\text{L}$  chitosan solutions were spreaded over the modified electrode and allowed to air dry for a while.

### 2.3.8. Preparation of GSH-Px<sub>(immob)</sub>/PtNp/GCPE

Bare GCPE was prepared in a portion of 80:20 (w/w, %) glassy carbon spherical powder/mineral oil by hand mixing using a spatula. A portion of the resulting paste was then packed firmly into the electrode cavity (3.0 mm diameter and 5.0 mm depth) of a Delrin tube where electrical contact was established via a copper wire. The surface of the resulting paste electrode was smoothed and rinsed carefully with double distilled water.

After electrodeposition of PtNp onto bare GCPE surface as described in section 2.3.5, the construction of biosensor was applied for the PtNp modified GCPE. Then, GSH-Px enzyme immobilization procedure was applied according to following process: 0.2 mg GSH-Px was diluted in 1 mL phosphate buffer solution (pH 7.0). 5 U of GSH-Px and gelatine (3 mg) were mixed at  $38^\circ\text{C}$  in potassium phosphate buffer (pH 7.0, 50  $\mu\text{L}$ ). 50  $\mu\text{L}$  of mixed solution was spread over the PtNp modified GCPE surface and allowed to dry at  $4^\circ\text{C}$  for 1 hour. Finally, it was immersed in 2.5% glutaraldehyde in phosphate buffer (0.05 M, pH 7.0) for 5 min for cross-linkage (Figure 2.4). The resulting biosensor was stirred in 7.0 PBS (pH 7.0) for 15 min to remove the excess from the surface of the electrode before the beginning of the measurement.

### **2.3.9. Preparation of 4% Fe<sub>3</sub>O<sub>4</sub> Np/GSH-Px<sub>(immob)</sub> modified GCPE**

Fe<sub>3</sub>O<sub>4</sub> Np modified (4%) GCPE was prepared by hand mixing of 56:20:4 (% w/w) glassy carbon spherical powders, mineral oil and Fe<sub>3</sub>O<sub>4</sub> Np using a spatula. A portion of the resulting paste was then packed firmly into the electrode cavity (3.0 mm diameter and 5.0 mm depth) of a Delrin tube where electrical contact was established via a copper wire. The surface of the resulting paste electrode was smoothed and rinsed carefully with double distilled water. Immobilization of GSH-Px was applied onto the 4% Fe<sub>3</sub>O<sub>4</sub> Np modified GCPE as usual procedure which was mentioned in section 2.3.8.

## **2.4. Procedures**

### **2.4.1. Procedure for BiFE**

The three electrodes were immersed into the 10 mL electrochemical cell. DP voltammetric measurements were carried out in 0.05 M phosphate buffer solution (pH 7.0) in the potential range between -0.3 V and -0.8 V.

### **2.4.2. Procedure for AuNp/Al<sub>2</sub>O<sub>3</sub>.TiO<sub>2</sub>/GCPE**

Prior to its use, the surface of the composite electrode was smoothed with a weighing paper. The three electrodes were immersed into the 10 mL electrochemical cell.

Cyclic voltammetric and DP voltammetric measurements were carried out in 0.05 M phosphate buffer (pH 7.0) medium in the potential range between -0.4 V/+1.0 V at 100 mV/s scan rate and 0 V/+1.2 V, respectively. The electrode surface was renewed prior to each measurement.

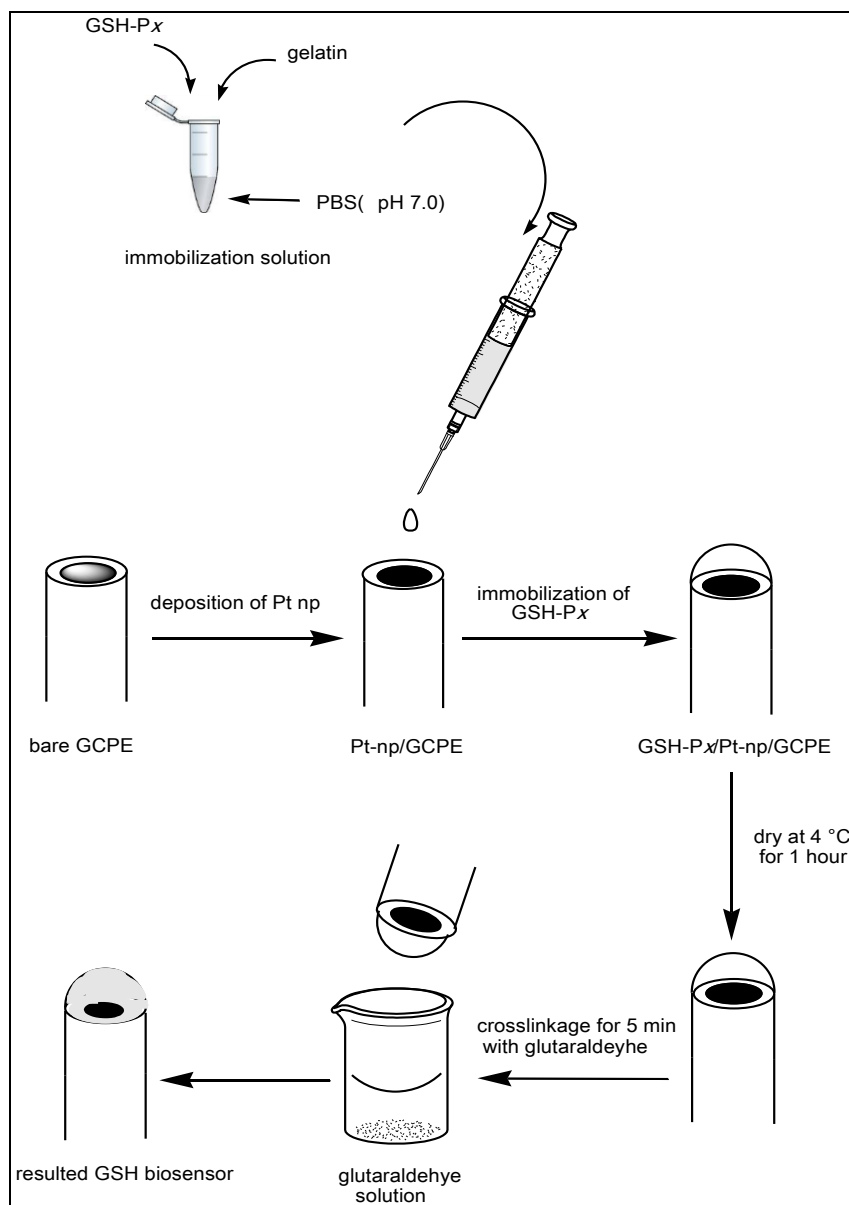


Figure 2.4. Schematic representation for the fabrication of a GSH biosensor.

### 2.4.3. Procedure for AuNp/nano-micro TiO<sub>2</sub> based GCPE

Prior to its use, the surface of the composite electrode was smoothed with a weighing paper. For the procedure of AuNp/nano-micro TiO<sub>2</sub> based GCPE, the three electrodes were immersed into the 10 mL electrochemical cell. DP voltammetric measurements were carried out in 0.05 M phosphate buffer (pH 7.0) medium in the potential range between 0 V and +1.0 V. The electrode surface was renewed prior to each measurement.

#### **2.4.4. Procedure for 4% MWCNT-CPE**

The GSH solution was placed in a beaker and 1.0 mg of silica gel and 30  $\mu\text{L}$  of AuNp solution were added (Figure 2.5). The stirred was switched on and the mixture was allowed to complete adsorption process for 7 min. Then, the mixture was placed into the centri-voltammetric cell and centrifuged for 4 min at 4000 rpm. The cell was carefully placed in the voltammetric stand and the reference and counter electrodes were immersed into the cell solution. DP voltammograms were recorded in the potential range between 0 V and +1.0 V in 0.05 M phosphate buffer (pH 7.0) medium. The electrode surface was renewed by stripping the surface and smoothing by a weighing paper prior to each use.

#### **2.4.5. Procedure for Chit/GSH-Px/PtNp onto the GCPE**

The chitosan, GSH-Px and PtNp modified GCPE was placed into the centri-voltammetric cell. 10 mL phosphate solution (0.05 M, pH 7.0) in the presence of various concentrations of GSH and  $\text{H}_2\text{O}_2$  was placed into the cell. Reference and counter electrodes were immersed into the solution for the centri-voltammetric measurements.  $\text{N}_2$  gas was passed through the solution before the measurements. The DP voltammograms were recorded in the range between 0 V and +0.7 V.

#### **2.4.6. Procedure for GSH-Px<sub>(immob)</sub>/PtNp/GCPE**

Prior to its use, the modified composite electrode was stirred in a phosphate buffer solution for 15 min to remove excess glutaraldehyde solution from the electrode surface after crosslinkage of glutaraldehyde. Proper amount of GSH and  $\text{H}_2\text{O}_2$  were put into the working cell including 0.05 M phosphate buffer (pH 7.5). The mixture was deaerated for 5 min by passing  $\text{N}_2$  gas through the solution. The cell was placed in the voltammetric stand and reference and counter electrodes were immersed into the solution. DP voltammograms were recorded in the range between 0 V and +0.7 V. The electrode was stirred for 15 min in phosphate buffer solution at each interval.



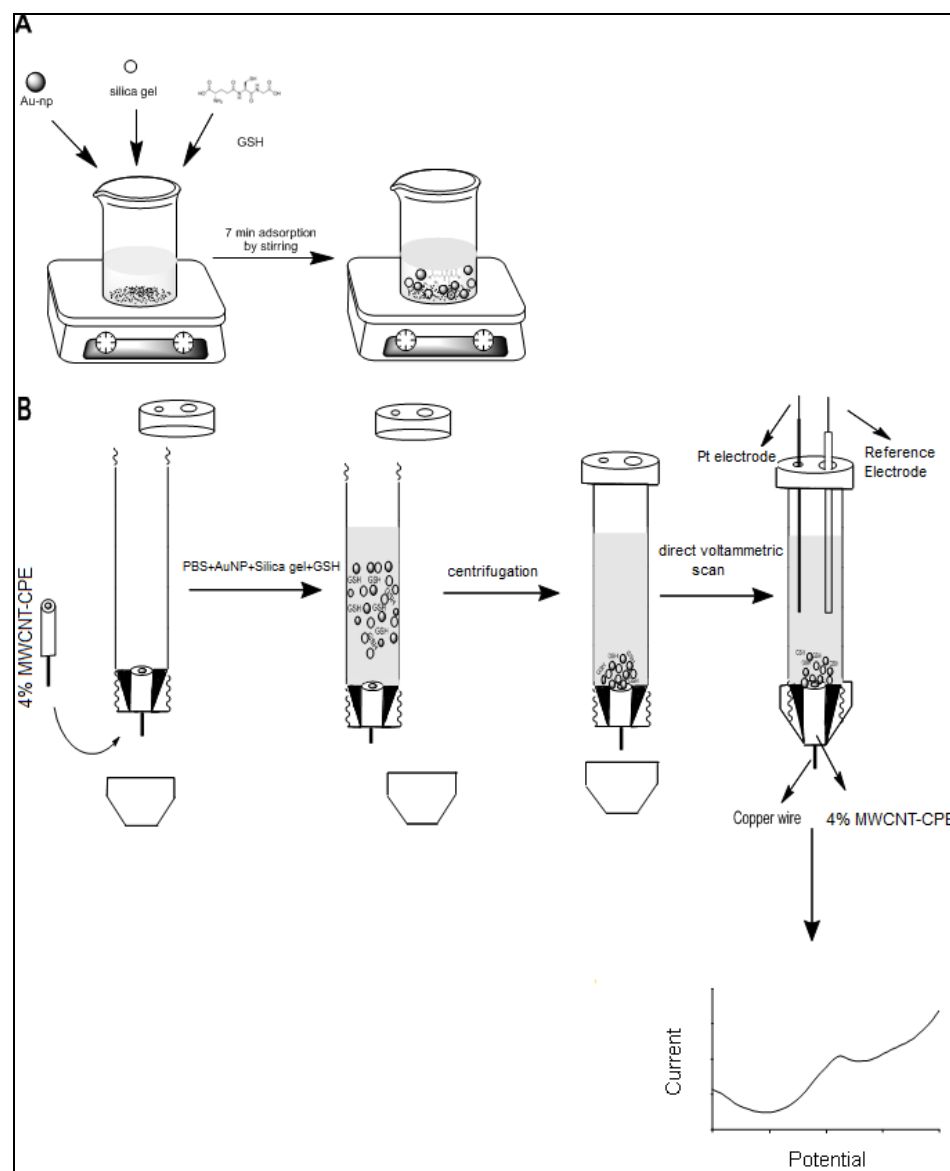


Figure 2.5 Demonstration of the centri-voltammetric procedure (A) Adsorption process, (B) the stages of centri-voltammetry

#### 2.4.7. Procedure for 4% $\text{Fe}_3\text{O}_4$ Np/GSH- $\text{P}x_{(\text{immob})}$ modified GCPE

The surface of the composite electrode was smoothed with a weighing paper after filling the resulting paste into the electrode cavity and then immobilization procedure was applied which was described in section 2.3.9. For the procedure of 4%  $\text{Fe}_3\text{O}_4$  Np/GSH- $\text{P}x_{(\text{immob})}$  modified GCPE, the three electrodes were immersed into the 10 mL electrochemical cell. DP voltammetric measurements were carried out in 0.05 M phosphate buffer (pH 7.0) medium in the potential range between 0 V and +0.7 V.

The electrode surface was renewed prior to each measurement. The N<sub>2</sub> gas was passed through the solution for 10 min at every beginning of measurement and the resulting electrode was stirred between each measurement for 15 min.

## **2.5. Sample Application**

### **2.5.1. Sample application for AuNp/Al<sub>2</sub>O<sub>3</sub>.TiO<sub>2</sub> Np/GCPE**

The performance of the AuNp/Al<sub>2</sub>O<sub>3</sub>.TiO<sub>2</sub> nanopowder/ GCPE sensor was tested by applying for GSH analysis in wine sample. A known amount of GSH (250 μM) was added to the reaction cell from the stock solution that was prepared by dilution of (1:100) wine sample with 0.05M phosphate buffer (pH 7.0). DP voltammetric measurements with the composite electrode were performed after transferring the corresponding analytical solution to the electrochemical cell with a potential range from 0 V and +1.2 V versus Ag/AgCl. After the measurement, the recovery values of the analytical signal for the diluted samples were calculated.

### **2.5.2. Sample application for 4% MWCNT-CPE**

The procedure was applied for the detection of GSH in food and clinical sample to show the versatility of the method developed. Synthetically prepared plasma sample and the red wine sample from local market were analyzed using the standard addition method. The wine sample was diluted in 1:100 ratio with 0.05 M phosphate buffer solutions (pH 7.0) and spiked with 100 μM GSH standard. The procedure described above was applied to each sample and recovery value was calculated upon three successive additions of standard GSH solution into the mixture. The synthetically plasma sample was prepared according to the procedure reported before (Çoldur et al., 2010). Synthetic plasma solution was comprised of 140 mM NaCl, 4.5 mM KCl, 2.5 mM CaCl<sub>2</sub>, 0.8 mM MgCl<sub>2</sub>, 2.5 mM urea, and 4.7 mM glucose. 10 mM TRIS-HCl buffer was used as the background of the synthetic plasma solution.

The final pH of the solution was adjusted to 7.3 with addition of proper amount of 1 M HCl. The standard solutions were prepared from using the synthetic plasma electrolyte as a background solution and then proper amount of analytes was spiked to the phosphate buffer solution (pH 7.0). The recovery values were calculated upon three successive additions of standard GSH solution into the mixtures.

### **2.5.3. Sample application for GSH biosensor**

The obtained biosensor was used for the GSH analysis in synthetically prepared plasma sample to show the applicability of the method for clinical analysis. These samples were analyzed using the standard addition method. The synthetically plasma sample was prepared according to the same procedure described above. Synthetic plasma solution was comprised of 140 mM NaCl, 4.5 mM KCl, 2.5 mM CaCl<sub>2</sub>, 0.8 mM MgCl<sub>2</sub>, 2.5 mM urea, and 4.7 mM glucose. 10 mM TRIS-HCl buffer was used as the background of the synthetic plasma solution. The final pH of the solution was adjusted to 7.3 with addition of proper amount of 1 M HCl. The standard solutions were prepared from using the synthetic plasma electrolyte as a background solution and then proper amount of analytes was spiked to the phosphate buffer solution (pH 7.5).

### 3. RESULT and DISCUSSION

The results of the thesis can be grouped under four subheadings; to develop composite electrodes including metallic film and CPE and metal/metal oxide particles for selective determination of GSH, the use of alternative platforms for centri-voltammetric studies, developing a biosensor for its determination and biocentri-voltammetric applications. Therefore, following sections are devoted to the all trial and error studies of each section and promising methods were optimized for sensitive method development.

#### 3.1. Development of Composite Electrodes for Voltammetric Studies

Recent developments in voltammetric analysis of biologically important molecules encourages searching for more selective carriers as well as new electrode materials adoptable to different measuring systems. In the following section, the use of a variety of modified electrodes including metallic film and metal/metal oxide modified electrodes for GSH determination were given.

##### 3.1.1. Studies with BiFE

BiFE are good alternative for mercury film electrodes being less toxic and easy to use. Therefore, it was prepared *ex-situ* and then, it was subjected to DP voltammetry between -0.2 V and -0.8 V in the phosphate buffer medium including various concentration of GSH from  $1 \times 10^{-6}$  to  $5 \times 10^{-4}$  M. No well-defined current peak was observed for oxidation of GSH.

##### 3.1.2. Studies with AuNp/Al<sub>2</sub>O<sub>3</sub>.TiO<sub>2</sub> Modified GCPE

*The electrochemical behavior of GSH:* Figure 3.1 shows the cyclic voltammetric responses of 1 mM GSH at 100 mV/s scan rate of the sensors for (a) bare GCPE, (b) AuNp modified GCPE, (c) AuNp and Al<sub>2</sub>O<sub>3</sub>.TiO<sub>2</sub> nanopowder modified GCPE. Whole electrodes display a well defined electrochemical response upon addition of GSH.

However, as can clearly be seen from the voltammograms, the electrocatalytic reactions at the AuNp/Al<sub>2</sub>O<sub>3</sub>.TiO<sub>2</sub> nanopowder/GCPE electrode begins at a substantially more positive potentials (around 0.5 V), compared to the other electrodes (0.75 V) counterpart. Besides, AuNp/Al<sub>2</sub>O<sub>3</sub>.TiO<sub>2</sub> nanopowder/GCPE nanocomposite yields also a substantially higher sensitivity over the entire potential range.

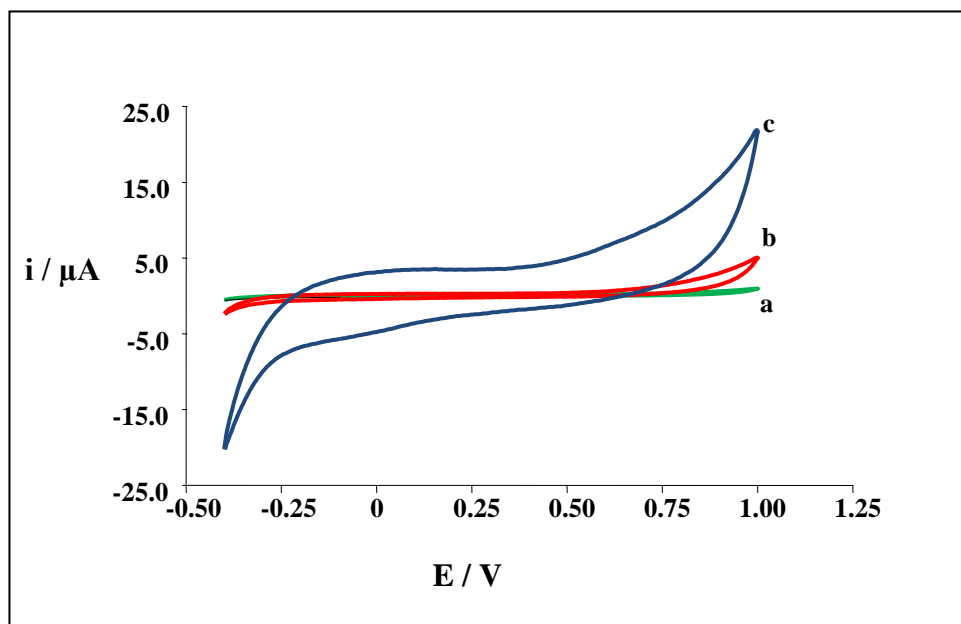


Figure 3.1. Cyclic voltammograms of 1 mM GSH at (a) for bare GCPE, (b) AuNp modified GCPE, and (c) AuNp and Al<sub>2</sub>O<sub>3</sub>.TiO<sub>2</sub> nanopowder modified GCPE in 0.05 M PBS (pH 7.0) at scan rate 100 mVs<sup>-1</sup>.

These results show the effective electrocatalytic ability of the composite electrode on GSH oxidation. The effect of the potential scan rate on the electro-oxidation of GSH was also studied by using cyclic voltammetry and the linear correlation of the peak current with  $v^{1/2}$  showed that the process is controlled by diffusion between 10 to 100 mVs<sup>-1</sup> (Figure 3.2). The curve deviates from linearity for higher scan rates indicating a quasi-reversible character of the oxidation process.

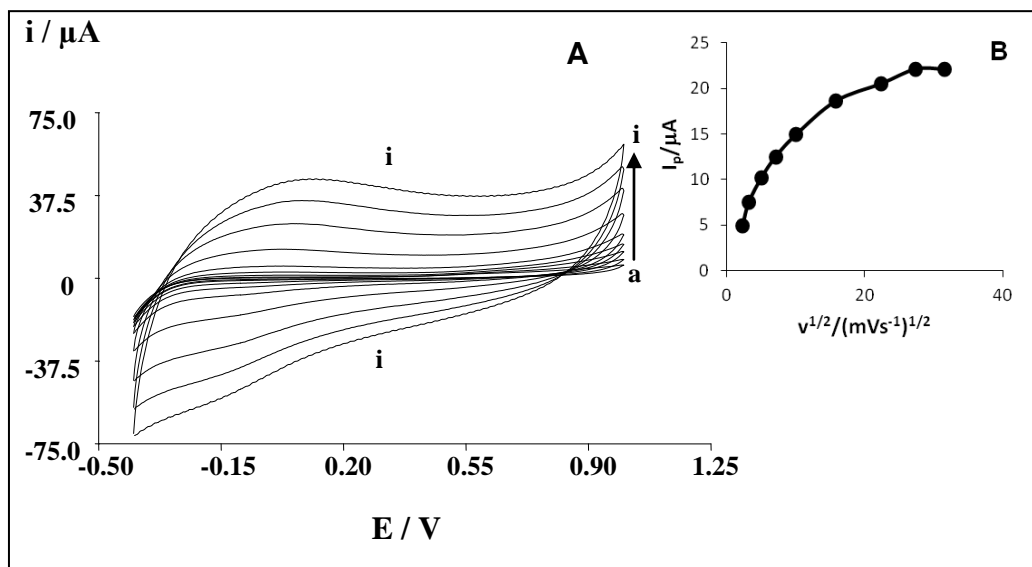


Figure 3.2. The different scan rates for 1mM GSH at the AuNp/Al<sub>2</sub>O<sub>3</sub>.TiO<sub>2</sub> nanopowder/GCPE (A) in 0.05 M PBS (pH 7.0); a) 5, (b) 10, (c) 25, (d) 50, (e) 100, (f) 250, (g) 500, (h) 750, and (i) 1000 mVs<sup>-1</sup>, (B) the curve of peak current ( $I_p$ ) vs  $v^{1/2}$ .

**Surface morphology of modified electrode:** Scanning electron microscopy was applied to characterize the surface morphology of the bare glassy carbon paste electrode (GCPE) (a) and the AuNp/Al<sub>2</sub>O<sub>3</sub>.TiO<sub>2</sub> nanopowder/GCPE (b, c, d) with different magnifications.

As shown in Figure 3.3, a spherical microparticles were observed on the bare GCPE surface with 2.00 kx magnification (a), and a highly packed non-porous surfaces characterizes the AuNp/Al<sub>2</sub>O<sub>3</sub>.TiO<sub>2</sub> nanopowder/GCPE with small dots onto the spherical micro-particles related to the AuNp (Çubukçu et al., 2007) and white cubical micro-particles which may be corresponded to the Al<sub>2</sub>O<sub>3</sub>.TiO<sub>2</sub> nanopowder with 1.00 kx (b), 2.00 kx (c), 3.52 kx (d) magnification, respectively.

From the images given in Figure 3.3, it can be concluded that commercially available Al<sub>2</sub>O<sub>3</sub>.TiO<sub>2</sub> nanopowder (the brand name) used in paste composition is not homogeneous and some pieces of the appeared to be larger than nano size.

**The Surface Characterization with QCM:** QCM technique is a simple and powerful tool which has been widely used in chemical and biological sensing. The QCM device comprise of a quartz crystal with different thickness sandwiched between two metal electrodes as a means of connecting the device to an external oscillator circuit that drives the quartz crystal at its resonant frequency.

Figure 3.4 shows the frequency responses of QCM sensors to adsorption of AuNp/Al<sub>2</sub>O<sub>3</sub>.TiO<sub>2</sub>/GSH suspension. From the obtained result, it can be concluded that the frequency was decreased as the surface mass of the QCM sensor with the adsorption of AuNp/Al<sub>2</sub>O<sub>3</sub>.TiO<sub>2</sub>/GSH suspension was increased.

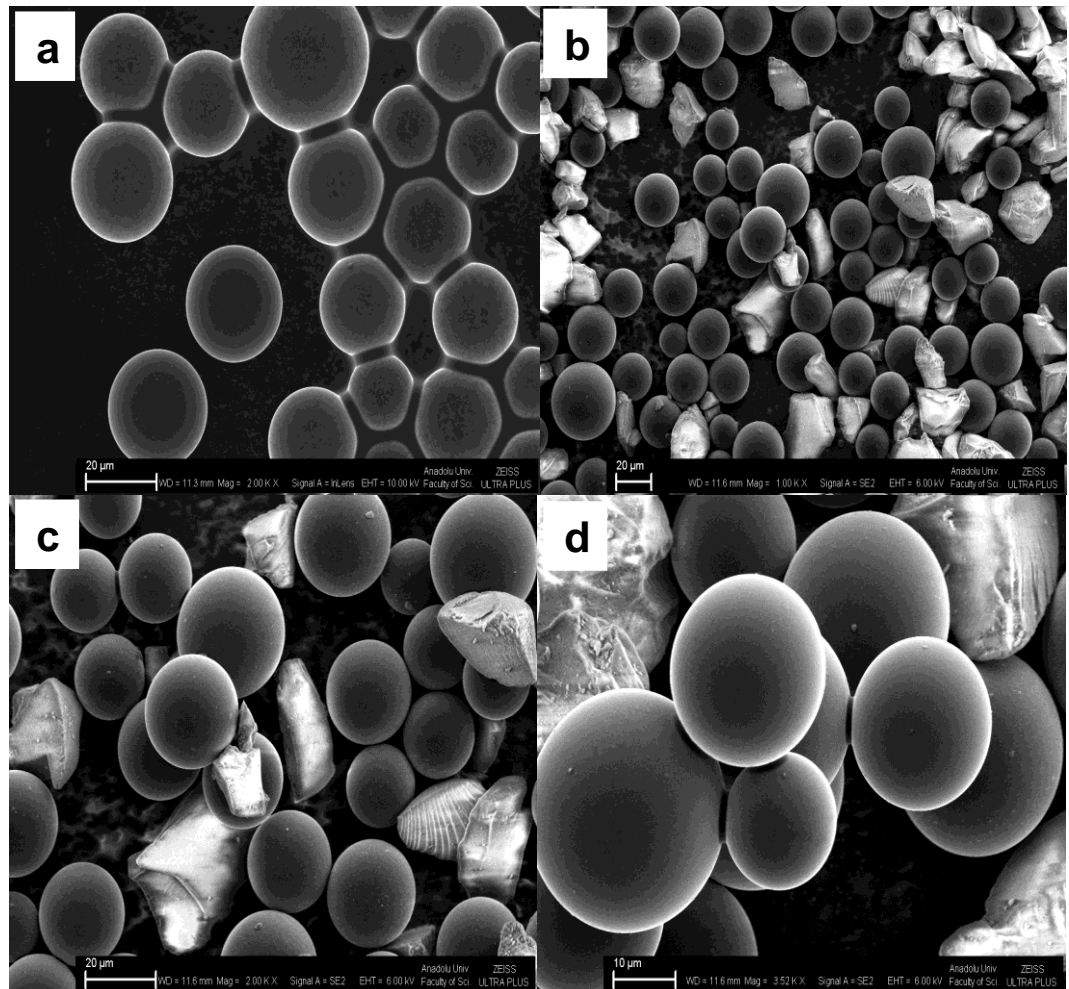


Figure 3.3. The SEM images of bare GCPE (a) with an accelerating potential of 10.00 kV, and AuNp/Al<sub>2</sub>O<sub>3</sub>.TiO<sub>2</sub> nanopowder/GCPE with different magnification of (b) 1.00 kx, (c) 2.00 kx, (d) 3.52 kx and accelerating potential of 6.00 kV.

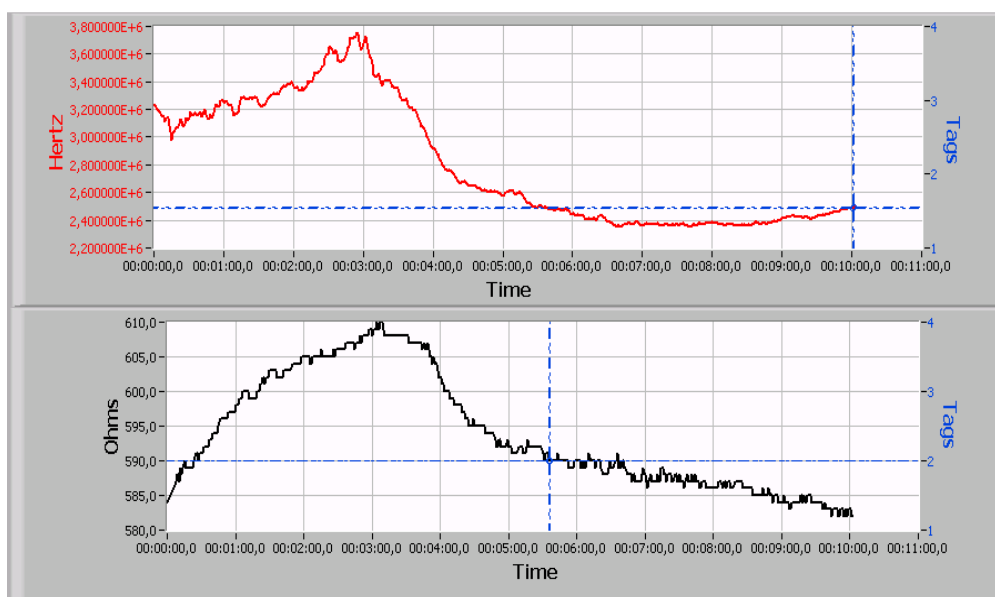


Figure 3.4. The frequency response of  $\text{Al}_2\text{O}_3.\text{TiO}_2/\text{AuNp}/\text{GSH}$  suspension modified QCM sensor.

### **3.1.2.1. Optimization of electrode composition**

***Influence of  $\text{Al}_2\text{O}_3.\text{TiO}_2$  nanopowder amount:*** In order to optimize the composition of the electrode, glassy carbon paste composites including various percentages of  $\text{Al}_2\text{O}_3.\text{TiO}_2$  nanopowder (2, 4, 8, 10, 20 and 30%) were prepared and their electroanalytical performances were examined by recording DP voltammograms of 0.25 mM GSH (Figure 3.5).

It can be followed from the figure that a large peak corresponding to the oxidation of gold particles were observed at 1.0 V and a small, broad peak at around 0.65 V corresponds to the oxidation of GSH. The height of this peak depends on the  $\text{Al}_2\text{O}_3.\text{TiO}_2$  nanopowder amount and increases from 2% to 20%, the peak current increases and then a slight decrease is obtained at  $\text{Al}_2\text{O}_3.\text{TiO}_2$  nanopowder amount higher than 20% (Figure 3.6). As a result 20%  $\text{Al}_2\text{O}_3.\text{TiO}_2$  nanopowder amount was chosen as optimum amount and used for further studies.



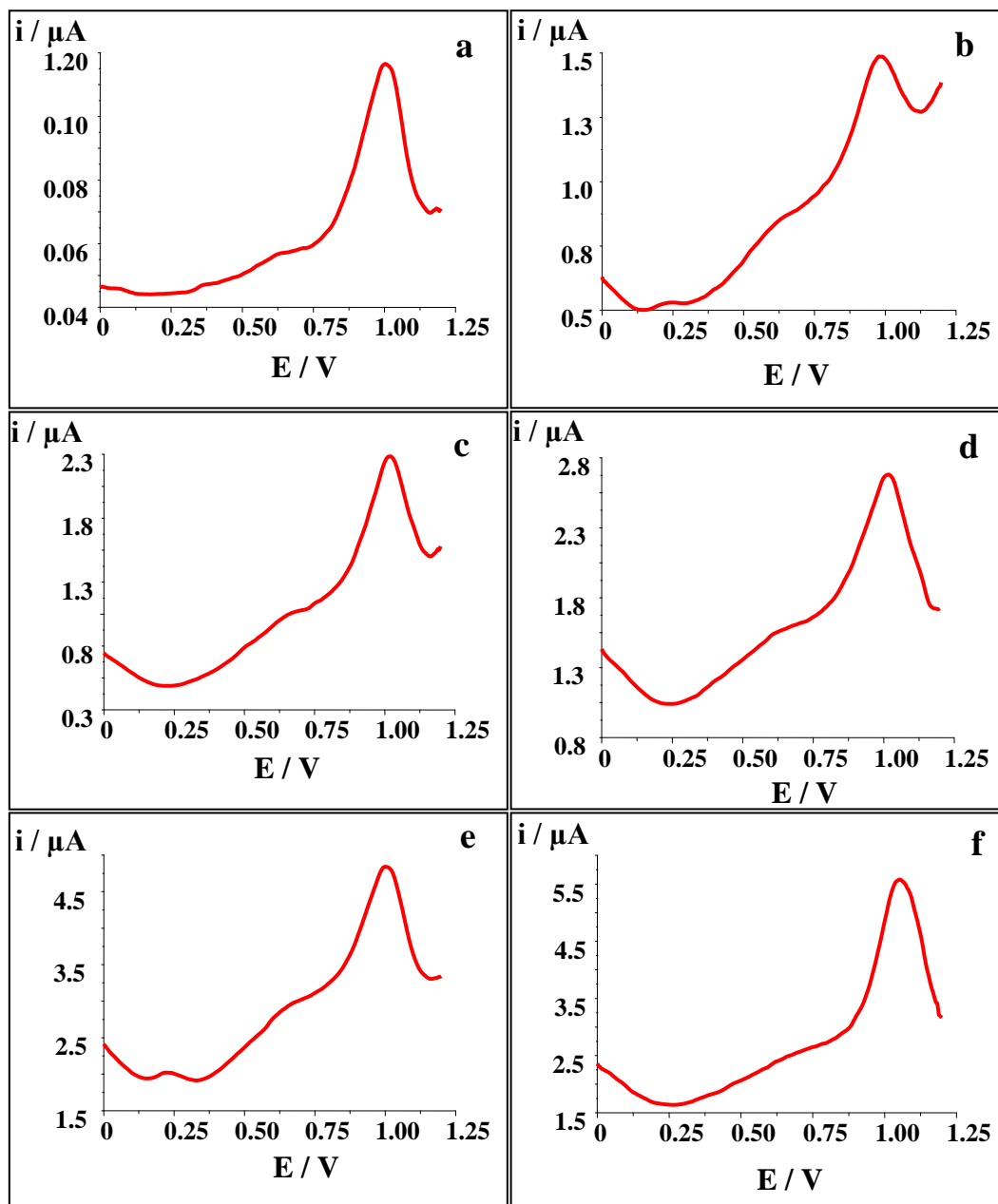


Figure 3.5. DP voltammograms of 250  $\mu\text{M}$  GSH on the sensor response at different portions of  $\text{Al}_2\text{O}_3\cdot\text{TiO}_2$  nanopowder: a to f: 2, 4, 8, 10, 20 and 30%, respectively; conditions: PBS (0.050 M, pH 7.0), 20  $\mu\text{L}$  AuNp added into 10 mL of PBS.

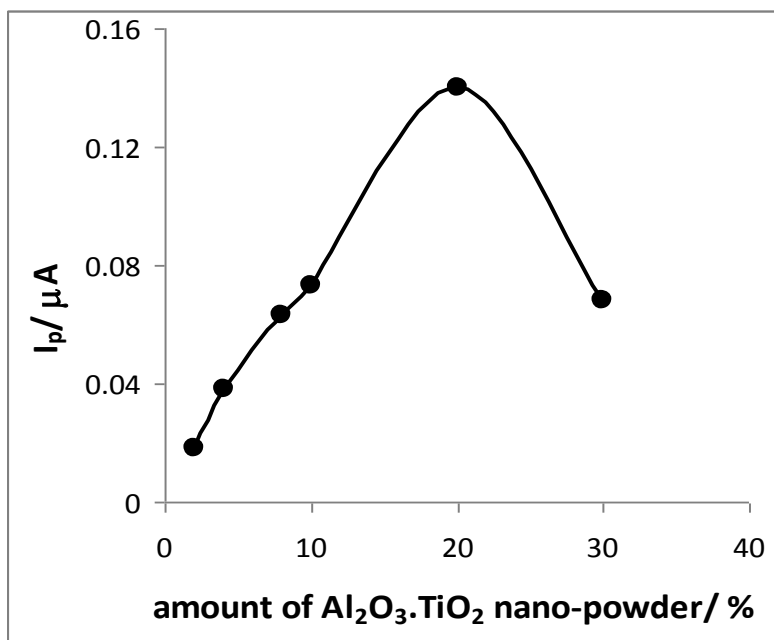


Figure 3.6. The effect of optimum Al<sub>2</sub>O<sub>3</sub>.TiO<sub>2</sub> nanopowder curve of AuNp/Al<sub>2</sub>O<sub>3</sub>.TiO<sub>2</sub> nanopowder/GCPE.

**Influence of AuNp amount:** The next step of the work consisted of finding the optimum AuNp amount. Figure 3.7 demonstrates the differential pulse voltammograms depending on various amounts AuNp (1, 2, 5, 10, 20 and 30 μL added into 10 mL of PBS) on the current response of 0.25 mM GSH.

As can clearly be seen from the figure, the current increases from 1 to 20 μL and then a decrease is obtained for volumes greater than 20 μL, so 20 μL of AuNp was chosen as optimum Au np amount (Figure 3.8).

According to our previous work, this decrease can be referred to increment of resistance and capacitance that are caused by double layer of the electrode since the active sites of the graphite decreases due to the increase in AuNp amount (Çubukçu et al., 2007).

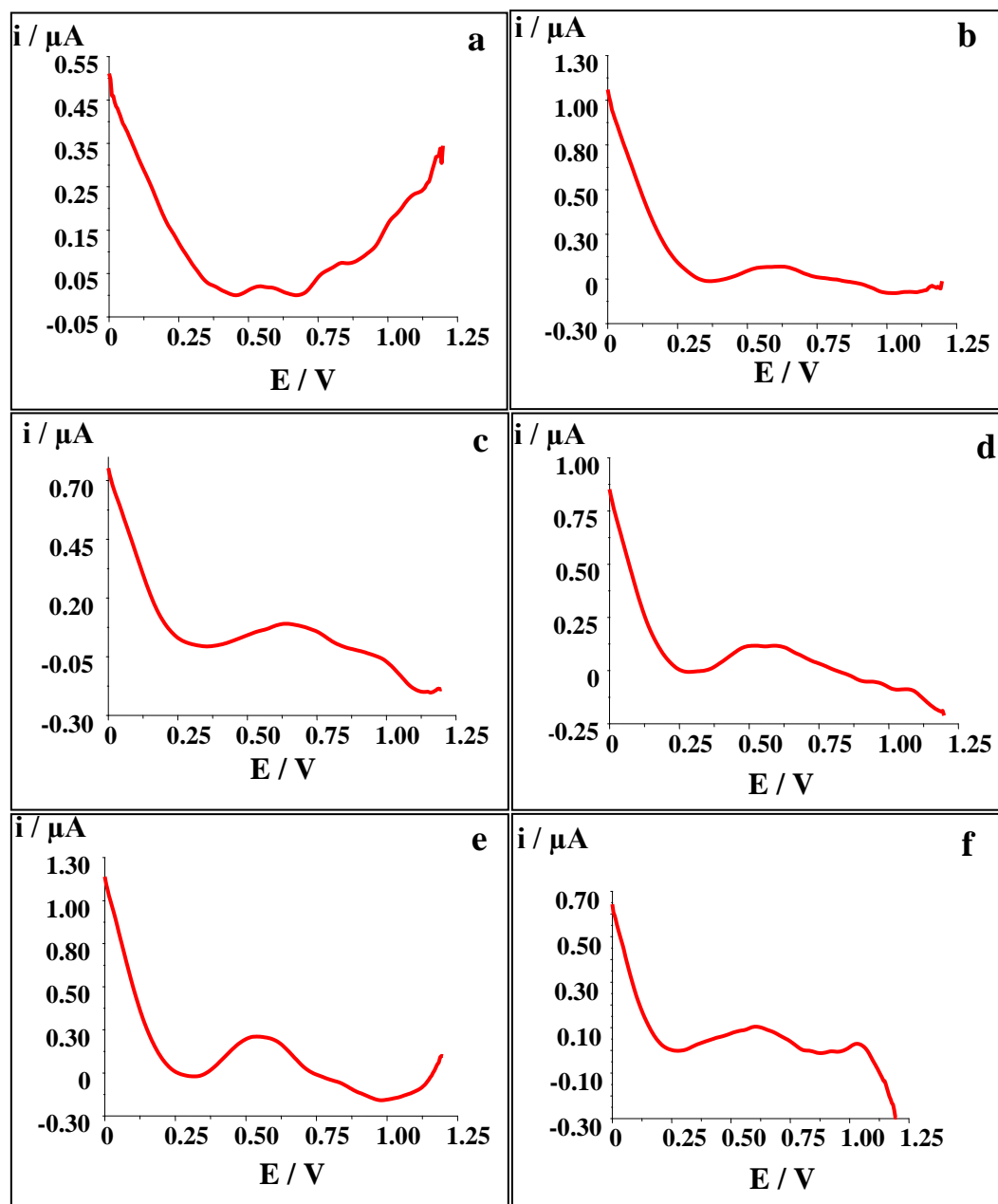


Figure 3.7. DP voltammograms of 250  $\mu\text{M}$  GSH on the sensor response at different volumes of AuNp (0.75A<sub>520</sub> units/mL; 10nm ~0.001% as HAuCl<sub>4</sub>): (a) 1  $\mu\text{L}$ , (b) 2  $\mu\text{L}$ , (c) 5  $\mu\text{L}$ , (d) 10  $\mu\text{L}$ , (e) 20  $\mu\text{L}$ , (f) 30  $\mu\text{L}$  in 10 mL of 0.05 M PBS (pH 7.0).

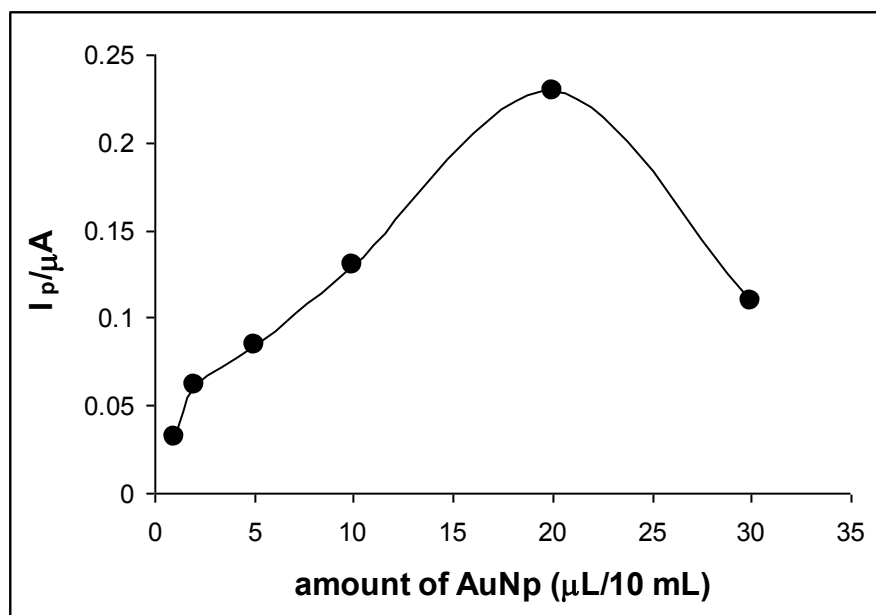


Figure 3.8. The effect of AuNp amount for 250  $\mu\text{M}$  GSH at AuNp/ $\text{Al}_2\text{O}_3$ . $\text{TiO}_2$  nanopowder/GCPE.

**Effect of pH:** The pH of the working buffer is usually regarded as a one of the most important factor determining the electrochemical behavior of GSH. Therefore, the electrochemical behavior of GSH in 0.05 M phosphate buffered solution with various pH ranges (6.0-8.5) was studied. Figure 3.9 shows that the DP voltammograms of AuNp/ $\text{Al}_2\text{O}_3$ . $\text{TiO}_2$  nanopowder/GCPE.

As can be seen from the Figure 3.10, the response current of the electrode to GSH reaches a maximum value at pH 7.0 and then decreases gradually with increasing of pH. Thus, pH 7.0 was taken as the optimum pH for the electrochemical determination of GSH.

Raof *et al.* (2009) studied the electrochemical behavior of GSH and Tryptophan (Trp) in 0.1 M phosphate buffered solution with various pHs ( $2.0 < \text{pH} < 12.0$ ) at the surface of  $\text{TiO}_2$  nanoparticles and ferrocene carboxylic acid (FCCa) modified carbon paste electrode (FCCa- $\text{TiO}_2$ MCPE) for simultaneous determination of GSH and Trp.

They showed that for both of compounds, the electrocatalytic peak current and peak potential depended on the solution pH, and therefore studied value at pH 7.0 (Raouf et al., 2009).

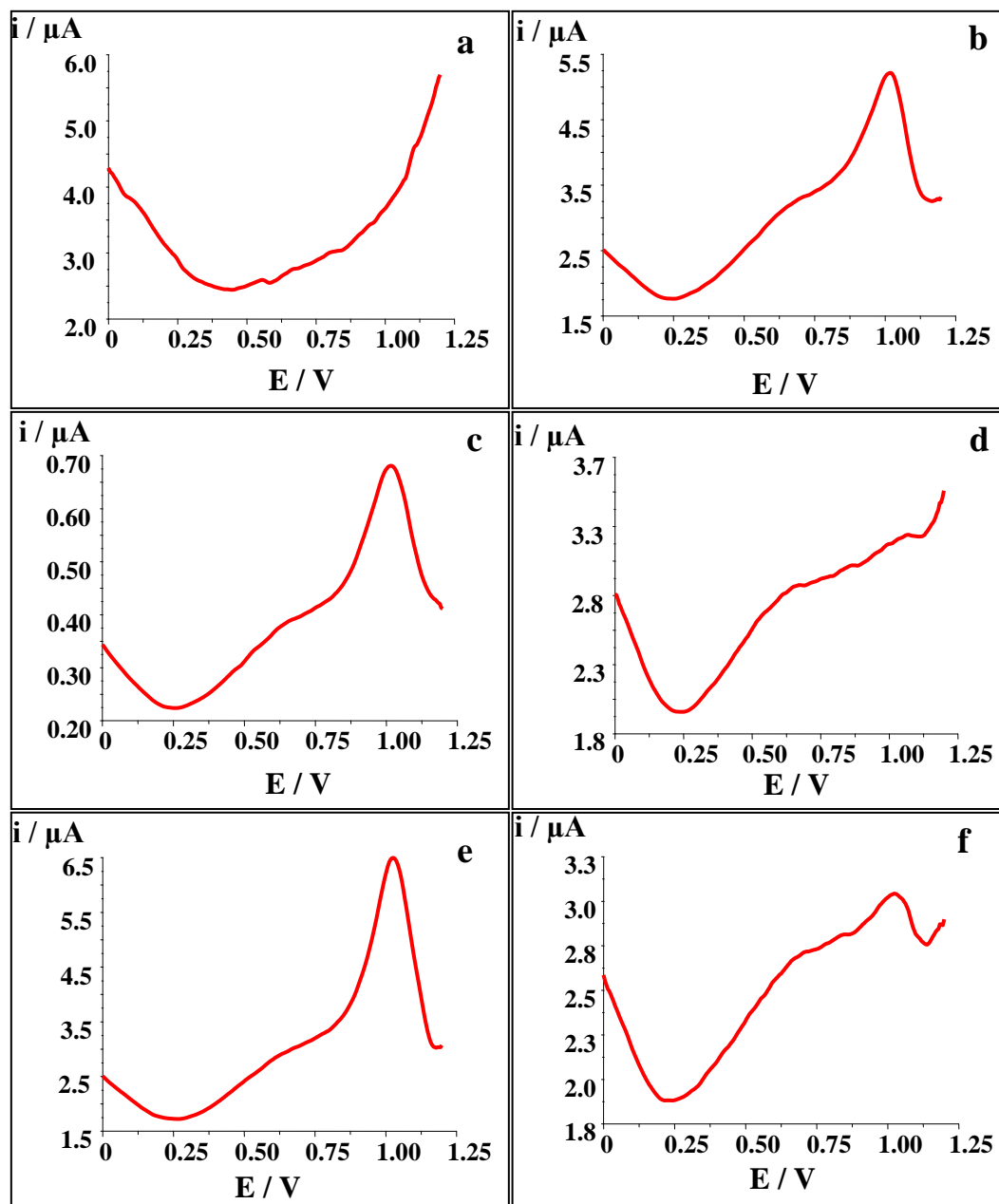


Figure 3.9. DP voltammograms of 250  $\mu\text{M}$  GSH on the sensor response at different pH ranges: (a) 6.0, (b) 6.5, (c) 7.0, (d) 7.5, (e) 8.0, (f) 8.5; conditions: 0.05M PBS, 20  $\mu\text{L}$  AuNp added into 10 ML of PBS.

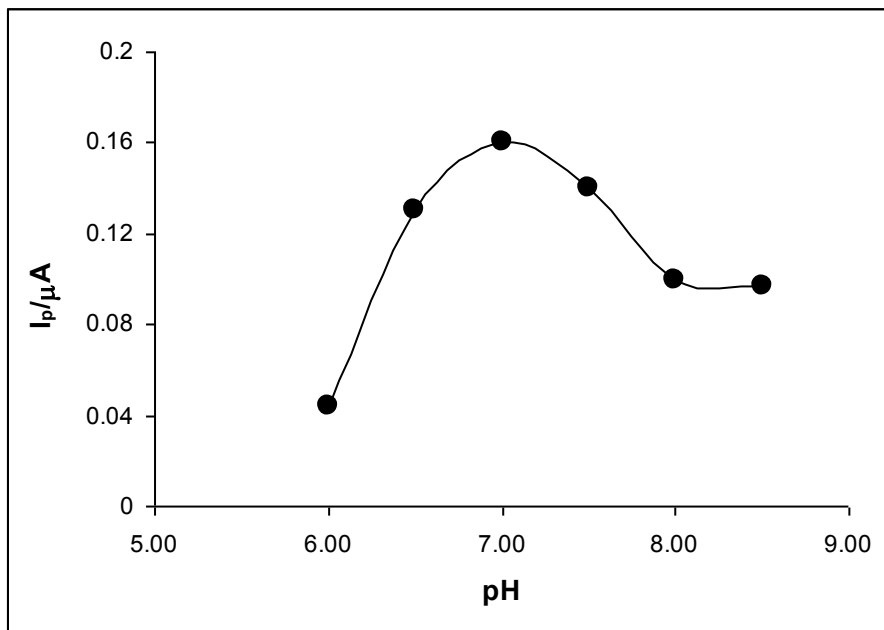


Figure 3.10. The effect of pH (from 6.0 to 8.5) on current values for 250  $\mu M$  GSH at AuNp/ $Al_2O_3$ .TiO<sub>2</sub> nanopowder /GCPE.

### **3.1.2.2. Analytical characteristics**

After the optimization of experimental parameters, analytical characteristics of the method were examined. Two linear ranges were obtained for the developed sensor between 5-50 and 100-750  $\mu M$  with the correlation coefficients of  $R^2=0.9943$  and  $R^2=0.9878$  respectively (Fig. 3.11-A and B). R.S.D values were calculated for 250  $\mu M$  GSH ( $n=6$ ) and found as 6.66%. The storage stability of the sensor is a very important parameter for long-term applications. The developed sensor was showed a long lifetime of one week when kept at room temperature in a dry atmosphere, it was observed that 80% of the activity was found to be recovered. During this stage 36 measurements were carried out and no decreases were found in the signal responses.

On the other hand, developed sensor performance was compared with other electrochemical sensors devoted for the determination of GSH in terms of analytical characteristics. The results were demonstrated in Table 3.1. Considering the linear range, it can be said that developed sensor's linear range is in acceptable limits and is similar with some of other electrodes.

Regarding to relative standard deviation (RSD) value nanostructure composite electrode has slightly higher RSD value that can be attributed to composite structure of the developed system.

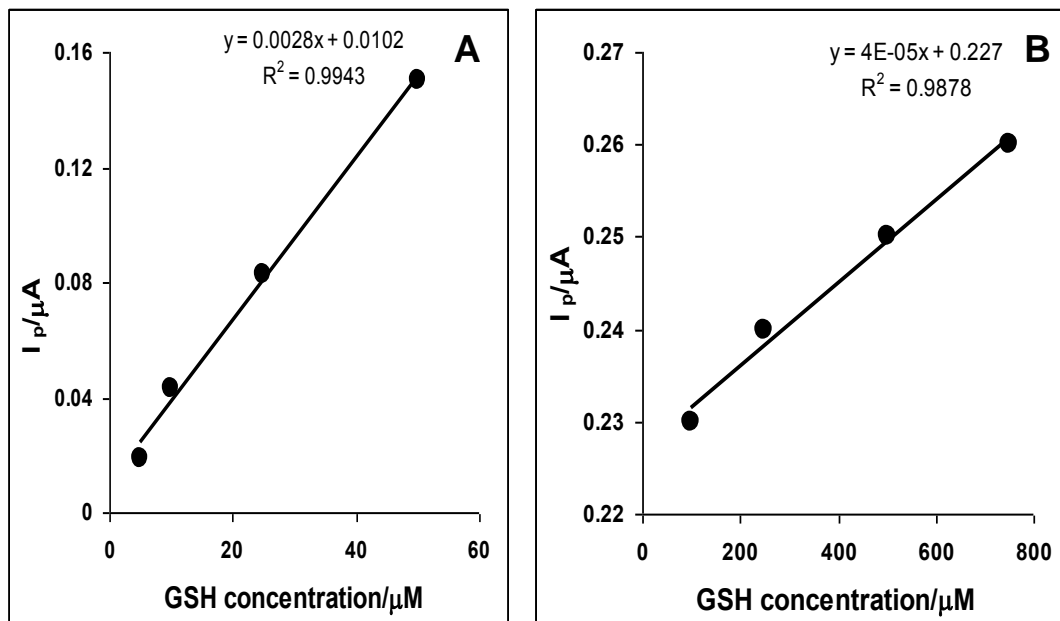


Figure 3.11. Calibration graph for GSH at AuNp/Al<sub>2</sub>O<sub>3</sub>.TiO<sub>2</sub> nanopowder/GCPE at lower concentration (A) and higher concentration (B) in 0.05 M PBS (pH 7.0), 25°C.

Table 3.1. A comparison of the analytical characteristics of differently modified electrochemical sensors for detection of GSH.

Electrode	Modifier	Linear Range ( $\mu M$ )	RSD (%)	References
CPE	TTF-TCNQ <sup>a</sup>	20-300	5.1	(Calvo-Marzal et al., 2004)
GC	OMC-Co <sup>b</sup>	1.0-7.0	2.1	(Hou et al., 2009)
GC	PmAP <sup>c</sup>	0.1-5.0	2.7	(Öztekin et al., 2011)
ITO NFE	CNFs-PDDA/PB <sup>d</sup>	6.0-17.4	5.2	(Muthirulan et al., 2011)
CPE	FM <sup>e</sup>	2.2-3500	-	(Raof et al., 2009)

<sup>a</sup> Tetrathiafulvalene (TTF)-tetracyanoquinodimethane, <sup>b</sup> ordered mesoporous carbon/Cobalt, <sup>c</sup> poly-m-aminophenol, <sup>d</sup> carbon nanofibers-poly(diallyldimethylammonium chloride)/Prussian blue, <sup>e</sup> ferrocene-modified, NFE: nanocomposite film electrode

### **3.1.2.3. Sample application**

As mentioned in the experimental part, prepared biosensor was applied for GSH detection in white wine sample by using standard addition method. A Turkish wine sample was diluted with phosphate buffer solution (0.05M, pH 7.0) in the ratio of 1:100 and a known amount of GSH (250  $\mu$ M) was added in the sample solution.

The change in peak current was monitored after the addition of known amount of GSH to diluted wine sample. Each analysis was performed three times and Recovery was calculated as  $100 \pm 0.14$  %.

### **3.1.3. Studies with AuNp/nano-micro TiO<sub>2</sub> based GCPE**

The commercial Al<sub>2</sub>O<sub>3</sub>.TiO<sub>2</sub> nanopowder was used in nano structure based composite electrode in determination of GSH which was investigated above study. In this part, the voltammetric responses were explored with the produced nano-micro TiO<sub>2</sub> structure incorporating into the same electrode system relating with the analysis of GSH.

***Nano-micro TiO<sub>2</sub> amount:*** Here, the amount of nano-micro TiO<sub>2</sub> only was optimized since the other parameters were optimized in previous study concerning to the optimization of working parameters of prepared sensors. According to this, Figure 3.12 shows the effect of nano-micro TiO<sub>2</sub> amount on the current response. As can be seen from the figure, the peak current increases from 2% to 4% and then a sharp decrease was obtained for higher amount of nano-micro TiO<sub>2</sub>. Thus, 4% nano-micro TiO<sub>2</sub> was chosen as the optimum amount.



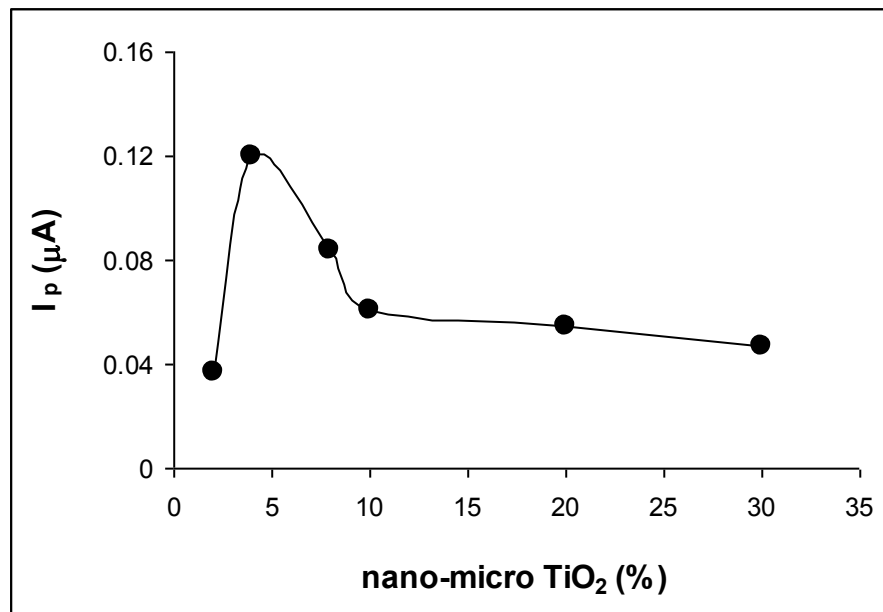


Figure 3.12. The effect of nano-micro TiO<sub>2</sub> amount on the sensor response.

### 3.1.3.1. Analytical characteristics

After the optimization of nano-micro TiO<sub>2</sub> amount, an analytical characteristic of the method was examined. The linear range was obtained for the developed sensor between 25-1000 µM with the correlation coefficients of  $R^2 = 0.9965$  (Figure 3.13). R.S.D values were calculated for 250 µM GSH ( $n=4$ ) and found as 8.44%.

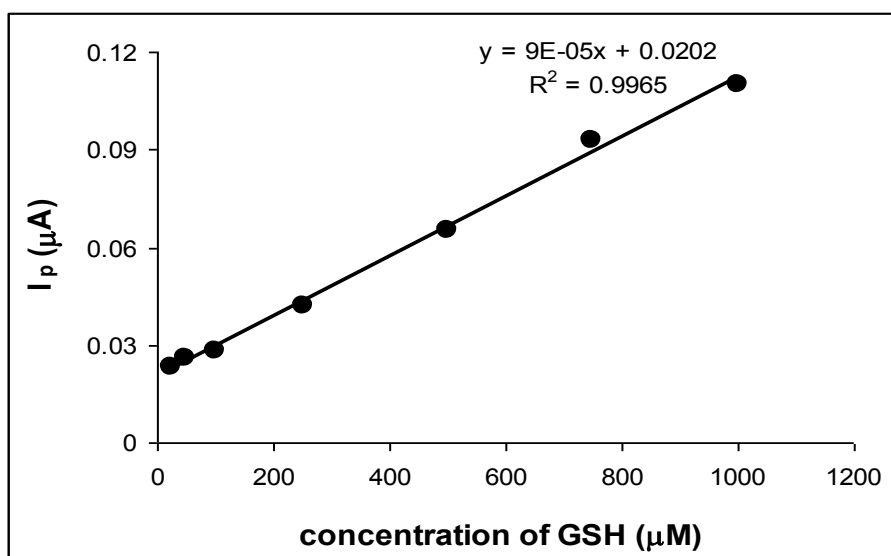


Figure 3.13. The linear range of nano-micro TiO<sub>2</sub>/AuNp/GCPE

### 3.2. Centri-voltammetric Studies

In this part of the thesis, centri-voltammetric studies were conducted to search any improvement in the sensitivity with the composite electrodes as it was pointed out in the aim of the thesis. For this purpose a home-made centri-voltammetric cell was constructed and employed in voltammetric analysis.

The first application of centri-voltammetry is the usage of AuNp/ $\text{Al}_2\text{O}_3\cdot\text{TiO}_2$  nanopowder/GCPE as a transducer in electrochemical detection of GSH. The composite sensor was prepared as usual procedure. The optimum amount of AuNp established in the former study and different concentrations of GSH were injected into the 0.05 M PBS (pH 7.0). The centri-voltammetric cell was centrifuged at 3000 rpm for 3 minutes and then, the DP voltammograms were recorded in the potential range 0 V and +1.2 and no well-defined peak was observed relating with the electrochemical detection of GSH in a concentration range of  $10\text{-}100 \times 10^{-6}$  M.

Another experiment was designed for centri-voltammetric analysis by using bare GCPE and addition of  $250 \mu\text{M}$   $\text{HAuCl}_4$  into the solution containing various amounts of GSH. Although an oxidation peak was observed relating to Au (III) around +0.8 V, no voltammetric signal corresponding to the GSH oxidation.

Alternatively, MWCNT modified electrodes were used. The effectiveness of the proposed method can be seen from Figure 3.14 where  $400 \mu\text{M}$  GSH was used. The wide peak of GSH at 0.6 V at a MWCNT-CPE (Fig. 3.14-b) has been observed after the addition of silica gel and centrifugation at 4000 rpm. It is known that this process produces a thin film on the electrode surface trapping in the GSH content of the solution (Fig. 3.14-c).

The improvement of the signal can be assigned to the enrichment of the analyte in this film at a certain extent. Actual improvement was observed when  $30 \mu\text{L}$  of AuNp solution was added into the cell content as described in the procedure. As a result, GSH peak has doubled (Fig. 3.14-d). Here, AuNP serves as a carrier reagent and as a modifier as well.

Due to strong affinity of these nanoparticles to the thiol groups, it has been believed that the accumulation process is strengthened and as a result more significant GSH peak was obtained.

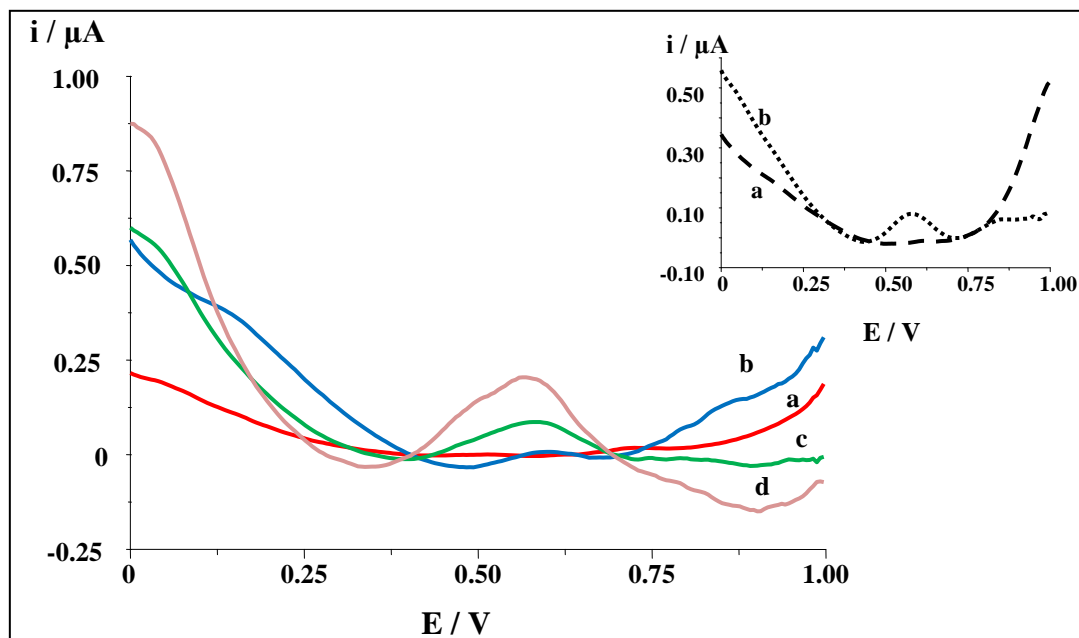


Figure 3.14. DP voltammetric responses of the 4% MWCNT/CPE with centri-voltammetry (a) background, (b) 400  $\mu\text{M}$  GSH, (c) a+ 1 mg silica gel, (d) c+ AuNp, in 0.05 M PBS (pH 7.0). Inset: A comparison of (a) bare CPE and (b) 4% MWCNT modified CPE for 400  $\mu\text{M}$  GSH including silica gel and AuNp.

The performance system was tested with bare and MWCNT modified CPE. It can be seen that when the 4% MWCNT was incorporated into the CPE, a significant and well-defined peak could be observed relating to electrochemical oxidation of GSH with centri-voltammetry whilst no distinct peak current was obtained with bare CPE (Fig. 3.14 inset). The voltammograms show that the plain CPE had a current value of 0.0047  $\mu\text{A}$  while the MWCNT including CPE had current value of 0.087  $\mu\text{A}$ . The significant increase in current value can be attributed to the electrocatalytic activity of CNT, which can mediate the electron transfer reactions (Anık and Çubukçu, 2008).

In our previous work, the effect of MWCNT and single-wall carbon nanotube (SWCNT) on CPE electrochemical response was examined by introducing various portions of CNT (2%, 4%, 8%, and 100%) into the CPE as xanthine biosensor transducers.

The optimum electrode structure was determined by comparing the electroanalytical performance of prepared electrodes towards ferricyanide (Anık and Çubukçu, 2008). From the obtained results, the best current values and hence optimum structures correspond to electrodes that contain 4% MWCNT.

### **3.2.1. Optimization of the experimental parameters**

The experimental parameters including silica gel and AuNp amounts, pH, adsorption time and centrifugation parameters were optimized before the examination of analytical characteristics.

*Effect of Silica Gel Amount:* Figure 3.15 demonstrates the centri-voltammetric responses of silica gel particles in various amounts on the current response of 250  $\mu$ M GSH.

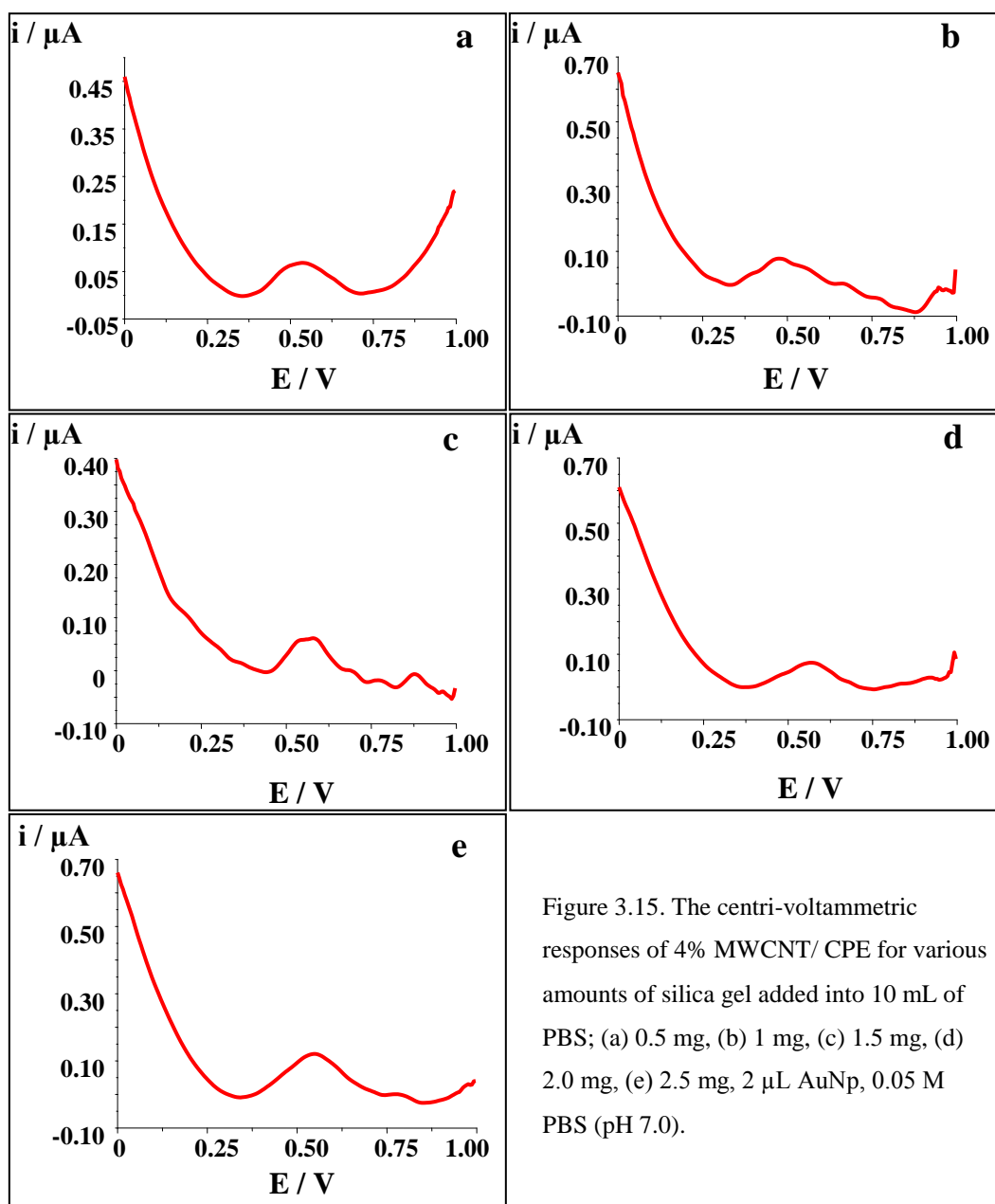


Figure 3.15. The centri-voltammetric responses of 4% MWCNT/ CPE for various amounts of silica gel added into 10 mL of PBS; (a) 0.5 mg, (b) 1 mg, (c) 1.5 mg, (d) 2.0 mg, (e) 2.5 mg, 2  $\mu\text{L}$  AuNp, 0.05 M PBS (pH 7.0).

As can clearly be seen from the Figure 3.16, the peak current increases when the silica gel amount was increased from 0.5 to 1.0 mg and then a slight decrease was obtained for amounts greater than 1.0 mg silica gel. This can be attributed to the altered surface conductivity of the electrode due to the thickening of the film. Therefore, 1.0 mg of silica gel was chosen as optimum amount of carrier material and used for further studies.

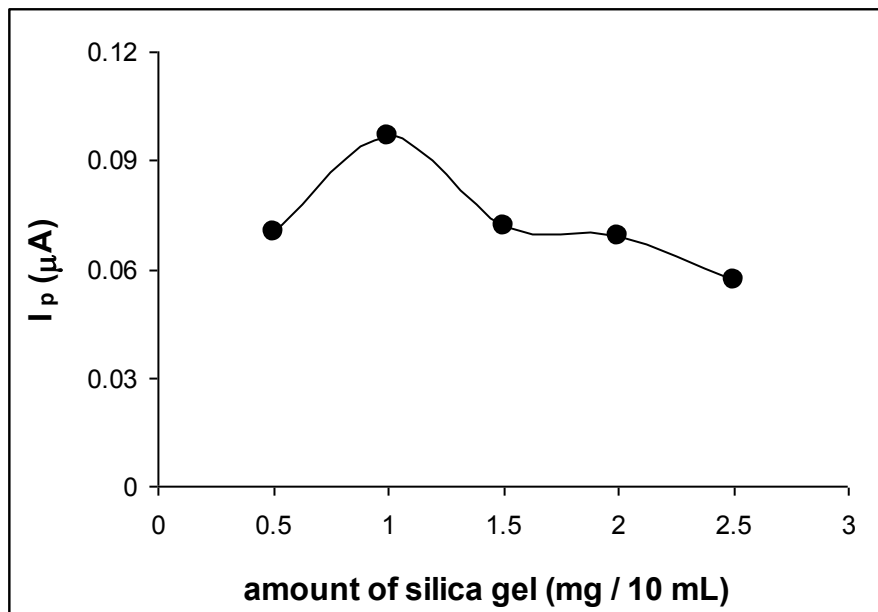


Figure 3.16. The effects of silica gel amount added into 10 mL of cell solution containing 250  $\mu\text{M}$  GSH on the sensor response.

***Influence of AuNp amount:*** Similarly, various amounts of AuNp (10, 20, 30, 40, and 50  $\mu\text{L}$  added into 10 mL of PBS) were tested by applying DP voltammetry to examine their effect on the current response of 250  $\mu\text{M}$  GSH (Figure 3.17). As can clearly be seen from the Figure 3.18, the amount of AuNp is critical for the signal formation. Best results were obtained with 30  $\mu\text{L}$  of AuNp solution. The decrease in the peak current for higher amounts of AuNp can be assigned to the thickening of the film which may have caused a change on the surface characteristics.

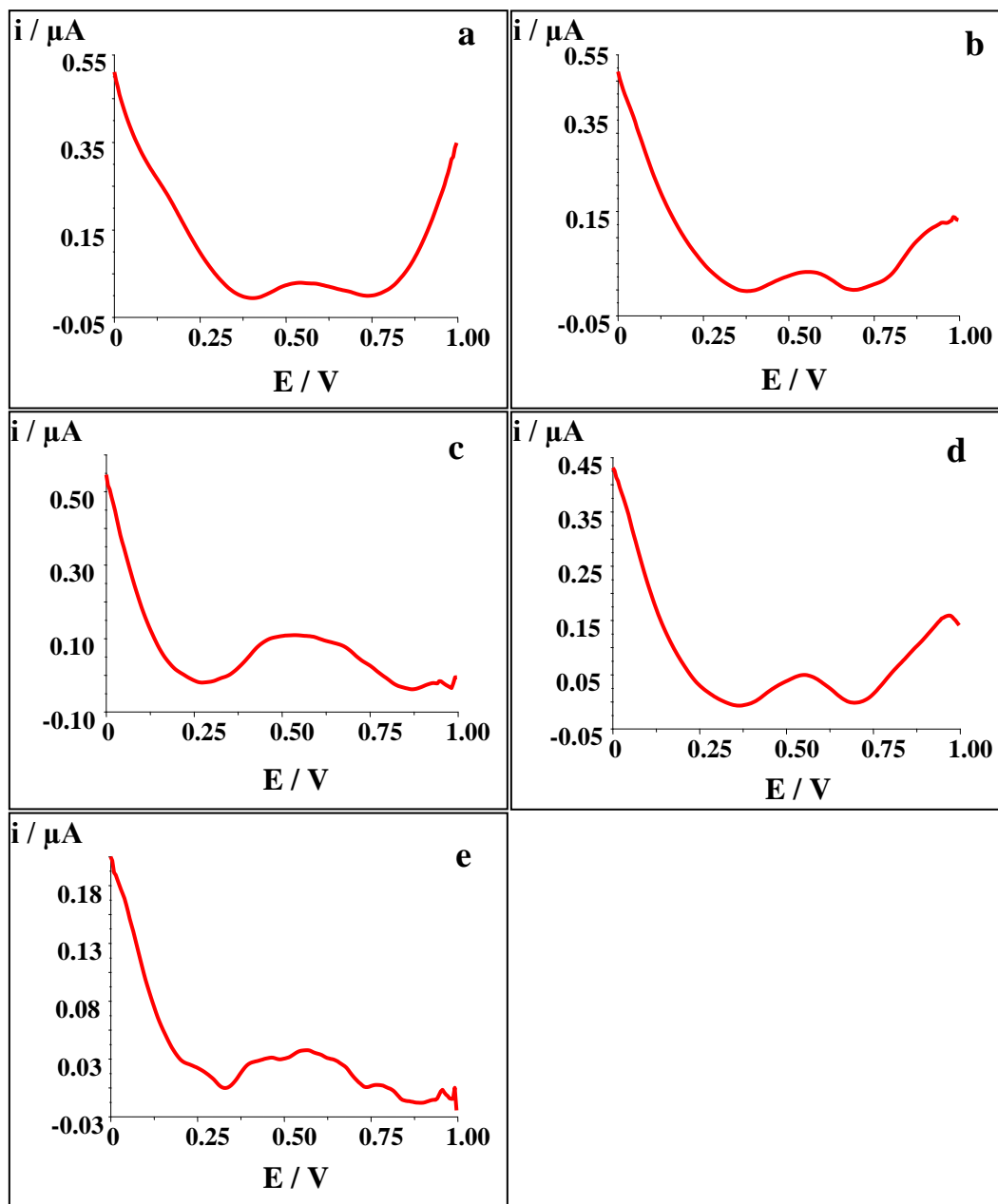


Figure 3.17. The centri-voltammetric responses of 4% MWCNT/ CPE for various amounts of AuNp; (a) 10  $\mu\text{L}$ , (b) 20  $\mu\text{L}$ , (c) 30  $\mu\text{L}$ , (d) 40  $\mu\text{L}$ , (e) 50  $\mu\text{L}$  were added into 10 mL of 0.05 M PBS (pH 7.0) containing 1 mg of silica gel.

**Influence of pH:** The medium pH is usually regarded as a one of the most important factors in electrochemical measurements. The electrochemical behavior of GSH in 0.05 M phosphate buffered solution was studied in a pH range of 6.0 to 8.0 and best results were obtained at pH 7.0. As can be seen from Figure 3.19, a gradual decrease was obtained as the pH value increases.

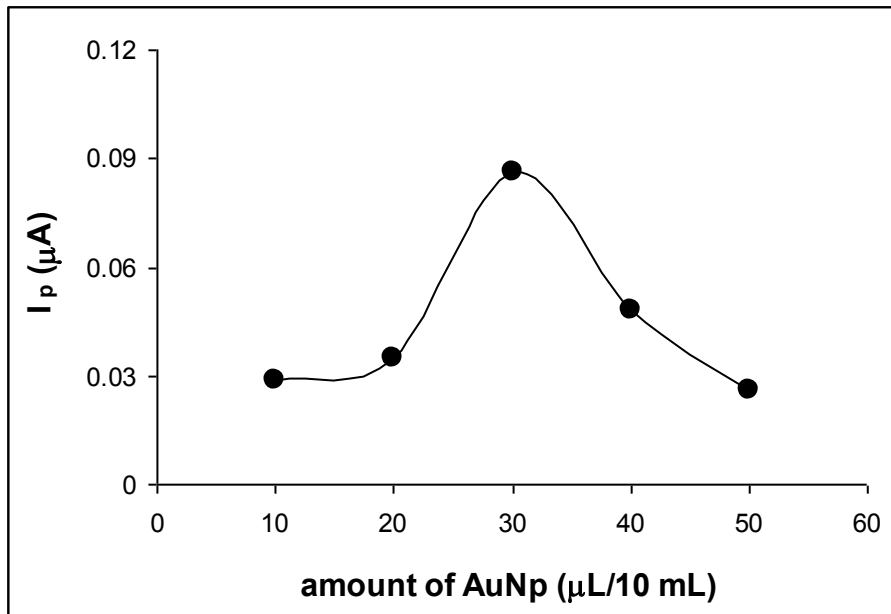


Figure 3.18. The effect of AuNp amount for 250  $\mu\text{M}$  GSH on the sensor response.

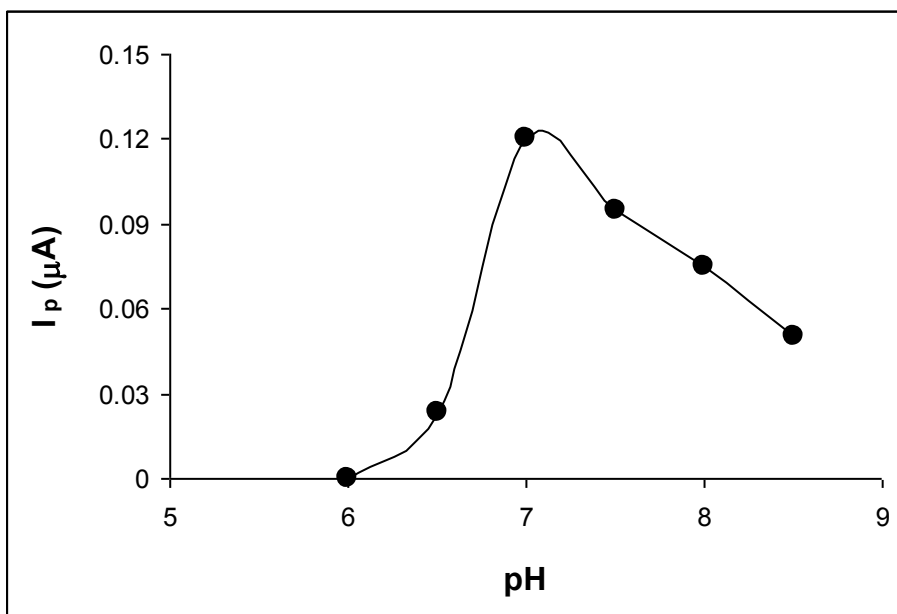


Figure 3.19. The effect of pH for 250  $\mu\text{M}$  GSH on the sensor response.



In accordance with previous studies on GSH (Lima et al., 2008; Çubukçu et al., 2012; Raoof et al., 2009; Mao and Yamamoto, 2000) this decrease can be attributed to structural effect that provides the increment of electronic density, facilitating the oxidation of the species formed in the chemical step (Lima et al., 2008).

***Influence of the adsorption time:*** The time elapsed in adsorption process is of great importance allowing the maturation of the precipitate and an effective enrichment of the analyte. The interaction of GSH with AuNps added into 250  $\mu\text{M}$  GSH solution was examined by allowing the mixture for adsorption for 1-20 min. The Figure 3.20 shows that the DP voltammetric signals of the developed sensor in different times of adsorption process.

It is evident from Fig. 3.21 that best peak current value was obtained when 7 min. was applied as adsorption period. The decline in the response observed for longer adsorption times can be attributed to the agglomeration in the solution at some extent which may cause an alteration in nanoparticle behavior and possible desorption process of the silica gel. Therefore, 7 min was selected as the optimum time and longer adsorption times were avoided.

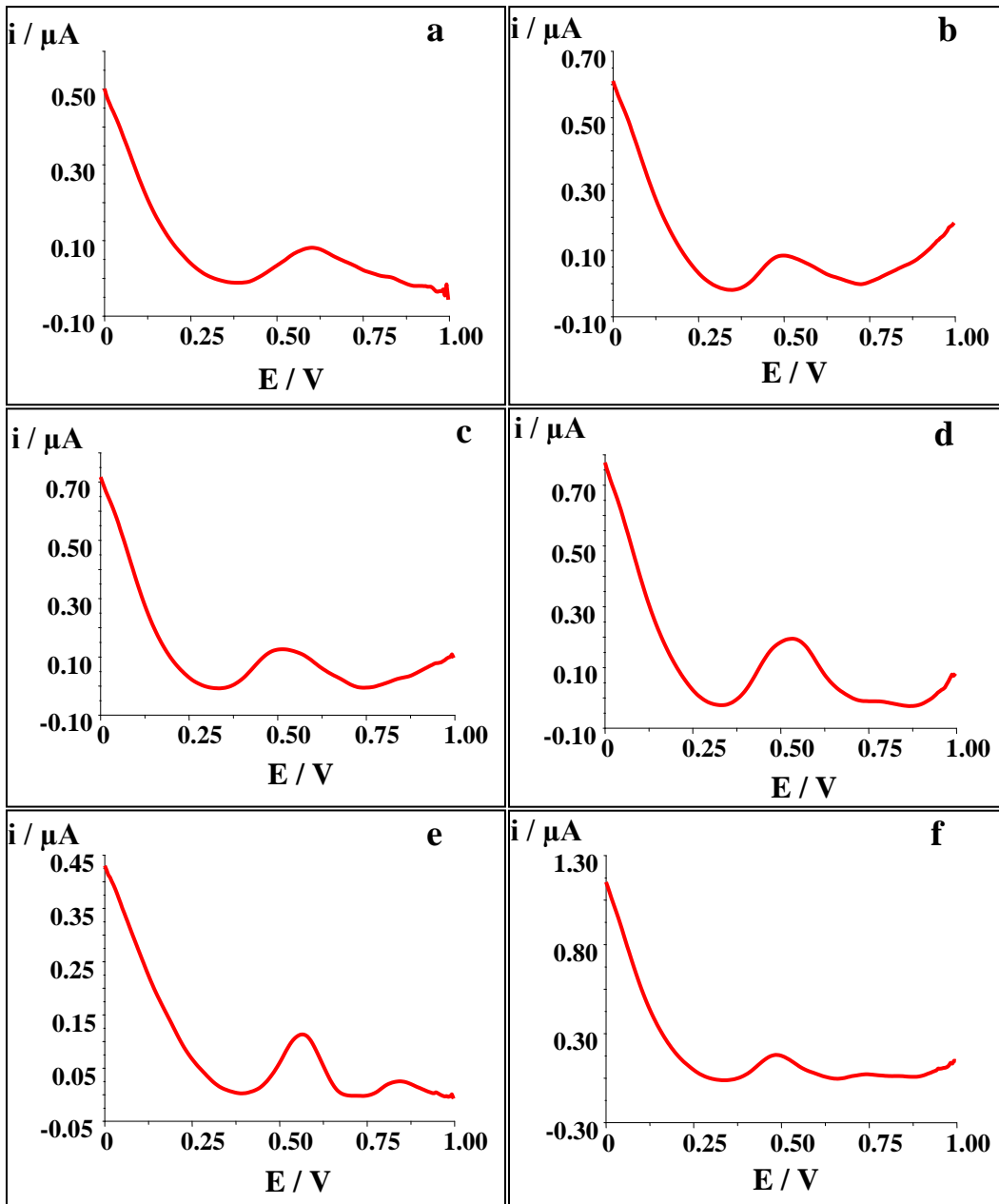


Figure 3.20. The centri-voltammetric responses of 4% MWCNT/ CPE for different adsorption time; (a) 1 min, (b) 2 min, (c) 5 min, (d) 7 min, (e) 10 min, (f) 20 min, 1 mg silica gel, 30  $\mu\text{L}$  AuNp, 0.05 M PBS (pH 7.0).

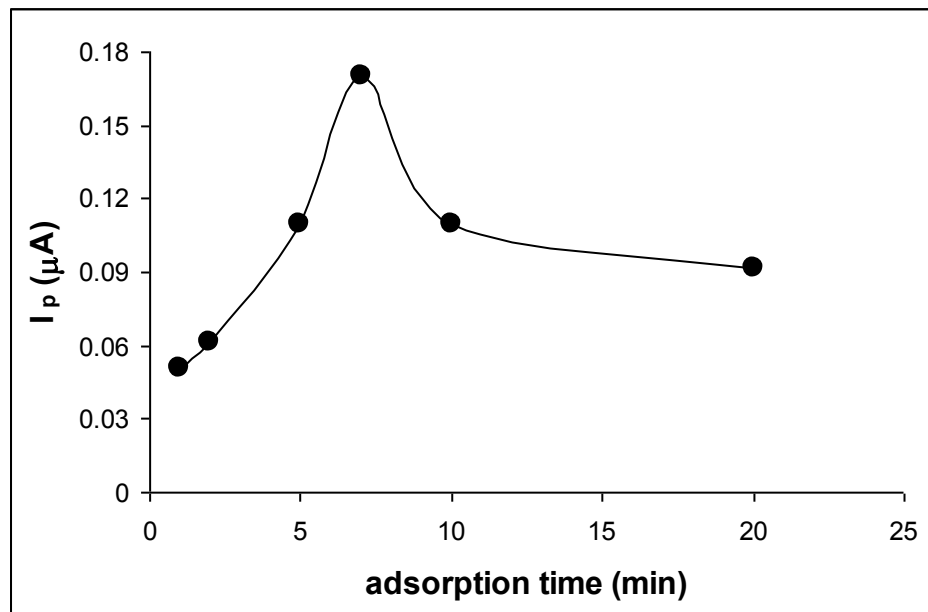


Figure 3.21. The effect of adsorption time for 250  $\mu\text{M}$  GSH on the sensor response.

**Centrifugation time:** The centrifugation parameters are vital for a sensitive and reproducible determination in centri-voltammetry. The influence of the centrifugation time on centri-voltammetric results of 250  $\mu\text{M}$  GSH was investigated. An increase in the current was observed from 1 to 4 min. and then, a sharp decrease was observed (Fig. 3.22-A). Longer times might cause dispersion of deposited analyte on the electrode surface that result with decrease in current values (Ürkmez et al., 2009). As a result, 4 min. was taken as optimum working potential and used for further studies.

**Centrifugation speed:** The effect of centrifugation speed on the centri-voltammetric results in the presence of 250  $\mu\text{M}$  GSH, 0.05M PBS (pH 7.0) for 4 min with adsorption time of 7 min.

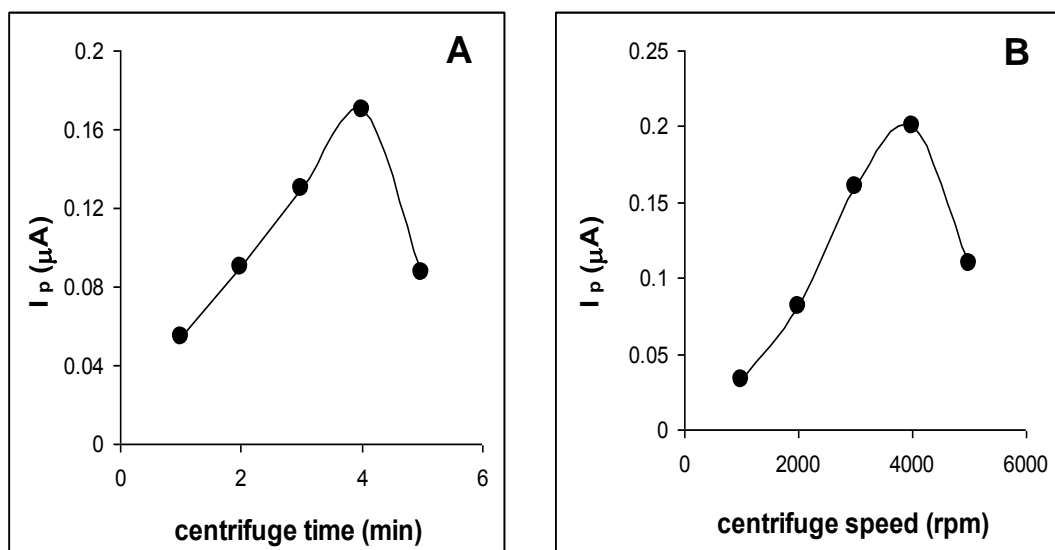


Figure 3.22. The effects of A) centrifugation time, B) centrifugation speed on the centri-voltammetric results obtained for 250  $\mu M$  GSH.

As can be seen from the Figure 3.22-B, the peak current gives a maximum at 4000 rpm and the decrease for higher speed is observed probably due the thickening of the film with a reduced conductivity.

### 3.2.2. Analytical characteristics

After the optimization of experimental parameters, analytical characteristics were examined. The linear range was obtained between 50-800  $\mu M$  where with the equation of  $y = 0.0002x + 0.0132$  and correlation coefficient of  $R^2 = 0.9915$  respectively (Figure 3.23). R.S.D values were calculated for 250  $\mu M$  GSH ( $n=6$ ) and found as 3.40%. LOD ( $S/N=3$ ) value was also calculated from the calibration graph and found as 51.15  $\mu M$ . These calculation was based on the formulation of  $3s/m$  (for LOD), where  $m$  is the slope of the calibration curve and  $s$  is the standard deviation of the blank current values.

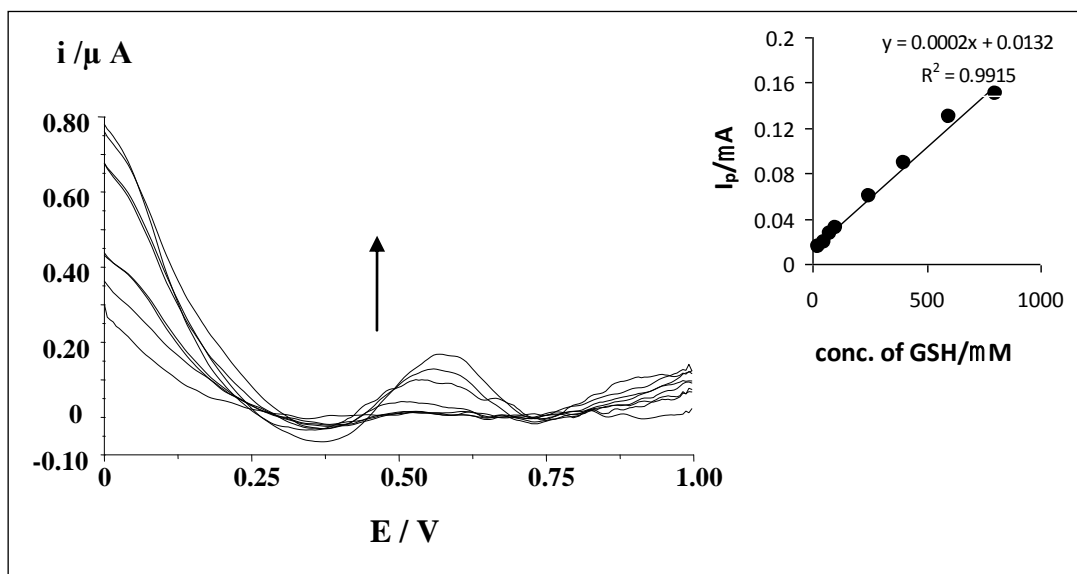


Figure 3.23. DP voltammetric response curves of 4% MWCNT-modified CPE obtained for different concentration GSH. Inset: the linear range of GSH sensor.

On the other hand, the performance of the developed method was compared with other methods devoted for the determination of GSH in terms of analytical characteristics. The results were demonstrated in Table 3.2. As can clearly be seen from the Table, the overall performance of the developed sensor is in acceptable limits.

The study of interference on the analysis signal is useful with the purpose of minimizing their effects. In this work, interferences in electroanalysis of GSH were considered to be common foreign species and the compounds that are structurally related to GSH. An equivalent concentration of ascorbic acid and L-cysteine showed a slight interference to the GSH detection in pH 7.0 as 8.4% and 9.4%, respectively and this indicates that the selectivity of this electrode in the detection of glutathione is acceptable.

Table 3.2 A summary of the recent investigations for GSH detection strategies based on various types of methods.

Methods	Analytical Range ( $\mu\text{M}$ )	LOD ( $\mu\text{M}$ )	R.S.D. (%)	R <sup>2</sup>	References
Fluorescence measurement	0-8x10 <sup>4</sup>	178	2.33	0.9941	Zeng et al., 2011
HPLC-ECD	0-195	0.0127	2.70	0.9989	Potesil et al., 2005
Spectrofluorometric assay	0-1000	-	5.10	1.00	Roušar et al., 2012
UPLC	0.98-325	0.06	3.80 6.20	0.998	Fracassetti et al., 2011
CE-LIF	1-130	0.065	6.00 6.35	0.999	Lavigne et al., 2007
CV FIA (Amperometry)	1.0x10 <sup>-4</sup> /5.0x10 <sup>-3</sup> 0.5-100	10 0.5	3.66	-	Chailapakul et al., 2001
Centri-voltammetry	50-800	51.15	3.40	0.9915	Present work

High-performance liquid chromatographic method with electrochemical detection: HPLC-ECD, Ultra-performance liquid chromatography: UPLC, Capillary electrophoresis coupled with laser-induced fluorescence: CE-LIF, Cyclic voltammetry: CV, Flow Injection Analysis: FIA

The comparison of centri-voltammetric methods with previously reported works was also provided with respect to analytical characteristics and demonstrated in Table 3.3. The Table 3.3 shows us that the centri-voltammetry can easily be applied on various kinds of analytes and presented promising analytical values.

Table 3.3. The comparison of analytical characteristics with reported on centri-voltammetry and biocentri-voltammetry

Analyte	Carrier Material	Linear Range ( $\mu\text{M}$ )	LOD ( $\mu\text{M}$ )	RSD (%)	R <sup>2</sup>	References
Pb(II) ions	Al(OH) <sub>3</sub>	0.01 to 1.0	0.0022	5.30	-	Anık-Kırgöz et al., 2004
Pb(II) ions	XAD-7 resin	0.05 to 1.0	0.0052	3.30	0.995	Anık-Kırgöz et al., 2005
Hg(II) ions	Not used	3.0x10 <sup>-6</sup> to 0.01	3x10 <sup>-6</sup>	-	0.9941	Ürkmez et al., 2009
Xanthine	Not used	0.1 to 1.0 5 to 50	0.092	3.43	0.984 0.997	Anık and Çevik, 2011
Acetylthiocholine chloride	Not used	1.0 to 350	-	3.60	0.99	Çevik et al., 2012
Mo	PGR					Koçak et al. 2012
GSH	Silica gel	25 to 800	264.2	3.40	0.9915	Present work

### 3.2.3. Sample application

In order to verify the applicability of the proposed method for clinical and food sample analysis, the wine sample and synthetically prepared plasma sample were analyzed as described in experimental section. Each experiment was employed for three times by applying standard addition method ( $n=3$ ). For wine samples the recovery of the analytical signal was calculated as 100.8%.

The synthetically plasma sample was prepared according to the procedure described in section 2.5.2. Synthetic plasma solution was comprised of NaCl, KCl, CaCl<sub>2</sub>, MgCl<sub>2</sub>, urea, and glucose in mM level.

10 mM TRIS-HCl buffer was used as the background of the synthetic plasma solution. The final pH of the solution was adjusted to 7.3 with addition of proper amount of 1 M HCl.

The standard solutions were prepared from using the synthetic plasma electrolyte as a background solution and then proper amount of analytes was spiked to the phosphate buffer solution (pH 7.0). The recovery values were calculated upon three successive additions of standard GSH solution into the mixtures and calculated as 100.0%.

### 3.3. Biosensor Studies with Pt Modified GCPE

#### 3.3.1. Electrodeposition of PtNps by cyclic voltammetry

PtNps were electrodeposited onto the bare GCPE using cyclic voltammetry between -0.70 V and +0.80 V at  $50 \text{ mV} \cdot \text{s}^{-1}$  in a solution of 0.1 M KCl containing 1.0 mM  $\text{H}_2\text{PtCl}_6$ . Figure 3.24 demonstrates the cyclic voltammogram obtained for the deposition of PtNps after 50 successive scans. Obtained two additional redox steps at -0.356 V and -0.424 V corresponded to  $\text{PtCl}_6^{2-}/\text{PtCl}_4^{2-}$  (I) and  $\text{PtCl}_4^{2-}/\text{Pt}^0$  (II), respectively (Wang and Lin, 2005).

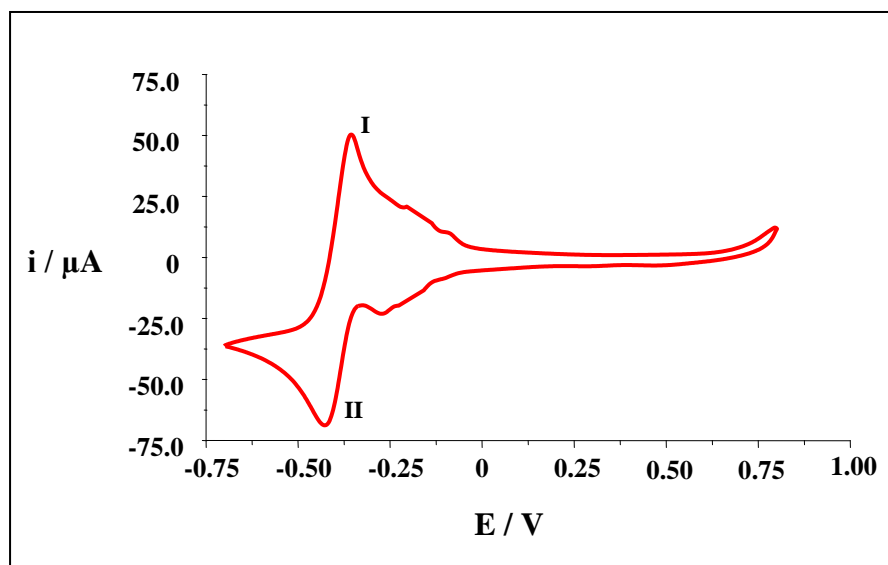


Figure 3.24. Electrodeposition of PtNps onto bare GCPE with cyclic voltammetry in 0.1 M at  $50 \text{ mV} \cdot \text{s}^{-1}$  for 50 cycles.



Afterwards, the electrode was modified with enzyme and other immobilization reagents namely gelatine and chitosan. The performance of the biosensors developed was tested by adding GSH in mM levels in a PBS solution at pH 7.0. Below figures demonstrate the performance of both electrodes in a concentration range of 100-500  $\mu\text{M}$  (Figure 3.25). Since enzymatic reaction consumes hydrogen peroxide in 2:1 stoichiometric ratio,  $\text{H}_2\text{O}_2$  was added into the solution providing this ratio for each GSH concentration studied. From the Figure 3.25, a current difference was obtained around 0.25  $\mu\text{A}$  between two differently prepared biosensor for 100  $\mu\text{M}$  GSH. Best results were obtained with the biosensors including gelatine and therefore, further experiments were carried out with this immobilizing agent.

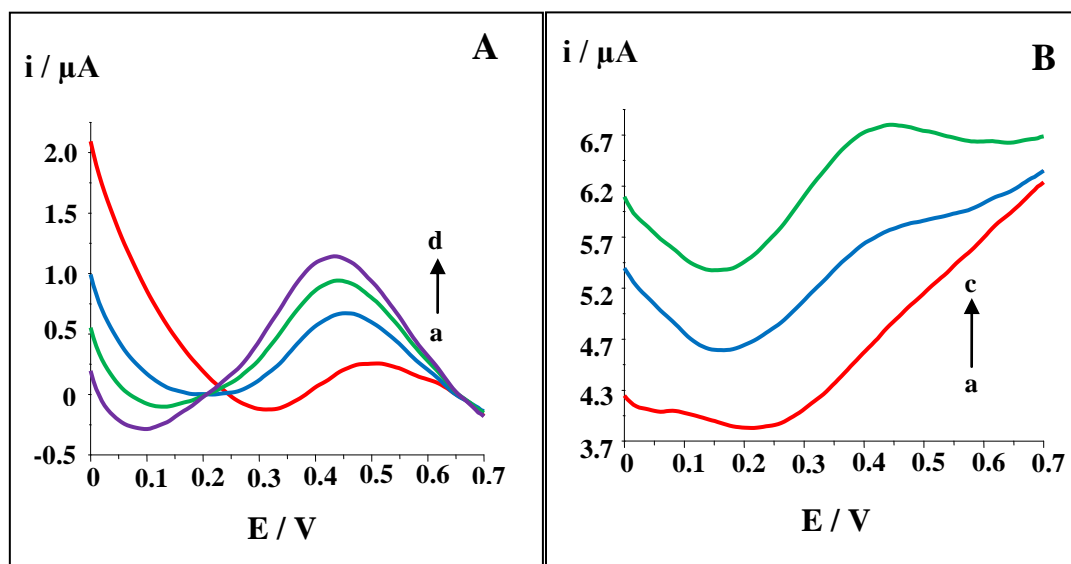


Figure 3.25. DP voltammetric responses of different concentration of GSH for (A) GSH- $\text{Px}_{(\text{immob})}/\text{PtNp}/\text{GCPE}$  and (B) Chit/GSH- $\text{Px}/\text{PtNp}/\text{GCPE}$ ; for (A) (a) background, (b) 100  $\mu\text{M}$  GSH:50  $\mu\text{M}$   $\text{H}_2\text{O}_2$ , (c) 250  $\mu\text{M}$  GSH:125  $\mu\text{M}$   $\text{H}_2\text{O}_2$  (d) 500  $\mu\text{M}$  GSH:250  $\mu\text{M}$   $\text{H}_2\text{O}_2$ , for (B) (a) background, (b) 100  $\mu\text{M}$  GSH:50  $\mu\text{M}$   $\text{H}_2\text{O}_2$ , (c) 500  $\mu\text{M}$  GSH:250  $\mu\text{M}$   $\text{H}_2\text{O}_2$  in 0.05 M PBS (pH 7.0).

Here, it should be mentioned that 50 is a large number for electrochemical nanoparticle matter formation as they grow towards microscale. Therefore, the experiment was repeated with platinum disc electrode and very small peak currents were obtained (Figure 3.26).

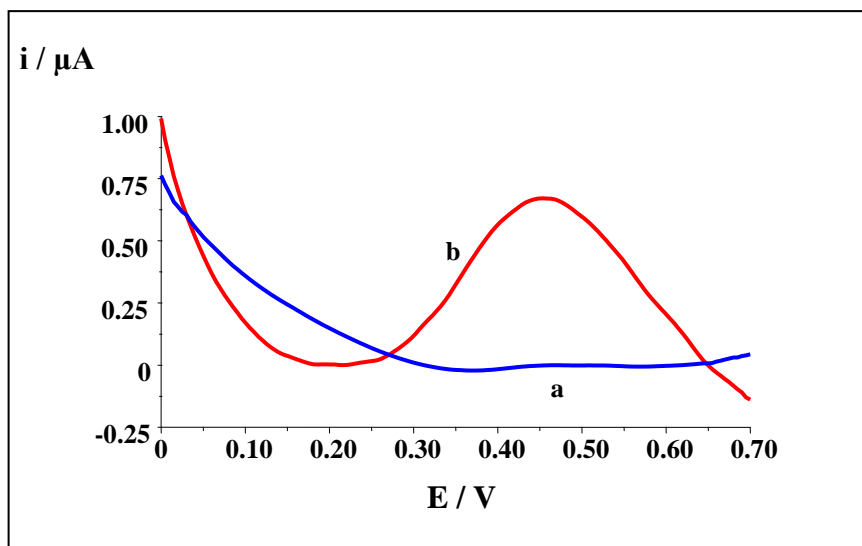


Figure 3.26. DP voltammetric responses of (a) GSH-Px immobilized Pt electrode, (b) GSH-Px<sub>(immob)</sub>/PtNp/GCPE for 100 μM GSH. Conditions: 0.05 M PBS (pH 7.5), GSH:H<sub>2</sub>O<sub>2</sub>=2:1 μM.

### 3.3.2. The presence of PtNps into electrode structure

Figure 3.27 shows the differential pulse voltammograms for the electrochemical oxidation of GSH in the presence of H<sub>2</sub>O<sub>2</sub> in phosphate buffer solution (pH 7.0) with GSH-Px<sub>(immob)</sub>/GCPE (Figure 3.27-b) and PtNp modified GSH-Px<sub>(immob)</sub>/GCPE (Figure 3.27-c). As can clearly be seen from the Figure, no anodic peak was observed for GSH at GSH-Px<sub>(immob)</sub>/GCPE (Figure 3.27-b) while a well-defined anodic peak was appeared when the PtNp was incorporated onto the electrode surface (Figure 3.27-c). This result demonstrates the electrocatalytic effect of PtNp on the peak current response.

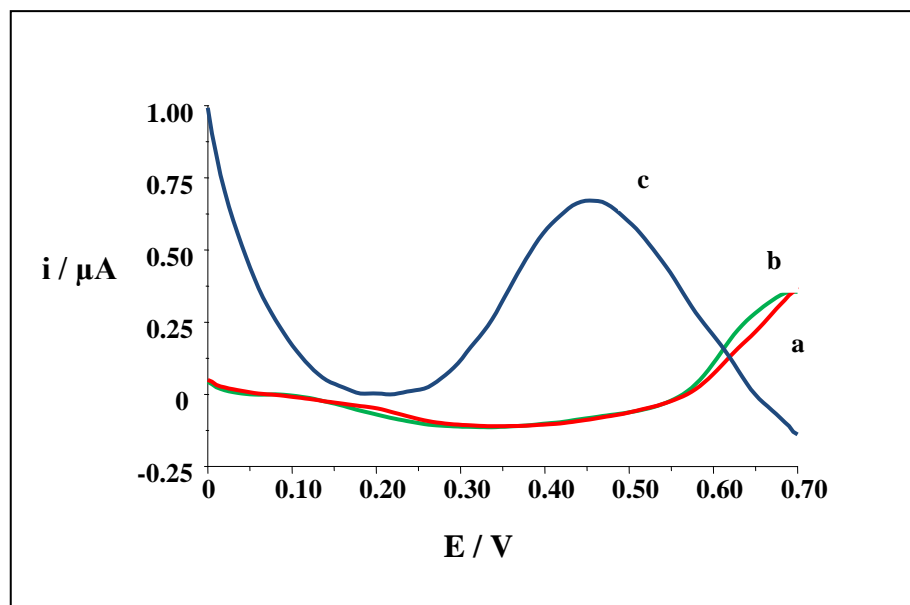


Figure 3.27. DP voltammograms of (a) background for GSH-Px<sub>(immob)</sub>/GCPE, and in the presence of 100 μM GSH:50 μM H<sub>2</sub>O<sub>2</sub> at a (b) GSH-Px<sub>(immob)</sub>/GCPE, (c) PtNp modified GSH-Px<sub>(immob)</sub>/GCPE in 0.05 M PBS (pH 7.0).

### 3.3.3. The EIS characterization of GSH biosensor

Nyquist plot ( $Z_{im}$  vs.  $Z_{re}$ ) is one of the typical electrochemical impedance spectrums which include a semicircle region lying on the  $Z_{re}$  axis observed at higher frequencies related with the electron-transfer-limited process and then followed by a linear part at lower frequencies representing the diffusion-limited electron transfer process. The semicircle diameter equals to the electron-transfer resistance,  $R_{et}$ , which is controlled by the surface modification of the electrode.

Accordingly, Figure 3.28 shows the electrochemical impedance spectra (EIS) of (a) bare GCPE, (b) GSH-Px immobilized GCPE, (c) PtNp/GSH-Px/GCPE for 1 mM  $[\text{Fe}(\text{CN})_6]^{3-/4-}$  redox couple.

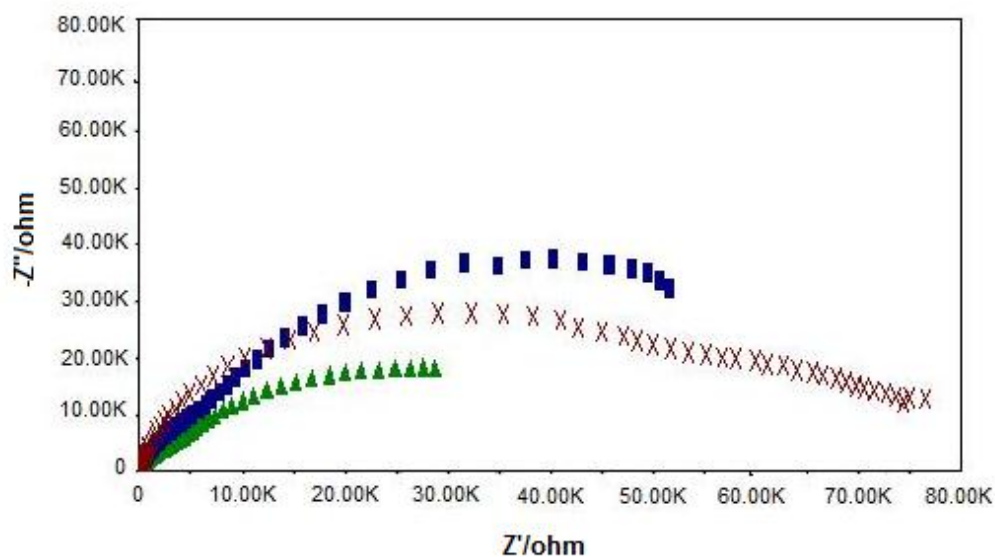


Figure 3.28. Nyquist plots of the biosensing electrode response at different stages in the electrode assembly process: bare GCPE (X); GSH-Px/GCPE (■) and PtNp/GSH-Px/GCPE (▲). All spectra were recorded in the presence of 1 mM  $[\text{Fe}(\text{CN})_6]^{3-/4-}$  in 0.05 M PBS (pH 7.5), as a redox-active indicator. Frequency range:  $10^4$  to 0.01 Hz, 0.05V amplitude.

From obtained spectra it can be said that bare GCPE shows a response corresponding to the electron-transfer-limited process while GSH-Px/GCPE exhibits a tendency to increase of semi-circle relating with the electron-transfer-limited process. This finding indicates that immobilization of GSH-Px via gelatine onto the electrode surface, the degradation of the interfacial electron transfer between the electrode and redox indicator in solution and the isolation of conductive supporting.

The electron transfer via redox couple is hindered by the presence of enzymes on electrode surface. The increased  $R_{\text{et}}$  value of GSH-Px/GCPE was due to the immobilization of enzymes onto GSH-Px/GCPE surface. This increase in  $R_{\text{et}}$  is attributed to the fact that most biological molecules, including enzymes, are poor electrical conductors at low frequencies (at least <10 kHz) and cause hindrance to the electron transfer (Chauhan et al., 2012).

When the PtNp was incorporated onto the GSH-Px/GCPE, a decrease was observed in  $R_{et}$ . Thus, there was a conducting PtNp on the electrode surface and this shows us the system tends to diffusion-limited electron transfer process from electron-transfer-limited process, relatively.

### 3.3.4. Optimization of experimental parameters

***Effect of Enzyme Amount:*** In order to investigate the optimum amount of enzyme, DP voltammetric responses of GSH were recorded with various amounts of GSH-Px. The effect of enzyme amount (1, 2, 5, 10 and 15 Unit) on obtained current values was investigated for 100  $\mu$ M GSH:50  $\mu$ M  $H_2O_2$  and shown in Figure 3.29.

As can be seen from the Figure 3.30, current values increase depending on the enzyme amount up to 5 Unit, and then a sharp decrease was observed for higher enzyme amount which can be attributed to diffusion problem (Anik et al., 2010). Here, the excess amount of protein might limit the efficient substrate-enzyme interaction that is required for this reaction. Since the best results were obtained with 5 Unit, further experiments were conducted with this amount.

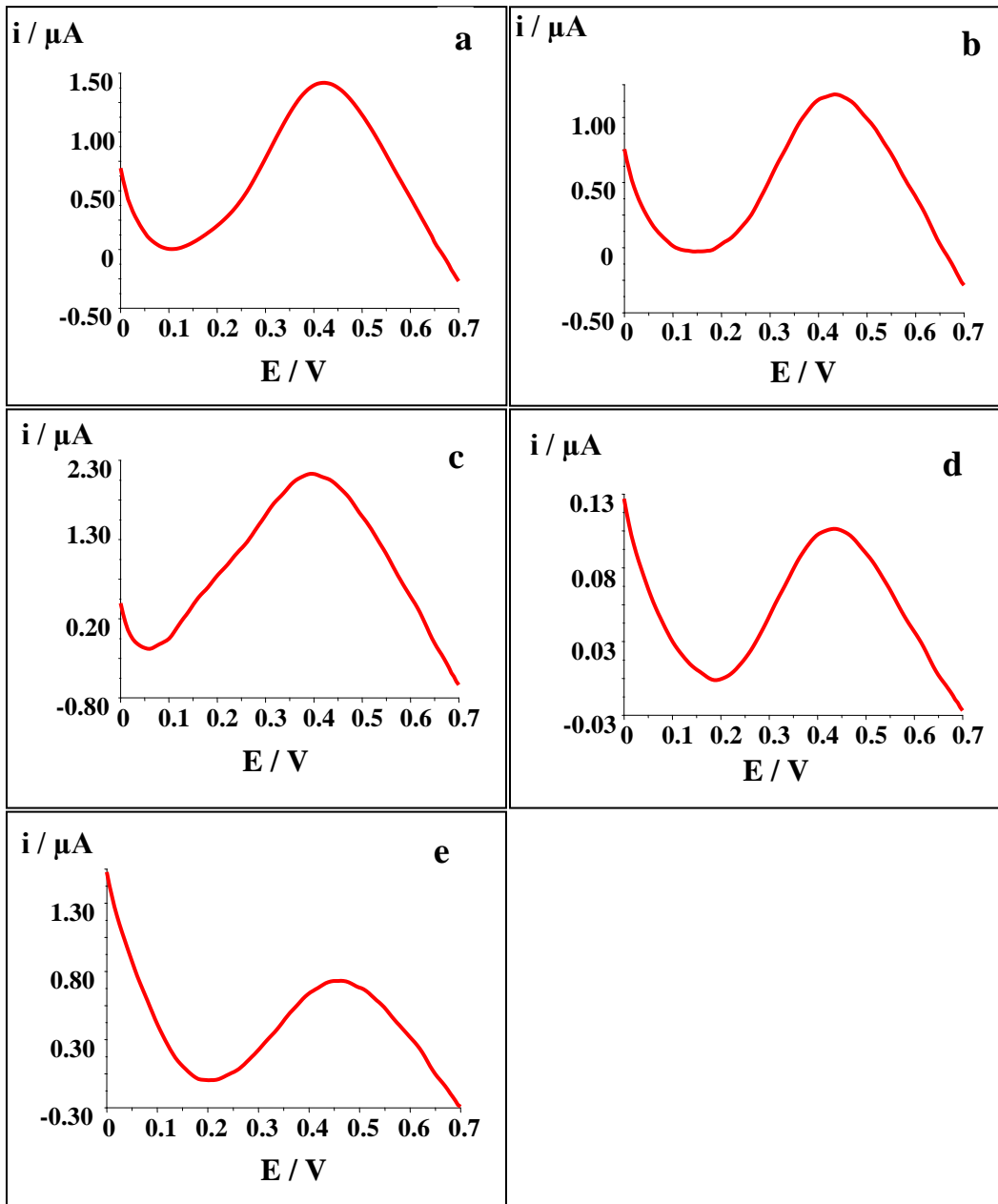


Figure 3.29. DP voltammetric responses of 100  $\mu\text{M}$  GSH: 50  $\mu\text{M}$   $\text{H}_2\text{O}_2$  on the biosensor response at various enzyme amount: (a) 1.0 U, (b) 2.0 U, (c) 5.0 U, (d) 10.0 U, (e) 15.0 U; in PBS (0.05 M, pH 7.0).

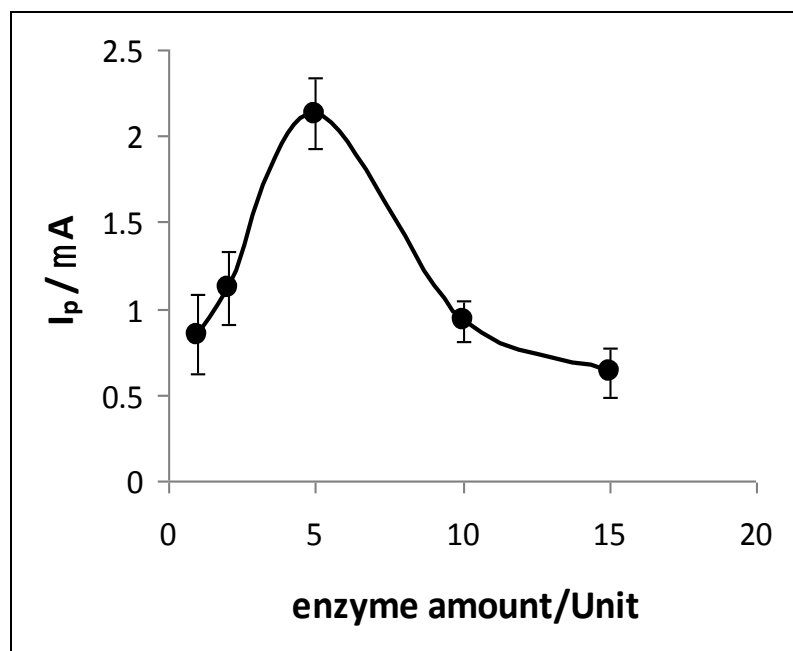


Figure 3.30. The effect of optimum enzyme amount curve of GSH- $Px_{(immob)}$ /PtNp/GCPE.

**Effect of GSH/ $H_2O_2$  Ratio:** According to the enzymatic mechanism proposed for the enzyme GSH- $Px$ , an enzyme pre-activation with peroxide was needed. It is also reported that in the absence of peroxide, no amperometric response was obtained based on the GSH electrooxidation (Rover et al., 2001). On the other hand, the peroxide concentration must be maintained at consistent levels since at high peroxide concentrations, an enzymatic inactivation can occur while the regeneration of oxidized enzyme with GSH (Rover et al., 2001; Satto et al., 1999). As a result, it is important to obtain the optimum peroxide amount for this reaction. For this purpose, the effect of  $H_2O_2$  amount on the assay response was evaluated by DP voltammetry, by varying the proportion between GSH and peroxide as 0.1:1, 0.5:1, 1:1, 2:1, 5:1 and 10:1 (Figure 3.31).

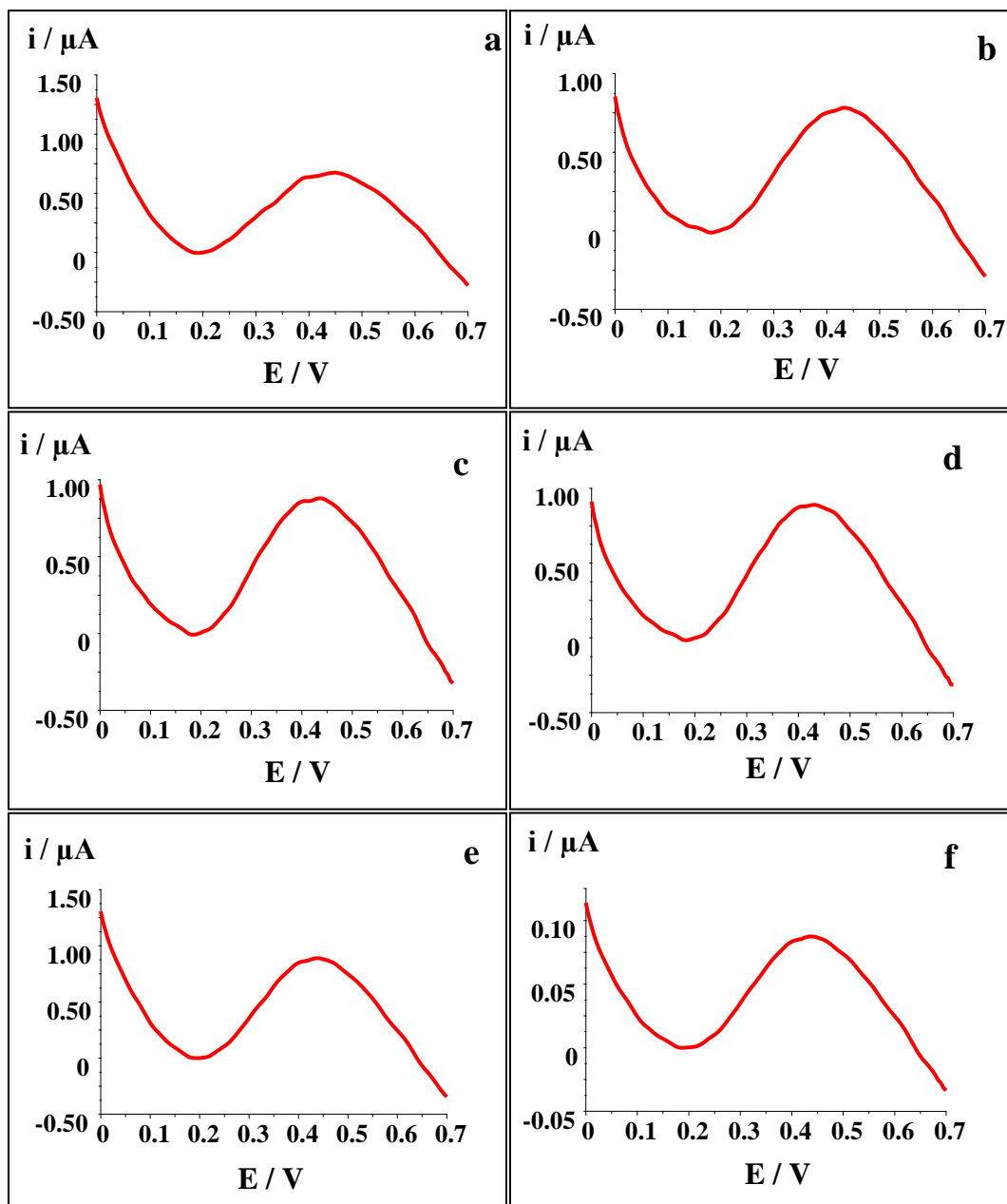


Figure 3.31. DP voltammetric responses of different GSH/H<sub>2</sub>O<sub>2</sub> ratio on the biosensor response; (a) 0.1:1 GSH:H<sub>2</sub>O<sub>2</sub>, (b) 0.5:1 GSH:H<sub>2</sub>O<sub>2</sub>, (c) 1:1 GSH:H<sub>2</sub>O<sub>2</sub>, (d) 2:1 GSH:H<sub>2</sub>O<sub>2</sub>, (e) 5:1 GSH:H<sub>2</sub>O<sub>2</sub>, (f) 10:1 GSH:H<sub>2</sub>O<sub>2</sub>. Conditions: PBS system (0.05 M, pH 7.0), [GSH]=50.0 μM, T=25°C.

At proportions higher than 2:1, a stabilization of the signal was observed; while for ratios lower than 1:1, the obtained response was considerably lower (Figure 3.32). As a result proportion of 2:1 was chosen as optimum value and used for further studies.



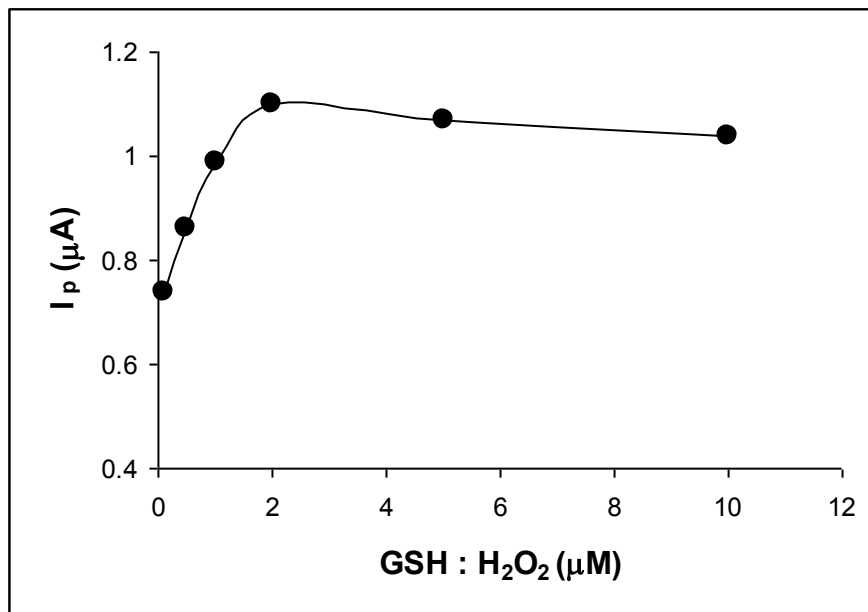


Figure 3.32. Effect of the GSH/H<sub>2</sub>O<sub>2</sub> ratio in the GSH biosensor performance.

**Effect of pH:** The medium pH is another important parameter to be optimized. Figure 3.33 showed that the electrochemical behavior of GSH was studied in 50 mM phosphate buffered solution with various pH ranges (5.0-8.0).

The obtained results showed that for pH values <7.5, the response decreases. This may be due to the lower activity of the enzyme in this media (Rover et al., 2001). However, for pH values higher than 8.0, there is not a significant amplification in the signal, presumably due to the reduced GSH to be unstable in alkaline solution as it is easily oxidized. Also there is a probability that protein denaturation might occur at alkaline media (Rover et al., 2001). Therefore, pH 7.5 was selected for further applications (Fig. 3.34).

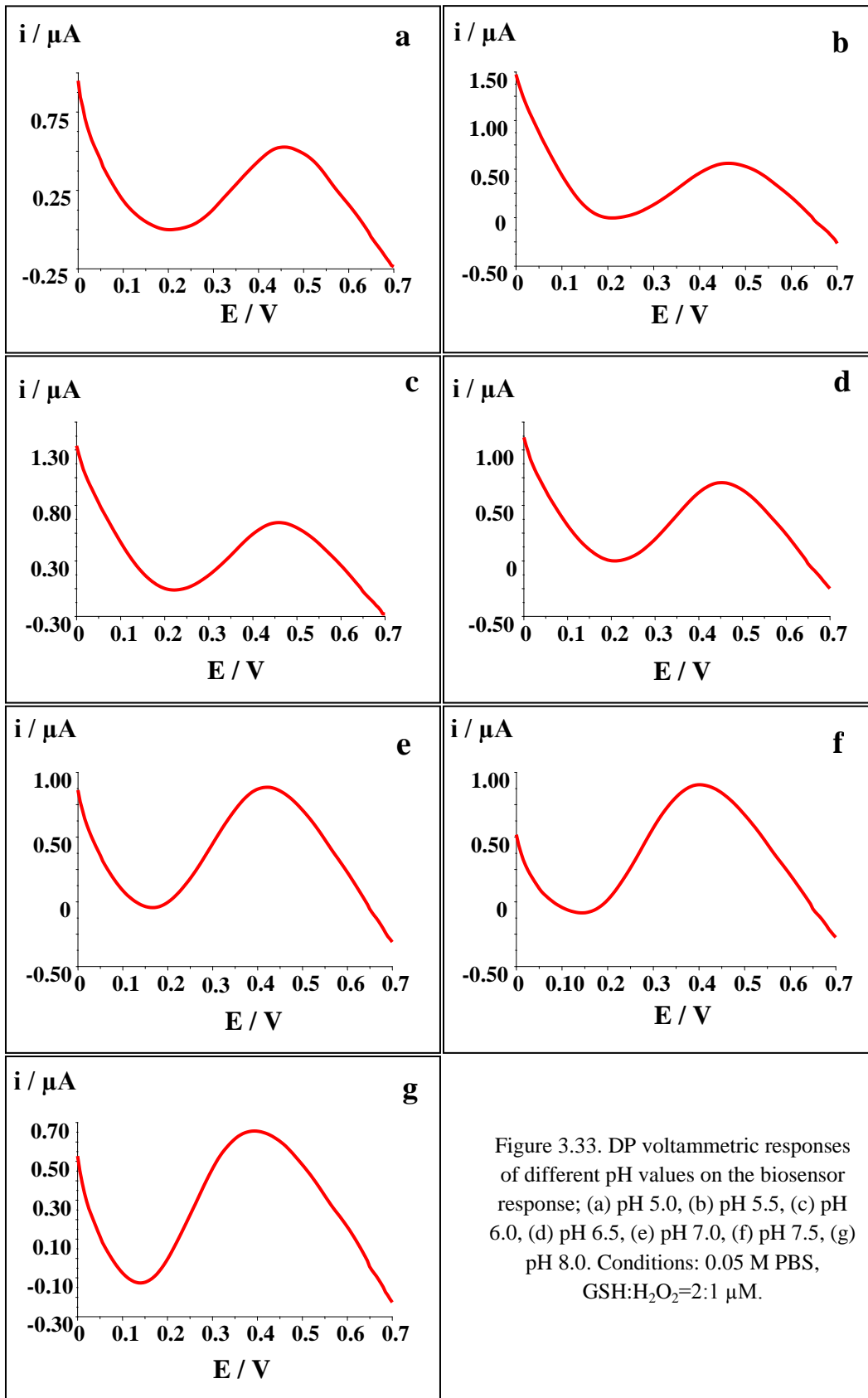


Figure 3.33. DP voltammetric responses of different pH values on the biosensor response; (a) pH 5.0, (b) pH 5.5, (c) pH 6.0, (d) pH 6.5, (e) pH 7.0, (f) pH 7.5, (g) pH 8.0. Conditions: 0.05 M PBS, GSH:H<sub>2</sub>O<sub>2</sub>=2:1  $\mu\text{M}$ .

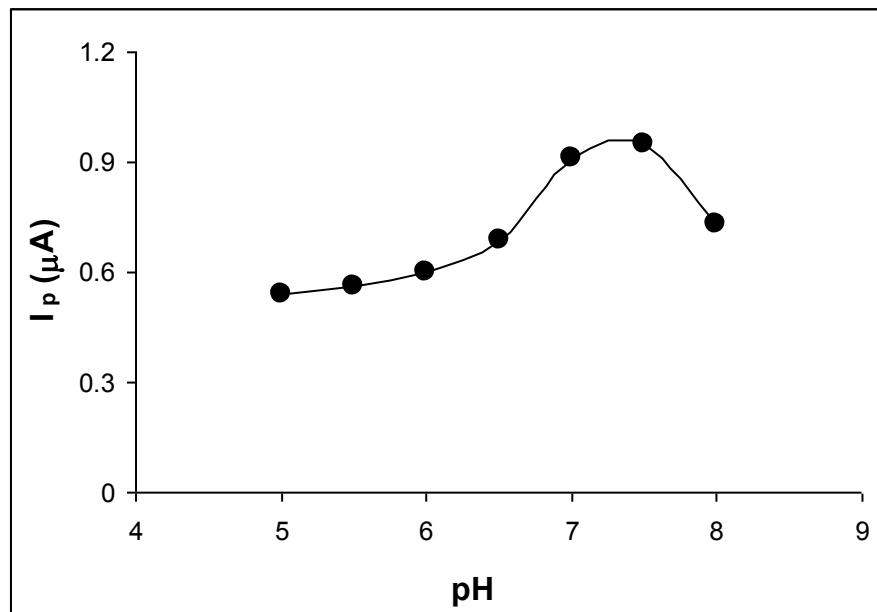


Figure 3.34. The effect of the pH in the GSH biosensor performance.

### 3.3.5. Analytical characteristics

After the optimization of experimental parameters, analytical characteristics were examined. The linear range was obtained for the developed biosensor between 10-250  $\mu\text{M}$  with the equation  $y = 0.0015x + 1.0618$  with the correlation coefficient of  $R^2 = 0.9968$ , respectively (Figure 3.35). Relative standard deviation (R.S.D) value was calculated for 25  $\mu\text{M}$  GSH ( $n=6$ ) and found as 2.92%.

The storage stability of the sensor is a very important parameter for long-term applications. When developed sensor was kept at 4  $^{\circ}\text{C}$  in a dry atmosphere for one week, it was observed that 98% of the activity was recovered. Moreover, during this period 50 measurements were carried out and no decrease was observed in the signal responses.

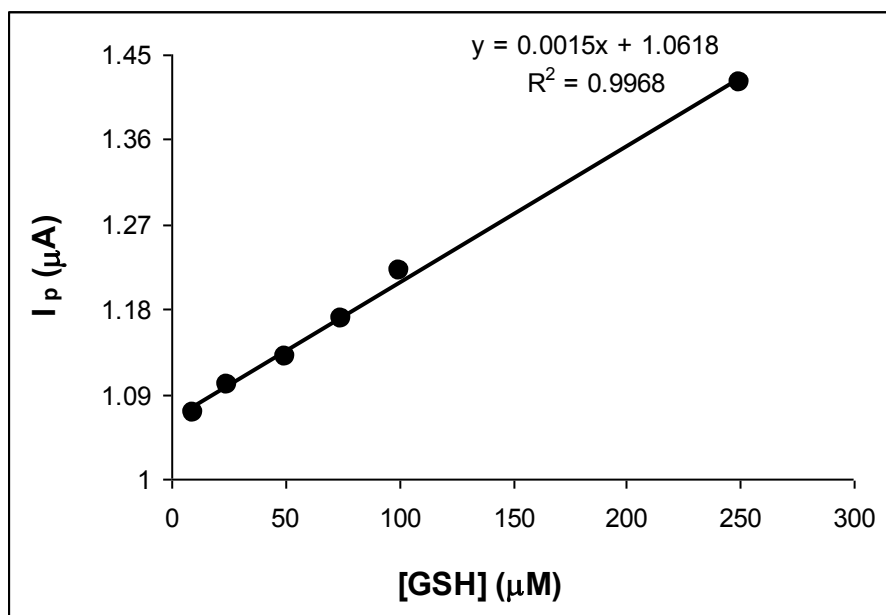


Figure 3.35. The linear range for the GSH biosensor.

In addition, the performance of developed biosensor was compared with other electrochemical biosensors devoted for the determination of GSH in terms of analytical characteristics. The results were demonstrated in Table 3.4.

Table 3.4. A comparison of the analytical characteristics of differently modified electrochemical biosensors for detection of GSH.

Biosensor	Analyte	Linear Range (μM)	RSD (%)	R <sup>2</sup>	LOD (μM)	References
GSH-Px immobilized EDAC/PGE	GSH	19-140	7.0	0.9993	-	Rover et al., 2001
Os-gel-HRP/GSH-SOx bilayer modified GCE	GSH	1-200	1.1	-	-	Mao and Yamamoto, 2000
GR-SOx /Chit/SGR bienzymatic	GSH	200-1000	1.9	0.9862	-	Timur et al., 2008
GSH-Px/PtNp/GCPE	GSH	10-250	2.92	0.9968	50.3	Present work

As can clearly be seen from the Table 3.4, GSH-P<sub>x(immob)</sub>/PtNp/GCPE biosensor overall performance is in acceptable limits. Even some parameters of developed system are better than other developed biosensors.

### 3.3.6. Interference study

In this work, the interferences were considered to be the compounds that are structurally related to GSH and present in biological samples, since this electrode was developed to analyze GSH in synthetically prepared plasma samples.

The two potential interfering substances with similar structure, such as ascorbic acid (AA) and cysteine were used to evaluate the selectivity of GSH-P<sub>x(immob)</sub>/PtNp/GCPE. 25  $\mu\text{molL}^{-1}$  GSH solution and interfering substances in the amount of 1, 5, 10, 50 and 100 fold more were added to the working medium. Up to 5 fold and 10 fold, it is found that developed system was affected as 7.9% and 5.3% for cysteine and AA, respectively.

These values are in acceptable limits and it can be concluded that the system works properly without any signal change in the presence of ten fold of AA and cysteine. The interference of cysteine arises due to the structural similarity between this compound and GSH molecule (Rover et al., 2001). High reactivity of AA may cause interference in determination of GSH. This interference can be minimized by using ascorbate oxidase enzyme exhibited high selectivity for the AA oxidation (Rover et al., 2001; Raoof et al., 2009).

### 3.3.7. Sample application

The synthetic plasma solution was prepared as described in sample preparation part. Then standard addition method was applied. Each analysis was performed three times and the recovery of the analytical signal for the diluted samples was calculated as  $104.6\% \pm 0.125$ . Thus it can be concluded that developed biosensor is reliable and sensitive enough for the usage of GSH in matrices like biological fluids (Figure 3.36).

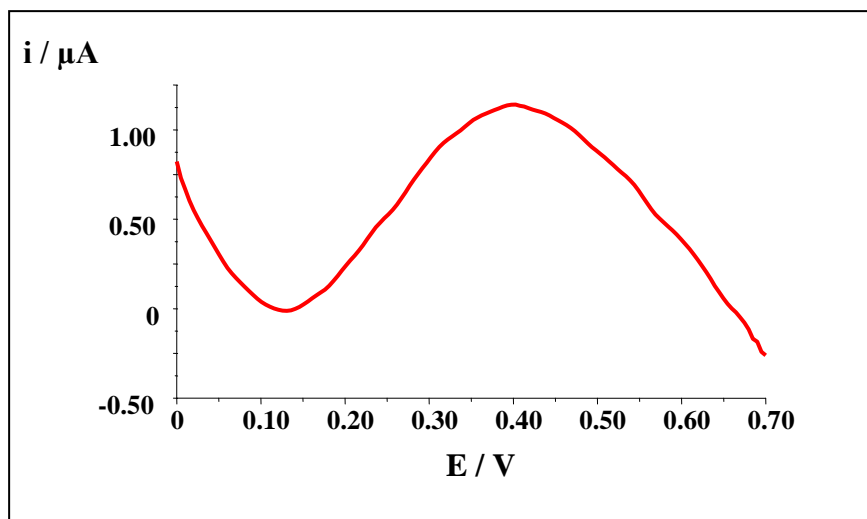


Figure 3.36. DP voltammetric response of the synthetic plasma sample for 25  $\mu\text{M}$  GSH in 0.05 M PBS, GSH:H<sub>2</sub>O<sub>2</sub>=2:1  $\mu\text{M}$ .

### 3.3.8 Biosensor studies with 4% Fe<sub>3</sub>O<sub>4</sub> Np modified GCPE

Nanoparticle modified paste electrodes were utilized to examine the electrochemical detection of GSH for this purpose. First of all, both GSH-Px immobilized bare GCPE and 4% Fe<sub>3</sub>O<sub>4</sub> Np modified with GSH-Px immobilized GCPE were prepared and then used for GSH analysis. Resulting DP voltammograms were given in Figure 3.37. As can be concluded from the figure, no significant peak was observed that can be utilized for GSH determination.

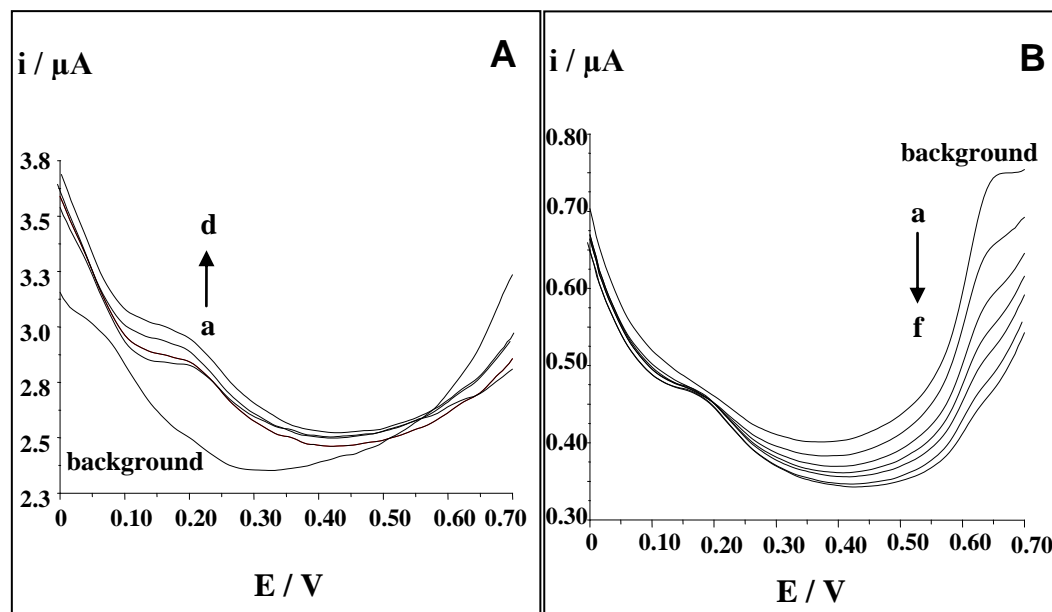


Figure 3.37. DP voltammograms recorded with (A) GCPE+GSH- $Px_{(immob)}$ , (B) GCPE+4%  $Fe_3O_4$  Np+GSH- $Px_{(immob)}$  for different concentrations of GSH: (a) 100  $\mu$ M GSH:50  $\mu$ M  $H_2O_2$ , (b) 200  $\mu$ M GSH:100  $\mu$ M  $H_2O_2$ , (c) 400  $\mu$ M GSH:200  $\mu$ M  $H_2O_2$ , (d) 600  $\mu$ M GSH:300  $\mu$ M  $H_2O_2$ , (e) 800  $\mu$ M GSH:400  $\mu$ M  $H_2O_2$ , (f) 1mM GSH:500  $\mu$ M  $H_2O_2$  in 0.05 M PBS (pH 7.0).

### 3.4. Biocentri-voltammetric Analysis of GSH

The biocentri-voltammetry is a rather new application area of centri-voltammetry with very promising results (Çevik et al., 2012a and 2012b). In this section, the use of the composite electrodes developed in biocentri-voltammetric analysis of GSH is given under subheadings according to the electrode type.

#### 3.4.1. Biocentri-voltammetry with GSH- $Px_{(immob)}/GCPE$

The enzyme immobilization procedure was carried out onto bare electrode as described in section 2.3.8 and 2.3.9, and then, this modified electrode was used for application of biocentri-voltammetric analysis of GSH (Figure 3.38).

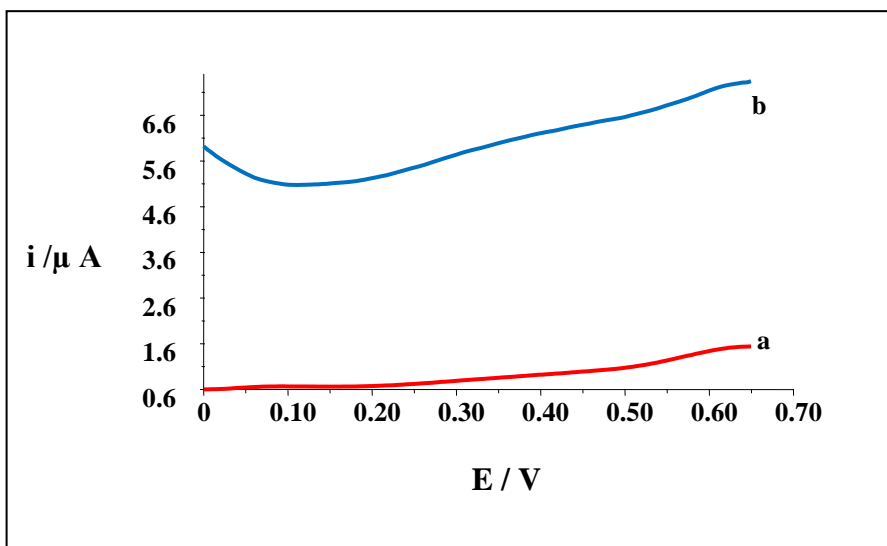


Figure 3.38. The biocentri-voltammograms of GCPE+GSH-P $x_{(immob)}$  for 50  $\mu$ M GSH+25  $\mu$ M H $_2$ O $_2$ ; (a) without centri, (b) with centri. Conditions: 0.05 M PBS (pH 7.0),  $V_{centr}$ : 3000 rpm,  $t_{centr}$ : 3 min.

According to the figure above, there is no observation of electrooxidation of GSH under these circumstances. The electrooxidation of GSH was investigated by using a carrier material for the same system. The electrode was prepared according to the above immobilization procedure. The proper amount of silica gel which is the carrier material and analyte was incorporated into the working buffer to observe the effect of the carrier material to the system. The DP voltammograms were recorded under centrifugal conditions (Figure 3.39).



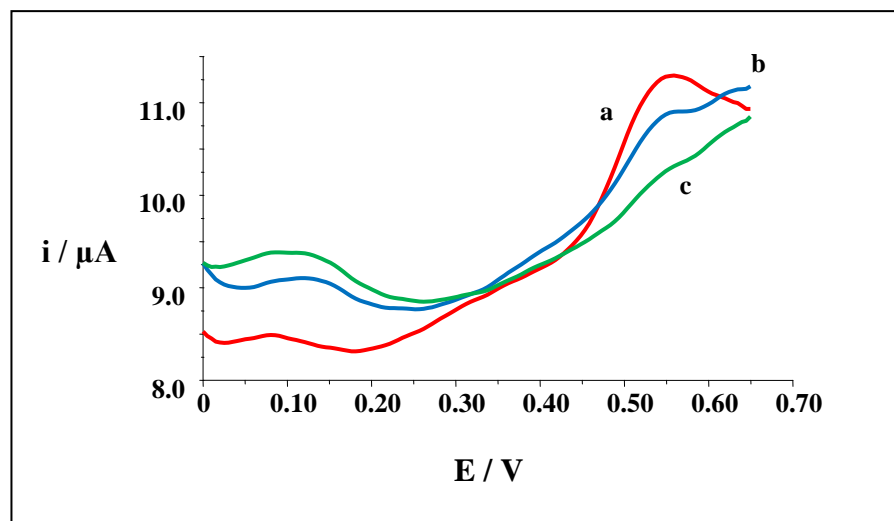


Figure 3.39. The centri-voltammograms recorded with GCPE+GSH-Px<sub>(immob)</sub>; (a) centri-voltammogram background, (b) 100  $\mu\text{M}$  GSH+50  $\mu\text{M}$  H<sub>2</sub>O<sub>2</sub>, (c) 100  $\mu\text{M}$  GSH+50  $\mu\text{M}$  H<sub>2</sub>O<sub>2</sub>+1mg silica gel. Conditions: 0.05 M PBS (pH 7.0),  $V_{\text{centr}}$ : 3000 rpm,  $t_{\text{centr}}$ : 3min.

As can be seen from the figure, when the carrier material was added to the system there is no expected observation in peak current relating with the concentration of GSH. Another way to monitor the electrooxidation of GSH was addition of the GSH-Px enzyme into the electrode paste. For this purpose, after obtaining the modified electrode the proper amount of analyte was incorporated into the working buffer. The DP voltammograms were recorded under centrifugal conditions and no significant improvement was obtained.

### 3.4.2. Biocentri-voltammetry with GSH-Px<sub>(immob)</sub>/PtNp/GCPE biosensor

The studies with this electrode were devoted to search for a proper carrier reagent such as Silica gel, Tenax and Activated Carbon. Figure 3.40 shows the resulting voltammograms in 0.05 M PBS (pH 7.5) for 5 min adsorption, 3 min centrifugation at 3000 rpm for 100  $\mu\text{M}$  GSH in the presence of 50  $\mu\text{M}$  H<sub>2</sub>O<sub>2</sub>. As can be seen from the figure, activated carbon has given promising results and the effectiveness of the activated carbon on the centri-voltammogram results can be seen in Figure 3.41 for 4000 rpm.

However, no linearity was observed for the DP voltammograms recorded for GSH concentration in a range of 50-250  $\mu\text{M}$  with the peak current at 0.4 V.

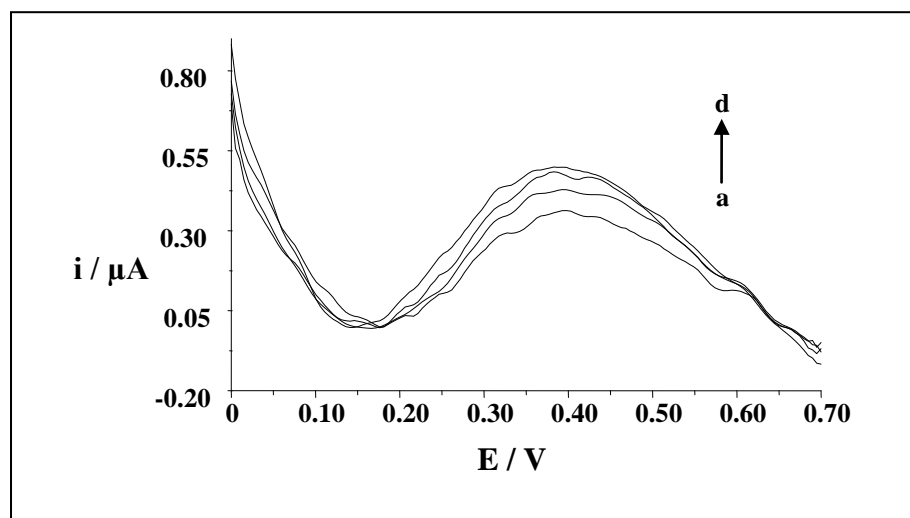


Figure 3.40. DP voltammetric responses of the developed biosensor for 100  $\mu\text{M}$  GSH:50  $\mu\text{M}$   $\text{H}_2\text{O}_2$ ; (a) no carrier material, (b) 0.5 mg Tenax, (c) 1 mg Silica gel, (d) 0.15 mg Activated Carbon in 0.05 M PBS (pH 7.5),  $t_{\text{ads}}$ :5 min,  $t_{\text{cent}}$ :3 min,  $V_{\text{cent}}$ :3000 rpm.

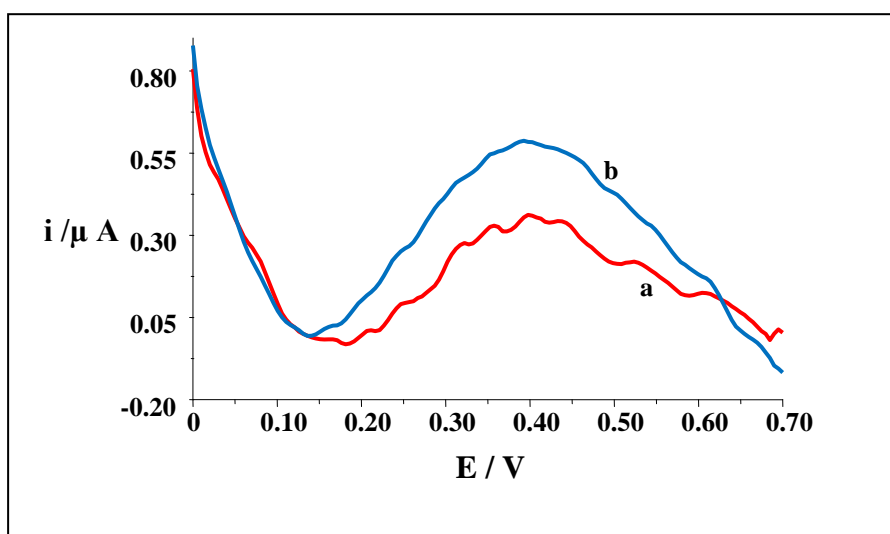


Figure 3.41. DP voltammetric responses of the developed biosensor (a) 100  $\mu\text{M}$  GSH: 50  $\mu\text{M}$   $\text{H}_2\text{O}_2$ , (b) 1 mg Activated Carbon. 0.05 M PBS,  $t_{\text{ads}}$ :5 min,  $t_{\text{cent}}$ :4 min,  $V_{\text{cent}}$ :4000 rpm

Therefore, further experiments were conducted with the same electrode and in the presence of  $\text{Cu(II)}$  ions which are known to give stable complexes with GSH. However, no significant improvement was observed for the quantization of GSH.

#### 4. CONCLUSION

In this thesis, novel electrode materials were utilized for biologically important thiol containing molecules. Development of composite electrodes including carbon based and metallic film electrodes as well as electrodes incorporated with metal/metal oxide nanoparticles was described. The results of this study were constituted alternative methods for the investigation of electrochemical detection methods for thiol containing biochemical compounds. The electrodes developed were utilized as novel platforms in centri-voltammetric and Bio-centri voltammetric studies for attaining more sensitive results.

The significance of thesis lies in the development of practical, economic, sensitive and selective electrochemical systems selected as a model related with detecting of biomolecules. For this purpose, one of the thiol containing biological molecules, GSH was analyzed by using different electrodes/biosensors and determined by utilizing centri-voltammetry method. Furthermore, various types of biomolecules were able to analyze by centri-voltammetric method without subjection of separation and filtration process after optimizing of centri-voltammetry method.

CPE, GCPE and GCE were utilized in this concept of the thesis. The surface of the electrodes was modified with nanoparticles and films. The role of centrifuging on the modification and corresponding response was studied as well. A home-made centri-voltammetric cell was used for this analysis. The cell was designed to be suitable for both centrifuging and voltammetric measurements afterwards.

A micro/nanostructured composite electrode was constructed by introducing various portions of  $\text{Al}_2\text{O}_3\cdot\text{TiO}_2$  nanopowder and AuNp into GCPE and used for GSH detection. A novel nanocomposite sensor was constructed by mixing proper amount of AuNp,  $\text{Al}_2\text{O}_3\cdot\text{TiO}_2$  nanopowder and GC micro particles and an organic pasting liquid.

The resulting nanocomposite sensor combines the electrochemical properties of GC with the various advantages of nanoparticles like AuNp and Al<sub>2</sub>O<sub>3</sub>.TiO<sub>2</sub> nanopowder.

The obtained sensor was validated for sensitivity, stability and repeatability and then applied for GSH detection in real samples. It has been demonstrated that resulting system works for GSH detection in real samples like wine and synthetic plasma samples without being affected by the nature of the sample. As a result, it can be concluded that a practical and a useful biosensor for GSH detection was constructed. By using this sensor, laborious sample treatment step that is commonly applied before the measuring step in the alternative methods was eliminated.

The GSH-P<sub>x</sub>(immob)/PtNp/GCPE was used as an electrochemical biosensor for determination of GSH. This study attempts to establish an efficient biosensor for the GSH determination. For this purpose, a biosensor was developed by using GSH-P<sub>x</sub> as the enzyme. Firstly PtNps were deposited onto GCPE then GSH-P<sub>x</sub> was immobilized by means of gelatine that was then crosslinked with glutaraldehyde. The measurement was based on the electrochemical oxidation of GSH to its disulfide form in the presence of H<sub>2</sub>O<sub>2</sub>. After the optimization of experimental parameters, the system was calibrated for GSH. According to obtained data, it can be concluded that sensitive, reproducible, stable and robust biosensor was obtained. The developed system was also applied for GSH detection in synthetically prepared plasma solution without applying any sample preparation procedure. Very satisfactory recovery values were obtained which indicates that GSH-P<sub>x</sub>(immob)/PtNp/GCPE biosensor can easily be adapted for GSH detection in real samples.

Centri-voltammetry allows concentrating of the analyte onto the working electrode with the aid of centrifuge in the presence or absence of a carrier precipitate, and then direct voltammetric scan was applied. Another obtained sensor describes the utility of centri-voltammetry as an efficient method for organic molecules as well as the metallic ions.

Here, the GSH content of a solution was driven onto the MWCNT modified CPE surface by means of a centrifugal force in the presence of silica gel. The addition of AuNps co-precipitating along with the analyte constitutes the original part of this work.

The insertion of AuNps into the film by this means would provide enhanced activity of the electrode surface by increasing the conductivity of the film. The analyte pre-concentrated as a thin film is then detected by applying voltammetric scan.

The performance of developed centri-voltammetric system was also tested by detecting GSH in wine and synthetic plasma samples without any need for sample preparation step. Recovery values demonstrate that centri-voltammetry provides a reliable tool for GSH detection in real samples since the technique is not affected by the sample matrix and the nature.

The obtained optimum systems were adapted for the sample application in the determination of thiol containing biological compounds.



## REFERENCES

- Allison, L.A., Mayer, G.S., and Shoup, R.E.**, 1984, o-Phthalaldehyde Derivatives of Amines for High-Speed Liquid Chromatography/Electrochemistry, *Anal Chem*, 56, 1089- 96.
- Anık-Kırgöz, Ü., Tural, H., and Ertaş, F.N.**, 2004, A New Procedure For Voltammetric Lead Determination Based On Coprecipitation And Centrifugation Preconcentration, *Electroanalysis*, 16, 765-768.
- Anık-Kırgöz, Ü., Tural, H., and Ertaş, F.N.**, 2005, Centri-Voltammetric Study With Amberlite XAD-7 Resin As A Carrier System, *Talanta*, 65, 48-53.
- Anık, Ü., and Çubukçu, M.**, 2008, Examination of the Electroanalytic Performance of Carbon Nanotube (CNT) Modified Carbon Paste Electrodes as Xanthine Biosensor Transducers, *Turkish Journal of Chemistry*, 32, 711-719.
- Anık, Ü., Çubukçu, M., Çevik, and S., Timur, S.**, 2010, Usage of Bismuth Film Electrode as Biosensor Transducer for Alkaline Phosphatase Assay, *Electroanalysis*, 22, 1519-1523.
- Anık, Ü., and Çevik, S.**, 2011, Centri-Voltammetry For Biosensing Systems: Biocentri-Voltammetric Xanthine Detection, *Microchim Acta*, 174, 207-212.
- Atmaca, G.**, 2004, Antioxidant Effects of Sulfur-containing Amino Acids, *Yonsei Med. J.*, 45(5) 776-788.
- Austin, L., Arthur, H., De Niese, M., Gurusinghe, A., and Baker, M.S.**, 1988, Micromethods in Single Muscle Fibers: 2. Determination of Glutathione Reductase and Glutathione Peroxidase, *Anal Biochem*, 174, 575-9.
- Bald, E., Chwatko, G., Glowacki, R., and Kusmierk, K.**, 2004, Analysis of Plasma Thiols by High-Performance Liquid Chromatography with Ultraviolet Detection, *J. Chromatogr. A*, 1032, 109-115.
- Banks, C.E., Davies, T.J., Wildgoose, G.G., and Compton, R.G.**, 2005, Electrocatalysis at Graphite And Carbon Nanotube Modified Electrodes: Edge-Plane Sites and Tube Ends are The Reactive Sites, *Chem Commun*, 7, 829-41.
- Benkova, B., Lozanov, V., Ivanov, I.P., Todorova, A., Milanov, I., and Mitev, V.**, 2008, Determination of Plasma Amino Thiols by High Performance Liquid Chromatography after Precolumn Derivatization with N-(2-Acridonyl)Maleimide, *J. Chromatogr. B*, 870, 103-108.

**REFERENCES (Continue)**

- Besada, A., Tadros, N.B., and Gawargious, Y.A.,** 1989, Copper(II)-neocuproine as Color Reagent For Some Biologically Activethiols-Spectrophotometric Determination Of Cysteine, Penicillamine, Glutathione And 6-Mercaptopurine, *Microchim Acta*, 3, 143-6.
- Brigelius-Flohé, R.,** 1999, Tissue-specific Functions of Individual Glutathione Peroxidases, *Free Radic. Biol. Med.*, 27(9-10) 951-65.
- Buchberger, W., and Winsauer, K.,** 1987, Determination of Glutathione in Biological Material by High-Performance Liquid Chromatography with Electrochemical Detection, *Anal Chim Acta*, 196, 251-4.
- Calvo-Marzal, P., Chumbimuni-Torres, K.Y., Hoehr, N.F., Neto, G.O., and Kubota, L.T.,** 2004, Determination of Reduced Glutathione Using an Amperometric Carbon Paste Electrode Chemically Modified with TTF-TCNQ, *Sensors and Actuators B*, 100, 333-340.
- Camera, E., Rinaldi, M., Briganti, S., Picardo, M., and Fanali, S.,** 2001, Simultaneous Determination of Reduced and Oxidized Glutathione in Peripheral Blood Mononuclear Cells by Liquid Chromatography-Electrospray Mass Spectrometry, *J Chromatogr B*, 757, 69-78.
- Cammarata, R.C.,** 2004, Nanocomposites, 199-213, Introduction to Nanoscale Science and Technology Di Ventra, M., Evoy, S., Heflin Jr., J.R., (Eds) Kluwer Academic Publishers, Boston, USA, 599p.
- Capitan, P., Malmezat, T., Breuille, D., and Obled, C.,** 1999, Gas Chromatographic-Mass Spectrometric Analysis of Stable Isotopes of Cysteine and Glutathione in Biological Samples, *J Chromatogr B*, 732, 127-35.
- Carru, C., Deiana, L., Sotgia, S., Pes, G.M., and Zinellu, A.,** 2004, Plasma Thiols Redox Status by Laser-Induced Fluorescence Capillary Electrophoresis, *Electrophoresis*, 25, 882-889.
- Carsol, M.A., Pouliquen, I., Lesgards, G., and Macini, M.,** 1996, Enzymatic Determination of Glutathione Using Electrochemical Sensor Based on Cobalt Phthalocyanine Screen-Printed Electrode, *Food Technol Biotechnol*, 34, 147-52.
- Causse, E., Malatray, P., Calaf, R., Charpiot, P., Candito, M., Bayle, C., Valdiguie, P., Salvayre, R., and Couderc, F.,** 2000, Plasma Total Homocysteine Aand Other Thiols Analyzed by Capillary Electrophoresis/Laser-Induced Fluorescence Detection: Comparison with Two Other Methods, *Electrophoresis*, 21, 2074-2079.
- Çevik, S., Timur, S., and Anık, Ü.,** 2012a, Biocentri-voltammetry for the Enzyme Assay: a model study, *RSC Adv*, 2, 4299-4303.



**REFERENCES (Continue)**

- Çevik, S., Timur, S., and Anık, Ü.**, 2012b, Biocentri-voltammetric biosensor for acetylcholine and choline, *Microchim Acta*, 179, 299-305.
- Chai, Y.C., Ashraf, S.S., Rokutan, K., Johnston, Jr R.B., and Thomas, J.A.**, 1994, S-Thiolation of Individual Human Neutrophil Proteins Including Actin by Stimulation of The Respiratory Burst: Evidence Against A Role for Glutathione Disulfide, *Arch Biochem Biophys*, 310, 273-81.
- Chailapakul, O., Fujishima, A., Tiphara, P., and Siriwongchai, H.**, 2001, Electroanalysis of Glutathione and Cephalexin Using The Boron-Doped Diamond Thin-Film Electrode Applied to Flow Injection Analysis, *Analytical Sciences*, 17, 419-422.
- Chambers, J.Q.**, 1978, Encyclopaedia of Electrochemistry of the Elements, Bard, A. J., Lund, H., (Eds), Marcel Dekker, New York, ch. XII-3, p. 329.
- Chauhan, N., Jagriti Narang, Meena, and C.S. Pundir**, 2012, An Amperometric Glutathione Biosensor Based on Chitosan–Iron Coated Gold Nanoparticles Modified Pt Electrode, *International Journal of Biological Macromolecules*, 51(5) 879-86.
- Chen, X.P., Cross, R.F., Clark, A.G., and Baker, W.L.**, 1999, Analysis of Reduced Glutathione Using A Reaction with 2,4'-dichloro-1-(naphthyl-4-ethoxy)-S-triazine (EDTN), *Microchim Acta*, 130, 225-31.
- Chen, J., He, Z., Liu, H., and Cha, C.**, 2006, Electrochemical Determination of Reduced Glutathione (GSH) by Applying the Powder Microelectrode Technique, *Journal of Electroanalytical Chemistry*, 588, 324-330.
- Cheng, W.H., Ho, Y.S., Valentine, B.A., Ross, D.A., Combs, G.F., and Lei, X.G.**, 1998, Cellular Glutathione Peroxidase is the Mediator of Body Selenium to Protect Against Paraquat Lethality in Transgenic Mice, *J. Nutr.*, 128(7) 1070-6.
- Chou, S.-T., Ko, L.-E., and Yang, C.-S.**, 2001, High Performance Liquid Chromatography with Fluorimetric Detection for The Determination of Total Homocysteine in Human Plasma: Method And Clinical Applications, *Anal. Chim. Acta*, 429, 331-336.
- Cohn, V.H., and Lyle, J.**, 1966, A Fluorometric Assay for Glutathione, *Anal Biochem*, 14, 434- 40.
- Compagnone, D., Massoud, R., Di Ilio, C., and Federici, G.**, 1991, Potentiometric Determination of Glutathione and Glutathione Transferase Activity, *Anal Lett*, 24, 993-1004.

**REFERENCES (Continue)**

- Compagnone, D., Federici, G., Scarciglia, L., and Palleschi, G.,** 1994, Flow Through Analysis of Glutathione in Human Erythrocytes with an Amperometric Biosensor, *Anal Lett*, 27, 15-27.
- Çoldur, F., Andaç, M., and Işıldak, I.,** 2010, Flow-injection Potentiometric Applications of Solid State Li<sup>+</sup> Selective Electrode in Biological and Pharmaceutical Samples, *J. Solid State Electrochem*, 14, 2241-2249.
- Çubukcu, M., Timur, S., and Anık, Ü.,** 2007, Examination of Performance of Glassy Carbon Paste Electrode Modified with Gold Nanoparticle and Xanthine Oxidase for Xanthine and Hypoxanthine Detection, *Talanta*, 74, 434-439.
- Çubukçu, M., Ertaş, and F.N., Anık, Ü.,** 2012, Metal/Metal Oxide Micro/Nanostructured Modified GCPE for GSH Detection, *Current Analytical Chemistry*, 8, 351-357.
- Dai, X., Nekrassova, O., Hyde, M.E., and Compton, R.G.,** 2004, Anodic Stripping Voltammetry of Arsenic(III) Using Gold Nanoparticle-Modified Electrodes, *Anal. Chem.*, 76, 5924-5929.
- Ellman, G.L.,** 1959, Tissue Sulfhydryl Groups. *Arch Biochem Biophys*, 82, 70-7.
- Failli, P., Palmien, L., Alfonso, C., Giovanelli, L., Generini, S., Rosso, A.D., Pignone, A., Stanflin, N., Orsi, S., Zilletti, L., and Matucci-Cerinic, M.,** 2002, Effect of N-acetyl-L-cysteine on Peroxynitrite and Superoxide Anion Production of Lung Alveolar Macrophages in Systemic Sclerosis, *Nitric Oxide Biol. Chem.*, 7, 277-282.
- Flohé, L.,** 1989, The Selenoprotein Glutathione Peroxidase, in Glutathione-Chemical, Biochemical, and Medical Aspects, D. Dolphin, R. Poulson, O. Avramovic (Eds), Wiley, New York, USA, 643p.
- Fracassetti, D., Lawrence, N., Tredoux, A.G.J., Tirelli, A., Nieuwoudt, H.H., and Du Toit, W.J.,** 2011, Quantification of Glutathione, Catechin and Caffeic Acid in Grape Juice and Wine by A Novel Ultra-Performance Liquid Chromatography Method, *Food Chemistry*, 128, 1136-1142.
- Fukunaga, K., and Nakazono, N.,** 1998, Yoshida, M., Determination of Reduced-Form Glutathione and Total Glutathione in Blood and Plasma by High-Performance Liquid Chromatography with On-Column Fluorescence Derivatization, *Chromatographia*, 48, 690-4.

## REFERENCES (Continue)

- Galley, H.F., Howdle, P.D., Walker, B.E., and Webster, N.R.**, 1997, The Effects of Intravenous Antioxidants in Patients with Septic Shock, *Free Radic. Biol. Med.*, 23(5) 768-74.
- Glatz, Z., and Maslanova, H.**, 2000, Specific thiol Determination by Micellar Electrokinetic Chromatography and On-Column Detection Reaction with 2,2'-dipyridyldisulfide, *J. Chromatogr. A*, 895, 179-187.
- Griffith, O.W., and Meister, A.**, 1985, Origin and Turnover Of Mitochondrial Glutathione, *Proc Natl Acad Sci U S A*, 82, 4668-72.
- Guan, X., Hoffman, B., Dwivedi, C., and Matthees, D.P.**, 2003, A Simultaneous Liquid Chromatography/Mass Spectrometric Assay of Glutathione, Cysteine, Homocysteine and Their Disulfides in Biological Samples, *J. Pharm. Biomed. Anal.*, 31, 251-261.
- Han, H., and Tachikawa, H.**, 2005, Electrochemical Determination of Thiols at Single-Wall Carbon Nanotubes and PQQ Modified Electrodes, *Front. Biosci.* 10, 931-9.
- Hansen, R.E., Østergaard, H., Nørgaard, P., and Winther, J.R.**, 2007, Quantification of Protein Thiols and Dithiols in The Picomolar Range Using Sodium Borohydride and 4,4'-Dithiodipyridine, *Anal. Biochem.* 363(1) 77-81.
- Hernandez-Santos, D., Diaz-Gonzales, M., Gonzales-Garcia, M.B., and Costa-Garcia, A.**, 2004, Enzymatic Genosensor on Streptavidin-Modified Screen-Printed Carbon Electrodes, *Anal. Chem.*, 76, 6887-6893.
- Hissin, P.J., and Hilf, R.**, 1976, A Fluorometric Method for Determination of Oxidized and Reduced Glutathione in Tissues, *Anal Biochem*, 74, 214-26.
- Holmgren A., and Sengupta, R.**, 2010, The Use of Thiols by Ribonucleotide Reductase, *Free Radical Biology & Medicine*, 49, 1617-1628.
- Hou, Y., Ndamanisha, J. C., Guo, L.-P., Peng, X.-J., and Bai, J.**, 2009, Synthesis of Ordered Mesoporous Carbon/Cobalt Oxide Nanocomposite for Determination of Glutathione. *Electrochimica Acta*, 54, 6166-6171.
- Hrapovic, S., Liu, Y., Male, K.B., and Luong, J.H.T.**, 2004, Electrochemical Biosensing Platforms Using Platinum Nanoparticles and Carbon Nanotubes, *Anal. Chem.*, 76, 1083-1088.
- Hua, C., Smyth, M.R., and O'Fagain, C.**, 1991, Determination of Glutathione at Enzyme-Modified and Unmodified Glassy Carbon Electrodes, *Analyst*, 116, 929-31.

## REFERENCES (Continue)

- Huang, Y.-Q., Ruan, G.-D., Liu, J.-Q., Gao, Q., and Feng, Y.-Q.,** 2011, Use of Isotope Differential Derivatization for Simultaneous Determination of Thiols and Oxidized Thiols by Liquid Chromatography Tandem Mass Spectrometry, *Analytical Biochemistry*, 416, 159-166.
- Inoue, T., and Kirchoff, J.R.,** 2000, Electrochemical Detection of Thiols with a Coenzyme Pyrroloquinoline Quinone Modified Electrode, *Anal. Chem.*, 72, 5755-5760.
- Ip, C., Hayes, C., Budnick, R.M., and Ganther, H.E.,** 1991, Chemical Form of Selenium, Critical Metabolites, and Cancer Prevention, *Cancer Res*, 51, 595-600.
- Jin, W., Li, W., and Xu, Q.,** 2000, Quantitative Determination of Glutathione in Single Human Erythrocytes by Capillary Zone Electrophoresis with Electrochemical Detection, *Electrophoresis*, 21, 774-9.
- Jones, D.P., and Liang, Y.,** 2009, Measuring the Poise Of Thiol/Disulfide Couples In Vivo, *Free Radic. Biol. Med.*, 47, 1329-1338.
- Jocelyn, P.C.,** 1972, Biochemistry of the SH Group; Academic Press: London, p165.
- Kand'ar, R., Zakova, P., Lotkova, H., Kucera, O., and Cervinkova, Z.,** 2007, Determination of Reduced and Oxidized Glutathione in Biological Samples Using Liquid Chromatography with Fluorimetric Detection, *J. Pharm. Biomed.Anal.*, 43, 1382-1387.
- Katz, E., Willner, I., and Wang, J.,** 2004, Electroanalytical and Bioelectroanalytical Systems Based on Metal and Semiconductor Nanoparticles, *Electroanalysis*, 16, 19-44.
- Kerman, K., Saito, M., Yamamura, S., Takamura, Y., and Tamiya, E.,** 2008, Nanomaterial-based Electrochemical Biosensors for Medical Applications, *Trends in Analytical Chemistry*, 27(7), 585-592.
- Kinoshita, H., Miya, T., and Kamihira, S.,** 1999, Amperometric Determination of Glutathione in Yeast Extract Using A Membrane-Covered Phthalocyanine Embedded Carbon-Paste Electrode, *Bunseki Kagaku*, 48,117-20.
- Kizek, R., Vacek, J., Trnkova, L., and Jelen, F.,** 2004, Cyclic Voltammetric Study of the Redox System of Glutathione Using the Disulfide Bond Reductant tris(2-carboxyethyl)phosphine, *Bioelectrochemistry*, 63(1-2) 19-24.
- Koçak, S.,** 2009, Centri-Voltammetric Molybdenum Determination and Electrochemical Polyoxomolybdate Formation and its Characterization, PhD Thesis, Ege University, Izmir, 154p.

## REFERENCES (Continue)

- Kubalczyk, P., and Bald, E.,** 2006, Transient Pseudo-isotachophoretic Stacking in Analysis of Plasma for Homocysteine by Capillary Zone Electrophoresis, *Anal. Bioanal. Chem.*, 384, 1181-1185.
- Kulys, J., and Drungiliene, A.,** 1991, Chemically Modified Electrodes for the Determination of Sulfhydryl Compounds, *Anal Chim Acta*, 243, 287-92.
- Kuwahara, S., Akita, S., Shirakihara, M., Sugai, T., Nakayama, Y., and Shinohara, H.,** 2006, Fabrication and Characterization of High-Resolution AFM Tips with High-Quality Double-Wall Carbon Nanotubes, *Chemical Physics Letters*, 429, 581-585.
- Lavigne, V., Pons, A., and Dubourdiu, D.,** 2007, Assay of Glutathione in Must and Wines Using Capillary Electrophoresis and Laser-Induced fluorescence Detection: Changes in Concentration in Dry White Wines During Alcoholic Fermentation and Aging, *Journal of Chromatography A*, 1139, 130-135.
- Lee, R., and Britz-McKibbin, P.,** 2009, Differential Rates of Glutathione Oxidation for Assessment of Cellular Redox Status and Antioxidant Capacity by Capillary Electrophoresis–Mass Spectrometry: An Elusive Biomarker of Oxidative Stress, *Anal. Chem.*, 81, 7047-7056.
- Lee, R., West, D., Phillips, S.M., and Britz-McKibbin, P.,** 2010, Differential Metabolomics for Quantitative Assessment of Oxidative Stress with Strenuous Exercise and Nutritional Intervention: Thiol-Specific Regulation of Cellular Metabolism With N-Acetyl-L-Cysteine Pretreatment, *Anal. Chem.*, 82, 2959-2968.
- Le Moan, N., Tacnet, F., and Toledano, M.B.,** 2008, Protein-thiol Oxidation, From Single Proteins to Proteome-Wide Analyses, *Methods Mol. Biol.*, 476, 181-198.
- Lehmann, C., Wollenberger, U., Brigelius-Flohe, R., and Scheller, F.W.,** 1998, Bioelectrocatalysis by a Selenoenzyme, *J Electroanal Chem*, 455, 259-63.
- Lehmann, C., Wollenberger, U., Brigelius-Flohe, R., and Scheller, F.W.,** 2001, Modified Gold Electrodes for Electrochemical Studies of the Reaction of Phospholipid Hydroperoxide Glutathione Peroxidase with Glutathione and Glutathione Disulfide, *Electroanalysis*, 13(5) 364-369.
- Lima, P.R., Santos, W.J.R., Oliveira, A.B., Goulart, M.O.F., and Kubota, L.T.,** 2008, Electrocatalytic Activity of 4-nitrophthalonitrile-Modified Electrode for the L-glutathione detection, *Journal of Pharmaceutical and Biomedical Analysis*, 47, 758-764.

**REFERENCES (Continue)**

- Liu, Y., Yin, F., Long, Y., Zhang, Z., and Yao, S.,** 2003, Study of the Immobilization of Alcohol Dehydrogenase on Au-Colloid Modified Gold Electrode by Piezoelectric Quartz Crystal Sensor, Cyclic Voltammetry, and Electrochemical Impedance Techniques, *J. Colloids Interf. Sci.*, 258, 75-81.
- Liu, S.Q., and Ju, H.X.,** 2003, Reagentless Glucose Biosensor Based on Direct Electron Transfer of Glucose Oxidase Immobilized on Colloidal Gold Modified Carbon Paste Electrode, *Biosens. Bioelectron.*, 19, 177-183.
- Liu, Y., Nie, L., Tao, W., and Yao, S.,** 2004, Amperometric Study of Au-Colloid Function on Xanthine Biosensor Based on Xanthine Oxidase Immobilized in Polypyrrole Layer, *Electroanalysis*, 16, 1271-1278.
- Liu, L.-P., Yin, Z.-J., and Yang, Z.-S.,** 2010, A L-cysteine Sensor Based on Pt Nanoparticles/Poly(*O*-Aminophenol) Film on Glassy Carbon Electrode, *Bioelectrochemistry*, 79, 84-89.
- Luo, X., Morrin, A., Killard, A.J., and Smyth, M.R.,** 2006, Application of Nanoparticles in Electrochemical Sensors and Biosensors, *Electroanalysis*, 18, 319-326.
- Maiorino, M., Aumann, K.D., Brigelius-Flohé, R., Doria, D., van der Heuvel, J., McCarthy, J., Roveri, A., Ursini, F., and Flohe, L.,** 1995, Probing the Presumed Catalytic Triad of Selenium-Containing Peroxidases by Mutational Analysis of Phospholipid Hydroperoxide Glutathione Peroxidase (PHGPx), *Biol. Chem. Hoppe-Seyler*, 376(11) 651-60.
- Majima, Y.,** 2002, Mucoactive Medications and Airway Disease, *Pediatr. Respir. Rev.*, 3, 104-9.
- Mannervik, B.,** 1985, Glutathione Peroxidase, *Methods in Enzymology*, vol. 113. New York: Academic Press, p490-5.
- Manso, J., Mena, M.L., Yáñez-Sedenó, P., and Pingarrón, J.M.,** 2007, Electrochemical Biosensors Based on Colloidal Gold–Carbon Nanotubes Composite Electrodes, *J. Electroanal. Chem.*, 603, 1-7.
- Mao, L., and Yamamoto, K.,** 2000, Amperometric Biosensor for Glutathione Based on Osmium-Polyvinylpyridine Gel Polymer and Glutathione Sulfhydryl Oxidase, *Electroanalysis*, 12, 577-582.
- Matés, J.M., Pérez-Gómez, C., and Núñez de Castro, I.,** 1999, Antioxidant Enzymes and Human Diseases, *Clin Biochem*, 32, 595-603.

**REFERENCES (Continue)**

- Matés, J.M., Pérez-Gómez, C., and Blanca, M.,** 2000, Chemical and Biological Activity of Free Radical “Scavengers” in Allergic Diseases: A Review, *Clin Chim Acta*, 296, 1-15.
- McCully, K.S.,** 1996, Homocysteine and Vascular Disease, *Nat. Med.*, 2, 386-389.
- McCully, K.S.,** 1997, *The Homocysteine Revolution*. New Canaan, CT: Keats Publishing.
- Meister, A.,** 1973, On the Enzymology of Amino Acid Transport, *Science*, 180, 33-9.
- Meister, A., and Anderson, M.E.,** 1983, Glutathione, *Ann Rev Biochem*, 52, 711-60.
- Meister, A., and Larsson, A.,** 1989, Glutathione Synthetase Deficiency and Other Disorders of the G-Glutamyl Cycle. In: Scriver CR, Beaudet AL, Sly WS, Valle D, editors. *The metabolic basis of inherited disease*. 6th ed. New York: McGraw-Hill; p. 855–68.
- Meister, A.,** 1994, Glutathione, Ascorbate, and Cellular Protection, *Cancer Res.*, 54, 1969S-1975S.
- Mena, M.L., Yáñez-Sedenó, P., and Pingarrón, J.M.,** 2005, A Comparison of Different Strategies for the Construction of Amperometric Enzyme Biosensors Using Gold Nanoparticle-Modified Electrodes, *Anal. Biochem.*, 336, 20-27.
- Merkoçi, A., Pumera, M., Llopis, X., Pérez, B., del Valle, M., and Alegret, S.,** 2005, New Materials for Electrochemical Sensing VI: Carbon Nanotubes, *Trends in Analytical Chemistry*, 24, 826-838.
- Monostori, P., Wittmann, G., Karg, E., and Túri, S.,** 2009, Determination of Glutathione And Glutathione Disulfide in Biological Samples: An In-Depth Review, *J. Chromatogr. B*, 877, 3331-3346.
- Moriarty-Craige, S.E., and Jones, D.P.,** 2004, Extracellular Thiols and Thiol/Disulfide Redox In Metabolism, *Annu. Rev. Nutr.* 24, 481-509.
- Muthirulan, P., and Velmurugan, R.,** 2011, Direct Electrochemistry and Electrocatalysis Of Reduced Glutathione on CNFs–PDDA/PB Nanocomposite Film Modified ITO Electrode for Biosensors, *Colloids and Surfaces B: Biointerfaces*, 83, 347-354.
- Nalini, B., and Narayanan, S.S.,** 1998, Electrocatalytic Oxidation Of Sulfhydryl Compounds at Ruthenium (III) Diphenyldithiocarbamate Modified Carbon Paste Electrode, *Electroanalysis*, 10,779-83.

**REFERENCES (Continue)**

- Narayan, J., and Tiwari, A.,** 2006, Methods of Forming Three-Dimensional Nanodot Arrays in a Matrix. U.S. Patent No. 7,105,118. Washington, DC: U.S.
- Nolin, T.D., McMenamin, M.E., and Himmelfarb, J.,** 2007, Simultaneous Determination of Total Homocysteine, Cysteine, Cysteinylglycine, And Glutathione in Human Plasma by High-Performance Liquid Chromatography: Application to Studies of Oxidative Stress, *J. Chromatogr. B*, 852, 554-561.
- Norris, R.L., Eaglesham, G.K., Shaw, G.R., Smith, M.J., Chiswell, R.K., Seawright, A.A., and Moore, M.R.,** 2001, A Sensitive and Specific Assay for Glutathione with Potential Application to Glutathione Disulphide, Using High-Performance Liquid Chromatography-Tandem Mass Spectrometry, *J Chromatogr B*, 762, 17-23.
- Owens, C.W.I., and Belcher, R.V.,** 1965, A Colorimetric Micro-Method for the Determination of Glutathione, *Biochem J*, 94, 705-11.
- Oztekin, Y., Ramanaviciene, A., and Ramanavicius, A.,** 2011, Electrochemical Glutathione Sensor Based on Electrochemically Deposited Poly-m-aminophenol, *Electroanalysis*, 23(3), 701-709.
- Parmentier, C., Leroy, P., Wellman, M., and Nicolas, A.,** 1998, Determination of Cellular Thiols and Glutathione-Related Enzyme Activities: Versatility of High-Performance Liquid Chromatography Spectrofluorimetric Detection, *J Chromatogr B*, 719, 37-46.
- Pastore, A., Federici, G., Bertini, E., and Piemonte, F.,** 2003, Analysis of Glutathione: Implication in Redox and Detoxification, *Clinica Chimica Acta*, 333, 19-39.
- Phung, X., Groza, J., Stach, E.A., Williams, L.N., and Ritchey, S.B.,** 2003, Surface Characterization of Metal Nanoparticles, *Mater Eng A*, 359, 261-8.
- Piccoli, G., Fiorani, M., Biagiarelli, B., Palma, F., Potenza, L., Amicucci, A., and Stocchi, V.,** 1994, Simultaneous High Performance Capillary Electrophoretic Determination of Reduced and Oxidized Glutathione in Red Blood Cells in the Femtomole Range, *J Chromatogr A*, 676, 239-46.
- Pingarrón, J.M., Yáñez-Sedenõ, P., and González-Cortés, A.,** 2008, Gold Nanoparticle-Based Electrochemical Biosensors, *Electrochimica Acta*, 53, 5848-5866.



## REFERENCES (Continue)

- Potesil, D., Petrlova, J., Adama, V., Vacek, J., Klejdus, B., Zehnalek, J., Trnkova, L., Havel, L., and Kizek, R.,** 2005, Simultaneous Femtomole Determination of Cysteine, Reduced and Oxidized Glutathione, and Phytochelatin in Maize (*Zea Mays* L.) Kernels Using High-Performance Liquid Chromatography with Electrochemical Detection, *Journal of Chromatography A*, 1084, 134-144.
- Rabenstein, D.L., and Saetre, R.,** 1977, Mercury-based Electrochemical Detector of Liquid Chromatography for the Detection of Glutathione and Other Sulfur-Containing Compounds, *Anal Chem*, 49, 1036- 9.
- Raggi, M.A., Nobile, L., and Giovannini, A.G.,** 1991, Spectrophotometric Determination of Glutathione and of its Oxidation-Product in Pharmaceutical Dosages Forms, *J Pharm Biomed Anal*, 9, 1037-40.
- Raj, C.R., Okajima, T., and Ohsaka, T.,** 2003, Gold Nanoparticle Arrays for the Voltammetric Sensing of Dopamine, *J. Electroanal. Chem.*, 543, 127-133.
- Rao, C.N.R., Müller, A., and Cheetham, A.K.,** (Eds), 2004, Nanomaterials-an Introduction, 1-12, *The Chemistry of Nanomaterials: Synthesis, Properties and Applications*, Vol.1, Wiley-VCH, Weinheim, p724.
- Raof, J.-B., Ojani, R., and Baghayeri, M.,** 2009, Simultaneous Electrochemical Determination of Glutathione and Tryptophan on a Nano-TiO<sub>2</sub>/Ferrocene Carboxylic Acid Modified Carbon Paste Electrode, *Sensors and Actuators B*, 143, 261-269.
- Rellinghaus, B., Stappert, S., Wassermann, E.F., Sauer, H., and Spliethoff, B.,** 2001, The Effect of Oxidation on The Structure of Nickel Nanoparticles, *Eur Phys J D*, 16, 249-252.
- Richie Jr, J.P., and Lang, C.A.,** 1987, The Determination of Glutathione, Cysteine and Other Thiols and Disulfides in Biological Samples Using High-Performance Liquid Chromatography with Dual Electrochemical Detection, *Anal Biochem*, 163, 9-15.
- Rivas, G.A., Rubianes, M.D., Rodriguez, M.C., Ferreyra, N.F., Luque, G.L., Pedano, M.L., Miscoria, S.A., and Parrado, C.,** 2007, Carbon Nanotubes for Electrochemical Biosensing, *Talanta*, 74(3) 291-307.
- Roederer, M., Ela, S.W., Staal, F.J.T., and Herzenberg, L.A.,** 1992, N-acetylcysteine: A New Approach To Anti-HIV Therapy, *AIDS Res. Hum. Retroviruses*, 8(2) 209-17.
- Romero, F.J., and Mueller-Klieser, W.,** 1998, Semiquantitative Bioluminescent Assay of Glutathione, *J Biolumin Chemilumin*, 13, 263-6.

**REFERENCES (Continue)**

- Roušar, T., Kucěra, O., Lotkova, H., and Červinkova, Z.,** 2012, Assessment of Reduced Glutathione: Comparison of an Optimized Fluorometric Assay with Enzymatic Recycling Method, *Analytical Biochemistry*, 423,236-240.
- Rover Jr, L., Tatsuo Kubota, L., and Fenalti Höehr, N.,** 2001, Development of an Amperometric Biosensor Based on Glutathione Peroxidase Immobilized in a Carbodiimide Matrix For The Analysis of Reduced Glutathione From Serum, *Clinica Chimica Acta*, 308, 55-67.
- Ruiz-Diaz, J.J., Torriero, A.A., Salinas, E., Marchevsky, E.J., Sanz, M.I., and Raba, J.,** 2006, Enzymatic Rotating Biosensor for Cysteine and Glutathione Determination in a FIA System, *Talanta*, 68, 1343-1352.
- Saitoh, K., Yamada, N., Ishikawa, E., Nakajima, H., and Shibukawa, M.,** 2006, On-Line Redox Derivatization Liquid Chromatography Using Double Separation Columns And One Derivatization Unit, *J. Sep. Sci.* 29, 49-56.
- Saitoh, K., Koichi, K., Yabiku, F., Noda, Y., Porter, M.D., and Shibukawa, M.,** 2008, On-Column Electrochemical Redox Derivatization for Enhancement of Separation Selectivity of Liquid Chromatography Use of Redox Reaction As Secondary Chemical Equilibrium, *J. Chromatogr. A*, 1180, 66-72.
- Salimi, A., and Pourbeyram, S.,** 2003, Renewable Sol-Gel Carbon Ceramic Electrodes Modified with a Ru-Complex for the Amperometric Detection of L-Cysteine and Glutathione, *Talanta*, 60, 205-214.
- Salimi, A., and Hallaj, R.,** 2005, Catalytic Oxidation of Thiols at Preheated Glassy Carbon Electrode Modified with Abrasive Immobilization of Multiwall Carbon Nanotubes: Applications to Amperometric Detection of Thiocytosine, L-Cysteine and Glutathione, *Talanta*, 66, 967-975.
- Satoh, I., Arakawa, S., and Okamoto, A.,** 1988, Flow-Injection Determination of Glutathione with Amperometric Monitoring of the Enzymatic Reaction, *Anal Chim Acta*, 214, 415-9.
- Satoh, I., Arakawa, S., and Okamoto, A.,** 1991, Calorimetric Flow-Injection Determination of Glutathione with Enzyme-Thermistor Detector, *Sens. Actuators B*, 5, 245-7.
- Satto, S.S., Kubota, L.T., and Neto, G.O.,** 1999, Biosensor for Phenol Based on the Direct Electron Transfer Blocking of Peroxidase Immobilising on Silica-Titanium, *Chim. Acta*, 390, 65-72.

**REFERENCES (Continue)**

- Schafer, F.Q., and Buettner, G.R.**, 2001, Redox Environment of the Cell as Viewed Through the Redox State of the Glutathione Disulfide/Glutathione Couple, *Free Radic. Biol. Med.* 30, 1191-1212.
- Scheller, F.W., Wollenberger, U., Lei, C., Jin, W., Ge, B., Lehmann, C., Lisdat, F., and Fridman, V.**, 2002. Bioelectrocatalysis by Redox Enzymes at Modified Electrodes, *ReViews in Molecular Biotechnology*, 82, 411-424.
- Sevcikova, P., and Glatz, Z.**, 2003, Specific Determination of Cysteine in Human Urine by Capillary Micellar Electrokinetic Chromatography, *J. Sep. Sci.*, 26, 734-738.
- Sevcikova, P., Glatz, Z., and Tomandl, J.**, 2003, Determination of Homocysteine in Human Plasma by Micellar Electrokinetic Chromatography and In-Capillary Detection Reaction With 2,2'-dipyridyl disulfide, *J. Chromatogr. A*, 990, 197-204.
- Shi, G., Lu, J., Xu, F., Sun, W., Jin, L., Yamamoto, K., Tao, S., and Jin, J.**, 1999, Determination of Glutathione in Vivo by Microdialysis Using Liquid Chromatography with a Cobalt Hexacyanoferrate Chemically Modified Electrode, *Anal Chim Acta*, 391, 307-313.
- Simonet, J.**, 1993, Electrochemical Behavior of Organic Molecules Containing Sulfur, Patai, S., and Rappoport, Z., (Eds), Supplement S, Wiley, The Chemistry of Sulfur Containing Functional Groups, Chichester, England, p439.
- Smith, I.K., Vierheller, T.L., and Thorne, C.A.**, 1988, Assay of Glutathione Reductase in a Crude Tissue Homogenates Using 5,5'-dithiobis(2-nitrobenzoic acid), *Anal Biochem*, 175, 408-13.
- Stulik, K.**, 1999, Challenges and Promises of Electrochemical Detection and Sensing, *Electroanalysis*, 11(14) 1001-1004.
- Thanh, N.T.K., and Green, L.A.W.**, 2010, Functionalisation of Nanoparticles for Biomedical Applications, *Nano Today*, 5, 213-230.
- Thomas, J.P., Maiorino, M., Ursini, F., and Girotti, A.W.**, 1990, Protective Action of Phospholipid Hydroperoxide Glutathione Peroxidase against Membrane-damaging Lipid Peroxidation, *J. Biol Chem.*, 265(1) 454-461.
- Tietze, F.**, 1969, Enzymic Method for Quantitative Determination of Nanogram Amounts of Total and Oxidized Glutathione: Application to Mammalian Blood and Other Tissues, *Anal Biochem*, 27, 502-22.

**REFERENCES (Continue)**

- Timur, S., Odaci, D., Dinçer, A., Zihnioglu, F., and Telefoncu, A.,** 2008, Biosensing Approach For Glutathione Detection Using Glutathione Reductase And Sulfhydryl Oxidase Bienzymatic System, *Talanta*, 74, 1492-1497.
- Toyo'oka, T., Tanabe, J., and Jinno, H.,** 2001, Determination of Rat Hepatocellular Glutathione By Reversed-Phase Liquid Chromatography with Fluorescence Detection and Cytotoxicity Evaluation of Environmental Pollutants Based on The Concentration Change, *Biomed. Chromatogr.*, 15, 240-247.
- Toyo'oka, T.,** 2009, Recent Advances in Separation and Detection Methods for Thiol Compounds in Biological Samples, *Journal of Chromatography B*, 877, 3318-3330.
- Tsikis, D., Sandmann, J., Ikic, M., Fauler, J., Stichtenoth, D.O., and Frölich, J.C,** 1998, Analysis of Cysteine and N-Acetylcysteine in Human Plasma by High-Performance Liquid Chromatography at the Basal State and After Oral Administration of N-Acetylcysteine. *J. Chromatogr. B*, 708(1-2) 55-60.
- Tsikis, D., Raida, M., Sandman, J., Rossa, S., Forssmann, W.G., and Frölich, J.C.,** 2000, Electrospray Ionization Mass Spectrometry of Low-Molecular-Mass S-Nitroso Compounds and Their Thiols, *J Chromatogr B*, 742, 99- 108.
- Ursini, F., Heim, S., Kiess, M., Maiorino, M., Roveri, A., Wissing, J., and Flohé, L.,** 1999, Dual Function of The Selenoprotein PHGPx During Sperm Maturation, *Science*, 285(5432) 1393-6.
- Ürkmez, İ., Gökçel, İ., Ertaş, F.N., and Tural, H.,** 2009, Centrifugation: An Efficient Technique For Preconcentration In Anodic Stripping Voltammetric Analysis Of Mercury Using A Gold Film Electrode, *Microchim. Acta*, 167, 225-230.
- Vignaud, C., Rakotozafy, L., Falguieres, A., Potus, J., and Nicolas, J.,** 2004, Separation and Identification by Gel Filtration and High-Performance Liquid Chromatography with UV or Electrochemical Detection of The Disulphides Produced From Cysteine and Glutathione Oxidation, *J. Chromatogr. A*, 1031(1-2) 125-33.
- Wang, J.,** 2003, Nanoparticle-Based Electrochemical DNA Detection, *Anal. Chim. Acta*, 500, 247-257.

## REFERENCES (Continue)

- Wang, H., Liang, S.-C., Zhang, Z.-M., and Zhang, H.-S.,** 2004, 3-Iodoacetylaminobenzanthrone as a Fluorescent Derivatizing Reagent for Thiols in High-Performance Liquid Chromatography, *Anal. Chim. Acta*, 512, 281-286.
- Wang, S., and Lin, X.,** 2005, Electrodeposition of Pt-Fe(III) Nanoparticle on Glassy Carbon Electrode for Electrochemical Nitric Oxide Sensor, *Electrochimica Acta*, 50, 2887-2891.
- Wang, J.,** 2006, Analytical Electrochemistry, 3rd Edition, Capt 1, 2, 3 Published by John Wiley & Sons, Inc., New Jersey, Canada, p245.
- Wang, Z., Ai, F., Xu, Q., Yang, Q., Yu, J.-H., Huang, W.-H., and Zhao, Y.-D.,** 2010, Electrocatalytic Activity of Salicylic Acid on the Platinum Nanoparticles Modified Electrode by Electrochemical Deposition, *Colloids and Surfaces B: Biointerfaces*, 76, 370-374.
- Welch, C.M., and Compton, R.G.,** 2006, The Use of Nanoparticles in Electroanalysis: A Review, *Anal Bioanal Chem*, 384, 601-619.
- White, P.C., Lawrence, N.S., Davis, J., and Compton, R.G.,** 2002, Electrochemical Determination of Thiols: A Perspective Electroanalysis, 14(2) 89-98.
- Wring, A.S., Hart, J.P., and Birch, B.J.,** 1989, Development of an Improved Carbon Electrode Chemically Modified With Cobalt Phthalocyanine as a Re-Usable Sensor for Glutathione, *Analyst*, 114, 1563-70.
- Wring, S.A., Hart, J.P., and Birch, B.J.,** 1992, Development of an Amperometric Assay for the Determination of Reduced Glutathione, Using Glutathione Peroxidase and Screen-Printed Carbon Electrodes Chemically Modified with Cobalt Phthalocyanine. *Electroanalysis*, 4, 299-309.
- Wu, B.Y., Hou, S.H., Yin, F., Li, J., and Zhao, Z.X.,** 2007, Amperometric Glucose Biosensor Based on Layer-By-Layer Assembly of Multilayer Films Composed of Chitosan, Gold Nanoparticles and Glucose Oxidase Modified Pt Electrode, *Biosens. Bioelectron.*, 22, 838-844.
- Wu, Y.,** 2009, Nano-TiO<sub>2</sub>/Dihexadecylphosphate Based Electrochemical Sensor for Sensitive Determination of Pentachlorophenol, *Sensors and Actuators B*, 137, 180-184.
- Zeng, X., Zhanga, X., Zhu, B., Jia, H., Yang, W., Li, Y., and Xue, J.,** 2011, A Colorimetric and Ratiometric Fluorescent Probe for Quantitative Detection of GSH at Physiologically Relevant Levels, *Sensors and Actuators B*, 159, 142-147.

**REFERENCES (Continue)**

- Zheng, N., Zhou, X., Yang, W., Li, X., and Yuan, Z.,** 2009, Direct Electrochemistry and Electrocatalysis of Hemoglobin Immobilized in a Magnetic Nanoparticles-Chitosan Film, *Talanta*, 79, 780-786.
- Zhang, S., Wang, N., Yu, H., Niu, Y., and Sun, C.,** 2005, Covalent Attachment of Glucose Oxidase to an Au Electrode Modified with Gold Nanoparticles for Use as Glucose Biosensor, *Bioelectrochemistry*, 67, 15-22.
- Zhang, L., Jiang, X., Wang, E., and Dong, S.,** 2005, Attachment of Gold Nanoparticles to Glassy Carbon Electrode and its Application for the Direct Electrochemistry and Electrocatalytic Behavior of Hemoglobin, *Biosens. Bioelectron.*, 21, 337-345.
- Zhong, Z., Chen, H., Tang, S., Ding, J., Lin, J., and Tan, K.L.,** 2000, Catalytic Growth of Carbon Nanoballs With and Without Cobalt Encapsulation, *Chem Phys Lett*, 330, 41-47.

## CURRICULUM VITAE

**Name, Surname** : Meliha ÇUBUKCU  
**Date of Birth** : 16/ 05/ 1982  
**Place of Birth** : Mugla  
**Marital Status** : Single  
**Nationality** : Turkish Republic  
**Tel:** 0252 262 4096 **mobile:** 0542 291 19 74  
**Email:** meli\_eagen@hotmail.com

### EDUCATION

- ✓ Abant İzzet Baysal University B.Sc.(Chemistry/*-in English*)  
2001-2005
- ✓ Mugla University M.Sc.(Chemistry/Anal. Chem.)  
2006-2008

**Languages** : English (advanced), German (elementary)

**Research Interest** : Electroanalytical chemistry, Bioelectroanalytical chemistry, Nanoparticle-nanotube based biosensors, Voltammetric techniques, Nanobioelectrochemistry, Biofuel cells, The electrochemical analysis of biological molecules, Centri-voltammetry

### THESIS

#### Master of Science Thesis (MSc.)

ÇUBUKCU, M., ANIK, Ü.,

“Nanocomposites and Applications of Electrochemical Biosensor”, 2008, Muğla University, Faculty of Art and Science, Chemistry Department, Analytical Chemistry Division.

### RESEARCH ACTIVITIES AT OTHER COUNTRIES

Working at Biosystems Technology at University of Applied Sciences Wildau with Prof. Dr. Fred Lisdat between 23 June-7 July 2011. The subjects of the project were:

- “The usage of glassy carbon paste electrodes as anode in Biofuel cell systems”

**CURRICULUM VITAE (Continue)****PUBLICATIONS:**

1. **Çubukcu, M.**, Timur, S., and Anık, Ü., 2007, Examination of Performance of Glassy Carbon Paste Electrode Modified with Gold Nanoparticle and Xanthine Oxidase for Xanthine and Hypoxanthine Detection, *Talanta*, 74, 434-439.
2. Anık, Ü., Timur, S., **Çubukcu, M.**, and Merkoçi, A., 2008, The usage of a bismuth film electrode as transducer in glucose biosensing, *Microchimica Acta*, 69(1-2) 269-273.
3. Anık, Ü., and **Çubukcu, M.**, 2008, Examination of the Electroanalytic Performance of Carbon Nanotube (CNT) Modified Carbon Paste Electrodes as Xanthine Biosensor Transducers, *Turkish Journal of Chemistry*, 32 (6) 711-719.
4. Merkoçi, A., Anık, Ü., Çevik, S., **Çubukcu, M.**, and Guix, M., 2010, Bismuth Film Combined with Screen-Printed Electrode as Biosensing Platform for Phenol Detection, *Electroanalysis*, 22(13) 1429–1436.
5. Anık, Ü., **Çubukcu, M.**, Çevik, S., and Timur, S., 2010, Usage of Bismuth Film Electrode as Biosensor Transducer for Alkaline Phosphatase Assay, *Electroanalysis*, 22(13) 1519–1523.
6. Anık, Ü., and **Çubukcu, M.**, 2012, Application of Bismuth (III) Entrapped XO Biosensing System for Xanthine Determination in Beverages, *Food Analytical Methods*, 5, 716-722.
7. **Çubukcu, M.**, Ertaş, F.N., and Anık, Ü., 2012, Metal/Metal Oxide Micro/Nanostructured Modified GCPE for GSH Detection, *Current Analytical Chemistry*, 8, 351-357.
8. Anık, Ü., **Çubukcu, M.**, and Yavuz, Y., Nanomaterial-based composite biosensor for glucose detection in alcoholic beverages, *Artificial Cells, Blood Substitutes and Biotechnology*, (doi:10.3109/10731199.2012.696071, pages 1-5).
9. **Çubukcu, M.**, Ertaş, F.N., and Anık, Ü., Centri-Voltammetric Determination of Glutathione, *Microchimica Acta*, (in press).
10. **Çubukcu, M.**, Ertaş, F.N., and Anık, Ü., An Effective Electrochemical Biosensing Platform for Reduced Glutathione Detection, *Sensor and Actuators B*, (in assessment).